

# 1 **Microscale evidence of liquefaction and its potential triggers during** 2 **soft-bed deformation within subglacial traction tills**

3  
4 Emrys R Phillips<sup>1\*</sup>, David J A Evans<sup>2</sup>, Jaap J M van der Meer<sup>3</sup> and Jonathan R Lee<sup>4</sup>

5 1. British Geological Survey, The Lyell Centre, Research Avenue South, Edinburgh EH14 4AP, UK

6 2. Department of Geography, University of Durham, South Road, Durham, DH1 3LE, UK

7 3. School of Geography, Queen Mary, University of London, Mile End Road, London E1 4NS, UK

8 4. British Geological Survey, Keyworth, Nottingham, NG12 5GG, UK

9 \* Corresponding author: e-mail - [erp@bgs.ac.uk](mailto:erp@bgs.ac.uk)

10 **Keywords:** glacier bed deformation, till liquefaction, pressurised meltwater, icequakes

## 11 **Highlights:**

12 Subglacial traction tills undergo repeated phases of liquefaction and deformation

13 This process lowers the shear strength of the till, facilitating glacier movement

14 This soft-bed sliding occurs in a series of 'stick-slip' events

15 Soft-bed sliding may be partially facilitated by glacier seismic activity

## 16 **Abstract**

17 Published conceptual models argue that much of the forward motion of modern and ancient glaciers  
18 is accommodated by deformation of soft-sediments within the underlying bed. At a microscale this  
19 deformation results in the development of a range of ductile and brittle structures in water-  
20 saturated sediments as they accommodate the stresses being applied by the overriding glacier.  
21 Detailed micromorphological studies of subglacial traction tills reveal that these polydeformed  
22 sediments may also contain evidence of having undergone repeated phases of liquefaction followed  
23 by solid-state shear deformation. This spatially and temporally restricted liquefaction of subglacial  
24 traction tills lowers the shear strength of the sediment and promotes the formation of "transient  
25 mobile zones" within the bed, which accommodate the shear imposed by the overriding ice. This  
26 process of soft-bed sliding, alternating with bed deformation, facilitates glacier movement by way of  
27 'stick-slip' events. The various controls on the slip events have previously been identified as: (i) the  
28 introduction of pressurised meltwater into the bed, a process limited by the porosity and  
29 permeability of the till; and (ii) pressurisation of porewater as a result of subglacial deformation; to

30 which we include (iii) episodic liquefaction of water-saturated subglacial traction tills in response to  
31 glacier seismic activity (icequakes), which are increasingly being recognized as significant processes  
32 in modern glaciers and ice sheets. As liquefaction operates only in materials already at very low  
33 values of effective stress, its process-form signatures are likely indicative of glacier sub-marginal tills.

34

## 35 **1. Introduction**

36 Deformation of the soft, unconsolidated sediments occurring beneath many glaciers is thought to  
37 account for a substantial component of their forward motion (e.g. Alley *et al.*, 1986; Boulton and  
38 Hindmarsh, 1987; Clarke, 1987; Alley *et al.*, 1987a, b; Alley, 1989a, b; Humphrey *et al.*, 1993; Boulton  
39 *et al.* 2001). This concept of a “deforming bed” was first proposed following experiments carried out  
40 upon the till beneath the margin of Breiðamerkurjökull in SE Iceland (Boulton, 1979; Boulton and  
41 Hindmarsh, 1987; Boulton and Dobbie, 1998) and further supported by high resolution seismic  
42 surveys beneath Ice Stream B in Antarctica (Blankenship *et al.*, 1986, 1987). Subsequent field studies  
43 and geotechnical experiments have identified a range of possible subglacial deformation responses  
44 to glacier basal shear stresses which give rise to increasing cumulative shear strain upwards through  
45 the till profile towards the ice base (Boulton *et al.*, 1974; Boulton and Jones; 1979; Boulton, 1986;  
46 Hindmarsh, 1997; Tulaczyk *et al.*, 2000a, b; Kavanaugh and Clarke, 2006). The water content,  
47 lithological composition and thickness of the tills, along with temporal and spatial changes in the  
48 porewater pressures that occur within the subglacial environment, are all considered to exert a  
49 strong control on the style and intensity of deformation (see Evans *et al.*, 2006 and references  
50 therein). However, the exact nature of the response of tills during subglacial deformation remains a  
51 subject of significant debate (cf. Boulton and Hindmarsh, 1987; Benn and Evans, 1996; Boulton 1996;  
52 Hindmarsh, 1997; Murray, 1997; Piotrowski and Kraus; 1997; Piotrowski *et al.*, 1997; Tulaczyk, 1999;  
53 Fuller and Murray, 2000; Tulaczyk *et al.*, 2000a, b; van der Meer *et al.*, 2003; Piotrowski *et al.*, 2004,  
54 2006; Kavanaugh and Clarke, 2006; Evans *et al.*, 2006; Damsgaard *et al.*, 2016), especially the  
55 responses that are likely to arise through changing water pressures. For example a number of  
56 studies of marine terminating ice streams in West Antarctic have suggested that tidal movements  
57 effecting the floating part of the glacier can influence the upstream distribution of pore water  
58 pressure leading to variations in the velocity of ice flow (e.g. Winberry *et al.*, 2011; Walker *et al.*,  
59 2013; Thompson *et al.*, 2014; Rosier *et al.*, 2015).

60 Boreholes through the Trapridge Glacier (NW Canada) indicate that subglacial deformation is  
61 driven by changes in shear stress due to the variation in ice-bed coupling and water pressure as well  
62 as possible changes in deforming layer thickness (Blake, 1992; Blake *et al.*, 1992; Kavanaugh and

63 Clarke, 2006). Iverson *et al.* (1994, 1995) used investigations at Storglaciären in northern Sweden to  
64 emphasize the complexity of subglacial deformation, concluding that the till acts as a “lubricant”  
65 with forward motion being dominated by basal sliding and ploughing of large clasts embedded in the  
66 base of the ice. Some subglacial experiments have revealed that, instead of increasing coupling at  
67 the ice-bed interface, ploughing clasts actually weaken sediment by elevating porewater pressures  
68 (PWP) in sediment prows (Iverson *et al.*, 1994; Iverson, 1999; Fischer *et al.*, 2001; Iverson, 2010).  
69 Hindmarsh (1996) suggested that the till itself may slide over an underlying hard substrate, giving  
70 rise to polished/striated bedrock surfaces. Similarly Truffer *et al.* (2000) and Kjær *et al.* (2006) have  
71 also argued for deformation having occurred deep within or beneath subglacial tills as a potential  
72 mechanism for rapid ice flow. Alternatively, Fuller and Murray (2000) recorded basal sliding over  
73 soft-sediments at the base of Hagafellsjökull in Iceland, associated with only a very thin (< 16 cm)  
74 layer of deformed sediment.

75         Reconciling these process studies with interpretations of the subglacial conditions recorded  
76 in ancient sedimentary sequences is particularly challenging, because palaeo-ice sheets and glaciers  
77 have left a legacy that comprises complex assemblages of deposits whose sedimentological and  
78 structural signatures are ambiguous. Consequently, our current understanding of the conditions  
79 encountered within the subglacial environment relies heavily upon theoretical models stemming  
80 from a modest number of glaciological process case studies and laboratory experiments. From this  
81 comes an understanding that increased porewater pressure (PWP) within the glacier bed, when it is  
82 at steady state consolidation, results in the “dilation” of the sediment and a fall in its shear strength  
83 (Fig. 1). Fluctuations in PWP will lead to repeated phases of “dilation” followed by “collapse” as the  
84 water pressure falls, the latter leading to an increase in the shear strength of the sediment (also see  
85 Damsgaard *et al.*, 2016; Winberry *et al.*, 2011); this response may be dampened by materials with  
86 lower diffusivity (Iverson, 2010). The computer simulations of the deformation of subglacial tills by  
87 Damsgaard *et al.* (2016) have demonstrated that creep in these modelled simple granular materials  
88 keeps porosities somewhat elevated between failure events. At the highest values of PWP the ice  
89 may become decoupled from its bed and there may be a significant fall in the shear stress translated  
90 to the underlying sediments, effectively switching off subglacial deformation and promoting basal  
91 sliding as the dominant mechanism of glacier forward motion. This stick-slip style of motion  
92 operating in soft glacier beds has been reported by Fischer and Clarke (1997) and Fischer *et al.*  
93 (1999) for the Trapridge Glacier, where decoupling of the ice takes place during periods of high  
94 water pressure. Boulton *et al.* (2001) also propose a stick-slip motion, operating diurnally, to explain  
95 their observations at Breiðamerkurjökull, Iceland, where rising water pressures initiate till dilation,  
96 followed by the reduction in ice-bed friction and then ice-till decoupling. Falling water pressures

97 then return the till to a deforming state and re-couple the ice-bed interface; a continued fall in water  
98 pressure below the threshold for failure causes the bed to stick and enhanced ice-bed traction.  
99 However, dilation increases the connectivity between intergranular pore spaces, temporarily  
100 increasing the permeability of the till promoting the dewatering of the sediment and dilatant arrest  
101 (Youd, 2003) or dilatant hardening (Iverson *et al.*, 1998; Moore and Iverson, 2002; Damsgaard *et al.*,  
102 2015). Consequently repeated phases of till dilation, in the absence of a mechanism to reintroduce  
103 water into these subglacial sediments, will cause an increase in ice-bed friction.

104 The above case studies notwithstanding, some significant uncertainties still exist in our  
105 understanding of till deformation processes and forms including: the spatial and temporal patterns  
106 of subglacial deformation, the variability of subglacial sediment rheology, and the inter-relationships  
107 of sediment deformation and subglacial hydrology, as well as the inter-relationships between sliding  
108 over soft-sediments with bed deformation. Given the constraints inherent within the discoveries  
109 outlined above, we should expect all subglacial tills to show at least some evidence of deformation.  
110 However, the massive nature of many subglacial tills exposed at the margins of contemporary  
111 glaciers and in the geological record has been used to question the pervasive nature of deformation,  
112 at least at the macroscale, even though shear-induced mixing has been invoked to explain such  
113 massive appearances (Piotrowski and Tulaczyk, 1999; Hooyer and Iverson, 2000). Due to this  
114 macroscopically massive nature of many tills, micromorphology is increasingly being used in the  
115 analysis of subglacial sediments (see Menzies and Maltman, 1992; van der Meer, 1993; Menzies *et al.*,  
116 1997; Khatwa and Tulaczyk, 2001; van der Meer *et al.*, 2003; Roberts and Hart, 2005; Hiemstra *et al.*,  
117 2005; Baroni and Fasano, 2006; Larsen *et al.*, 2006, 2007; Phillips *et al.*, 2011; Neudorf *et al.*,  
118 2013; Spagnolo *et al.*, 2016). In particular, this approach has been used to unravel the complex  
119 deformation histories recorded by glacial sequences (van der Meer, 1993; Phillips and Auton,  
120 2000; van der Wateren *et al.*, 2000; Menzies, 2000; Phillips *et al.*, 2007; Lee and Phillips, 2008; Denis  
121 *et al.*, 2010; Vaughan-Hirsch *et al.*, 2013; Narloch *et al.*, 2012, 2013) as well as to investigate the role  
122 played by pressurised meltwater during deformation events (Hiemstra and van der Meer, 1997;  
123 Phillips and Merritt, 2008; van der Meer *et al.*, 2009; Denis *et al.*, 2010; Phillips *et al.*, 2013a, b;  
124 Narloch *et al.*, 2012, 2013). The development of a quantitative microstructural mapping technique  
125 (Phillips *et al.*, 2011) has the potential to increase our understanding of subglacial processes by  
126 highlighting the relationships between the various microstructures developed within tills, thereby  
127 allowing a detailed relative chronology of events to be established.

128 This paper presents the results of a number of detailed micromorphological and  
129 microstructural studies carried out on subglacial tills and identifies significant structures indicative of

130 liquefaction events during till production. It is argued that this evidence is entirely consistent with  
131 the stick-slip processes that appear to be operating during soft-bed sliding/ploughing (Brown *et al.*,  
132 1987; Tulaczyk *et al.*, 2001; Clark *et al.*, 2003; Podolskiy and Walter, 2016) and, moreover, could  
133 record the impacts of glacier seismic activity that are now widely reported from modern glacier and  
134 ice sheet systems.

135

## 136 **2. Microscale evidence of subglacial deformation processes and** 137 **liquefaction (Scotland and Switzerland case studies)**

138 Intensive micromorphological analyses of the subglacial traction tills from two case studies are here  
139 reported as examples of subglacial process-form products from one lowland (Nairn, Scotland) and  
140 one upland (Galmis, Switzerland) setting. Previous investigations at both locations have  
141 demonstrated the subglacial genesis of the tills and hence we concentrate here on the microscale  
142 evidence for the interactions between bed shearing and porewater fluctuations.

143 Figure 2 shows the compiled results of a micromorphological study of subglacial traction tills  
144 exposed at a number of sites in the Nairn area of NE Scotland (Fig. 3). All the sites occur to the north  
145 of the Cairngorm plateau and comprise a sequence of brown sandy and silty tills (up to 10 m thick)  
146 interstratified with sands and gravels (outwash) containing a high proportion of locally-derived  
147 sedimentary, igneous and metamorphic rock fragments (Auton *et al.*, 1990; Phillips *et al.*, 2011;  
148 Merritt *et al.*, 2017). The tills were deposited by ice flowing northwards from the Central Highlands  
149 towards the coast (Fig. 3) during the main phase of the Late Devensian (Late Weichselian; Marine  
150 Isotope Stage 2) glaciation of NE Scotland (see Auton *et al.*, 1990; Phillips *et al.*, 2011; Phillips *et al.*,  
151 2013; Merritt *et al.*, 2017). Typical of subglacial traction tills (*sensu* Evans *et al.*, 2006), the  
152 diamictons used in this study have developed in a zone of enhanced glacier bed deformation,  
153 termed the 'mobile' or 'active' layer by Evans *et al.* (2006). From hereon we use the term 'transient  
154 mobile zone' (TMZ) in order to emphasize the spatial and temporal variations in subglacial  
155 deforming bed processes proposed by a number of researchers (cf. Piotrowski and Kraus, 1997;  
156 Boyce and Eyles, 2000; van der Meer *et al.*, 2003; Larsen *et al.*, 2004, 2007; Piotrowski *et al.*, 2004,  
157 2006; Evans *et al.*, 2006; Meriano and Eyles, 2009).

158 In thin section, the Scottish tills are composed of coarse-grained, poorly-sorted, matrix-  
159 supported, massive to weakly-stratified, sandy diamictons containing angular to subangular granule  
160 to pebble-sized rock fragments. Sand grains are mainly composed of monocrystalline quartz and  
161 subordinate amounts of feldspar which exhibit preferred shape alignments (see rose diagrams on  
162 Figs. 4 to 11). Detailed microstructural mapping of the thin sections has revealed a complex, but

163 systematic, array of deformation fabrics developed within the diamictons (Figs. 2, 4 to 11). These are  
164 interpreted as having formed by the passive rotation of sand grains into the planes of the foliations,  
165 defining a number of clast microfabrics (Phillips *et al.*, 2011). Although from different localities  
166 across NE Scotland, the tills show a remarkably similar range of microstructures (see Figs. 4 to 11)  
167 indicating that there are a number of common processes occurring during their formation, and that  
168 subglacial deformation was dominated by foliation development.

169 Three successive generations of microfabric of varying intensity have been identified,  
170 reflecting the heterogeneous nature of subglacial deformation (cf. Phillips *et al.*, 2011). The spacing  
171 of these microfabrics is controlled by the grain size of the diamicton matrix and spatial distribution  
172 of larger clasts (Figs. 2, 4 and 5), which acted as rigid bodies during foliation development. The  
173 earliest fabric (S1) dips down-ice (purple on Figs. 2 and 4 to 11) and is either crenulated (folded) (Fig.  
174 6) or cross-cut (Fig. 7) by a more pervasive, up-ice dipping second (S2) foliation (green on Figs. 2 and  
175 4 to 11). Both S1 and S2 are cross-cut by a heterogeneous third (S3) fabric (dark green on Figs. 2 and  
176 4 to 11) which is thought to record the progressive partitioning of deformation into narrow  
177 subhorizontal and down-ice dipping shear zones formed during the later stages of deformation. The  
178 geometry of the microfabrics is consistent with the formation of a conjugate set of Riedel shears  
179 (Passchier and Trouw, 1996) and subhorizontal shear foliation (Fig. 2) in response to shearing  
180 imposed by the overriding ice (cf. Phillips *et al.*, 2011; Spagnolo *et al.*, 2016). The orientation,  
181 geometry and kinematic indicators (e.g. asymmetry of S-shaped microfabrics) recorded by the  
182 fabrics (Figs. 2 and 4 to 11) are consistent throughout the tills and record a north-directed sense of  
183 shear, coincident with the regional ice flow pattern across this part of NE Scotland (see Fig. 3).

184 Microstructures formed in response to the rotation of granule and pebble-sized clasts  
185 (arcuate grain alignments, small-scale crenulations) during deformation are preserved within the  
186 matrix immediately adjacent to these larger clasts, as well as within the microlithons separating the  
187 S1 and S2 microfabrics (Figs. 2, 4 and 5). Rotational structures, including turbate structures (van der  
188 Meer, 1993, 1997; Menzies, 2000; Hiemstra and Rijdsdijk, 2003), are truncated by the clast  
189 microfabrics, indicating that they formed prior to, or during the early stages of foliation  
190 development. Comparable rotational structures have also been identified in mass flow deposits  
191 where they have been interpreted as forming in response to turbulent flow during emplacement  
192 (Lachniet *et al.*, 2001; Phillips, 2006). Turbate structures form where clasts rotate through angles of  
193 up to, and greater than 360°, entraining the adjacent finer-grained matrix (van der Meer, 1993;  
194 Menzies, 2000). This requires either very high shear strains or the lowering of the shear strength of

195 the till due to liquefaction, allowing the rotation of the clasts at much lower strains (Evans *et al.*,  
196 2006).

197 In samples N7126 and N7128 the style and relative intensity of the fabrics is highly variable  
198 (Figs. 2, 6 and 7). In the more matrix-rich areas, although both S2 and S3 are present, the earlier S1  
199 fabric is relatively weak or absent. In sample N7128 (Fig. 7), S1 is most pronounced within the upper  
200 part of the thin section where it is deformed by an open fold and its associated up-ice dipping axial  
201 planar S2 fabric. In the slightly sandier core of this fold, however, S1 is apparently absent. The finer  
202 grained areas are interpreted as veins and patches of liquefied sediment injected into the till during  
203 deformation, between the imposition of S1 and the later S2 and S3 foliations (Phillips *et al.*, 2011).  
204 Variation in the overburden pressure exerted in the TMZ by the overlying ice may have resulted in  
205 the collapse of the till and “squeezing out” of the liquefied sediment which is then injected into  
206 lower strain areas to form cross-cutting veinlets and/or patches of massive till. Deformation of the  
207 relatively weak till within the TMZ appears to have been associated with expansion (volume  
208 increase) and resulted in localised folding of S1. Subsequent shearing within the TMZ would then  
209 lead to renewed foliation development and deformation of the recently injected veins (see Fig. 2).  
210 Engineering studies have shown that the inherent density contrasts between an injected fluid and  
211 the host material will result in the escaping water-sediment mix being driven upwards towards the  
212 surface (Abou-Sayed *et al.*, 1984). In the subglacial environment this means that the liquefied till will  
213 be preferentially injected upwards towards the top of the TMZ and the ice-bed interface (Fig. 2; also  
214 see Fig. 14), as long as water pressures at the ice-bed interface are not elevated due to strong  
215 surface melting.

216 Although the majority of the tills from the Nairn area, like many other subglacial traction  
217 tills, appear massive in the field, a subhorizontal stratification is locally apparent in thin section  
218 where it is defined by laterally impersistent, wispy-looking lenses composed of slightly darker, more  
219 matrix-rich diamicton (N12280, N12281; Figs. 2, 8 and 9). The margins of these lenses are highly  
220 irregular to flame-like in nature and are gradational over several millimetres (Fig. 8), resulting in a  
221 distinctive “diffuse” to “mottled” appearance to the diamicton. Samples N12280 and N12281 were  
222 collected from the same till unit (N12281 collected 50 cm above N12280) and demonstrate that the  
223 stratification is variably developed/preserved. The shear related microfabrics clearly cross-cut the  
224 layering (Figs. 2, 8 and 9) indicating that their imposition post-dated this stratification.

225 The simplest interpretation of the highly complex stratification present within these two thin  
226 sections is that they record the progressive overprinting of the primary layering (e.g. bedding) within  
227 this till (Fig 2). Rather than being a product of deformation, the complexity of this stratification is

228 indicative of the disruption typically associated with liquefaction (Phillips *et al.*, 2007; Phillips *et al.*,  
229 2013b). Localised saturation of the till may have occurred in response to either the migration of  
230 porewater through the sediment and/or the introduction of pressurised meltwater into the bed  
231 from the overlying ice. The migration and/or introduction of pressurised meltwater into the bed is  
232 supported by a number of studies on modern glaciers (Hooke, 1984; Engelhardt and Kamb, 1997;  
233 Hooke *et al.*, 1997; Bartholomaeus *et al.*, 2008; Schoof *et al.*, 2014; Andrews *et al.*, 2014) which have  
234 shown that subglacial water pressures are extremely variable over space and time. Loading  
235 (compression) or shear (simple shear) of these water-saturated sediments will lead to an increase in  
236 intergranular PWP, lowering of the shear strength of the till, and ultimately a loss in the integrity of  
237 the sediment. The increase in intergranular PWP forced the constituent grains apart, leading to a  
238 reduction in intergranular contacts, lowering the density of the packing of the constituent sand  
239 grains, and increasing the volume of the sediment, which ultimately led to localised liquefaction. The  
240 increase in the connectivity of the intergranular pore spaces during this process would result in an  
241 increase in permeability, enabling the porewater to move/disperse through the sediment and drain  
242 away from the liquefied till, leading to “collapse” and solidification the sediment. Repeated phases  
243 of liquefaction, potentially coupled with the mobilisation/displacement of the liquefied sediment,  
244 would result in a loss of integrity of the original compositional layering, leading to mixing and  
245 eventual homogenisation of the till. The shear related microfabrics clearly cross-cut the layering  
246 (Figs. 2, 8 and 9), indicating that their imposition post-dated liquefaction and the disruption of this  
247 stratification.

248 Two samples of till from the Nairn area (N12278, Fig. 10 and N1279, Fig. 11) are cut by  
249 irregular, down-ice dipping veins of silty sand (Fig. 2). The sand is lithologically similar (contains the  
250 same range of clast types) to the matrix of the host diamicton indicating that they were derived from  
251 the same source. Rather than being sharp planar features, the vein margins are highly complex to  
252 gradational, suggesting that they were introduced into the till whilst it was still relatively weak  
253 (water-rich/saturated). The veins are coplanar to S3 (Fig. 11) and the down-ice dipping Riedel shears  
254 (R-type shears; see inset Fig. 2). Extension occurring across these narrow ductile shear zones aided  
255 hydrofracture propagation and the simultaneous injection of the liquefied sand (c.f. cut-and-fill of  
256 hydrofractures proposed by Larsen and Mangerud, 1992), indicating that liquefaction was also  
257 occurring during the imposition of S3 and the final stages of subglacial deformation. Shear induced  
258 by the injection of the pressurised liquefied sediment may have resulted in the observed complex,  
259 soft-sediment deformation along the walls of the vein.



260 Further evidence for the liquefaction, mobilisation and injection of till within the subglacial  
261 environment is provided by a detailed microstructural and sedimentological study of thinly stratified  
262 tills exposed at Galmis, Switzerland (van der Meer, 1979; 1982; Phillips *et al.*, 2013b). Phillips *et al.*  
263 (2013b) interpreted the micromorphology of the Galmis till as recording a complex history of  
264 deformation, liquefaction and sedimentation during repeated phases of basal sliding as the ice  
265 overrode a soft-sediment bed (Fig. 12). The till comprises alternating layers of massive to weakly  
266 foliated diamicton and variably deformed laminated silt and clay. It is argued that elevated  
267 porewater contents encountered immediately prior to, and during, basal sliding promoted localised  
268 liquefaction of the underlying diamicton, with the decoupling of the glacier from its bed enabling the  
269 injection of this liquefied sediment along the ice-bed interface and/or into the laminated sediments.  
270 Phillips *et al.* (2013b) concluded that the laminated sediments record the settling out of fines (clay,  
271 silt) from meltwater trapped along the ice-bed interface after an individual phase of basal sliding has  
272 ceased. Injection of the pressurised till into the locally water-saturated silts and clays resulted in  
273 partial liquefaction and incomplete mixing ('vinaigrette-like' texture) of these fine-grained sediments  
274 with the diamicton (Fig. 12). Recoupling of the ice with its bed led to bed deformation and localised  
275 folding and thrusting of the laminated sediments, as well as incipient microfabric development  
276 within the diamicton layers. Initial estimates of the strains imposed on these stratified tills indicates  
277 that the amount of shear transmitted into the soft-sediment bed during basal sliding are relatively  
278 low, allowing the preservation of the fine-scale stratification within the Galmis tills.

### 279 **3. Soft bed deformation/sliding and the potential for till liquefaction**

280 The concept of subglacial till-forming mosaics, in which the processes of deformation and soft bed  
281 sliding/ploughing operate as a spatial and temporal continuum, has been widely promoted (e.g.  
282 Piotrowski and Kraus, 1997; Boyce and Eyles, 2000; van der Meer *et al.*, 2003; Larsen *et al.*, 2004,  
283 2007; Piotrowski *et al.*, 2004, 2006; Evans *et al.*, 2006; Lee and Phillips, 2008; Meriano and Eyles,  
284 2009) and is encapsulated herein by our transient mobile zone (TMZ). This recognition of the spatial  
285 and temporal variations in subglacial deforming bed processes also acknowledges that changing  
286 water pressures, even at diurnal temporal scales, may result in cycles of decoupling and coupling of  
287 the glacier from its bed (e.g. Boulton and Dobbie, 1998; Boulton *et al.*, 2001) and the operation of  
288 stick-slip ice motion (e.g. Fischer and Clarke, 1997). The spatial variability in sliding versus  
289 deformation also gives rise to the development of 'sticky spots' on the glacier bed (Alley, 1993;  
290 Stokes *et al.*, 2007).

291 The stick-slip cycle of sliding and deformation proposed by Boulton *et al.* (2001) accounts for  
292 the soft-bed sliding (ploughing) process (Brown *et al.*, 1987; Tulaczyk *et al.*, 2001; Clark *et al.*, 2003),  
293 when shear stress and water pressure build to the point where till dilates, ice-bed friction is reduced

294 and ice-till decoupling takes place. When water pressures in the dilatant till fall, deformation and ice-  
295 bed coupling take over and there is a reduction in the amount of sliding. A continued fall in water  
296 pressures then consolidates the dilatant till, enhancing the transmission of strain through this  
297 sediment and deeper into the bed, thereby causing the shear zone to migrate downwards through  
298 the till. Deformation may stop once the water pressure falls below the critical level for failure,  
299 forming a sticky spot. The diurnal changes in water pressure are thought to lead to repeat cycles of  
300 dilation and collapse so that the classic curvilinear till displacement curve, which represents  
301 cumulative strain, becomes more pronounced with time.

302         Given the important role of variable porewater pressure cycles in driving the stick-slip  
303 motion observed at modern glacier beds, the evidence for potential multiple liquefaction events in  
304 the subglacial traction tills reported in the Scotland and Switzerland case studies is highly-significant  
305 with respect to the exact modes of operation of the subglacial deforming layer and till production.  
306 The micromorphological evidence for repeated phases of liquefaction followed by solid-state shear  
307 deformation, indicates that the operation of the TMZ involves slip events driven by not only the  
308 already widely acknowledged processes of pressurised meltwater and porewater but also the  
309 episodic liquefaction of water-saturated till.

310

#### 311 **4. Potential controls on liquefaction and soft-bed deformation/sliding**

312 As identified above, rather than being a continuous uninterrupted cyclical process, the generally  
313 accepted view of the forward motion of a glacier is in terms of a series of 'stick-slip' events (Fischer  
314 and Clarke, 1997; Fischer *et al.*, 1999; Wiens *et al.*, 2008). One major controlling factor responsible  
315 for the glacier 'sticking' to its bed is the downward force imposed by the overlying ice. This  
316 overburden pressure results in an increase in the packing of the sediments (consolidation),  
317 increasing their shear strength, which in turn restricts forward motion of the glacier as a result of  
318 soft-bed sliding. The individual slip events will likely be relatively short-lived, but over time allow the  
319 glacier to move forward without becoming unstable. Importantly the slip events occur repeatedly  
320 throughout both the summer and winter months requiring that any potential control on soft-bed  
321 sliding needs to operate throughout the year. Three potential controls on soft-bed sliding appear to  
322 be operating in glacial systems, one of which we hypothesize to be the now widely recognized  
323 phenomenon of glacier-related seismicity.

##### 324 **4.1. Control 1: pressurised meltwater**

325 The most commonly cited control on enhanced bed deformation is the introduction of pressurised  
326 meltwater into the subglacial environment (e.g. Bartholomaus *et al.*, 2008). This hypothesis is

327 supported by a number of studies of modern glacier systems which have clearly demonstrated that  
328 higher meltwater production during the spring and summer months coincide with an increase in ice  
329 surface velocity (Iken *et al.*, 1983; Iken and Bindschadler, 1986; Nienow *et al.*, 2005). This spring-  
330 summer 'speed-up' is subsequently followed by a decrease in velocity during the autumn and winter  
331 as meltwater production declines and the subglacial hydrogeological system in many glaciers begins  
332 to shut down. It is possible that the decrease in surface velocity towards the end of the spring-  
333 summer 'speed-up' is also governed by the increased maturation of the subglacial drainage system  
334 (e.g. Werder *et al.*, 2013) and the formation of channels which help drain the bed. The porosity and  
335 permeability of subglacial sediments will directly affect the rate at which meltwater can penetrate  
336 into and migrate through the bed. Several micromorphology studies (Kilfeather and van der Meer,  
337 2006; Tarplee *et al.*, 2010) have demonstrated that porosity in tills plays a much more important role  
338 in bed deformation than previously thought, confirming the relationship between porosity and bed  
339 deformation proposed by Tulaczyk *et al.*, (2000b) in his undrained plastic bed model.

340           Although clay-rich sediments possess a high intergranular porosity, they typically act as an  
341 aquitard forming an impermeable barrier at the base of the glacier, leading to the concentration of  
342 meltwater and therefore displacement at, or close to, the ice-bed interface (Boulton, 1996a, b;  
343 Engelhardt and Kamb, 1998; Tulaczyk, 1999). For example, at one location at the base of Ice Stream  
344 B (Whillans Ice Stream), Engelhardt and Kamb (1998) demonstrated that glacier flow was controlled  
345 by sliding over a clay-rich till. The clay-rich nature of the till retards water migration allowing the  
346 build-up of high porewater pressures and leading to glacier decoupling and thereby promoting  
347 forward motion due to basal sliding. This periodic decoupling of the glacier from its bed due to  
348 increased basal water pressures prevents the transmission of stress to the substrate (cf. Fischer and  
349 Clarke, 1997; Winberry *et al.*, 2009; Iverson, 2010) effectively switching off bed deformation and/or  
350 soft-bed sliding, and promoting basal sliding. This has been proposed in order to explain the  
351 apparent lack of pervasive subglacial deformation structures within a number of till sequences found  
352 in the geological record (Brown *et al.*, 1987; Clark and Hansel, 1989; Piotrowski and Kraus, 1997;  
353 Piotrowski and Tulaczyk, 1999; Piotrowski *et al.*, 1999, 2001, 2002; Hoffmann and Piotrowski, 2001;  
354 Lee and Phillips, 2008; Phillips *et al.*, 2013b; Lee *et al.*, 2016).

355           In contrast to clay-rich subglacial sediments, highly-permeable sands and gravels provide an  
356 ideal fluid pathway which can promote dewatering of the bed, effectively switching off soft-bed  
357 sliding and basal-slip. This illustrates the potential lithological control on not only the subglacial  
358 hydrological system but also the mechanism for glacier motion across its bed. In a theoretical  
359 overview of the deformation process, Boulton (1996) suggested that clay-rich tills do not couple to

360 the ice base as well as coarse-grained tills and will only deform to a shallow depth. This implies that  
361 the relative importance of sliding versus deformation will vary according to the granulometry of the  
362 glacier bed. Consequently, it is possible that the presence of coarse-grained, permeable sediments  
363 beneath glaciers could represent a major factor governing the formation of “sticky spots” beneath  
364 the overriding ice. However, a study by Salamon (2016) on the subglacial conditions beneath the  
365 Weichselian Scandinavian ice sheet in southern Poland suggests that despite the high permeability  
366 of the coarse-grained sediments within its bed, ice sheet movement was not impeded. In this case  
367 forward motion is believed to have been accomplished by a combination of basal slip and localised  
368 shallow bed deformation due to high basal water pressures resulting from permafrost restricting  
369 subglacial groundwater outflow. Consequently the potential for soft-bed sliding to be initiated is not  
370 only dependent on the permeability of the substratum, but also the connectivity of the aquifer and  
371 the presence of hydraulic pathways which facilitate/promote the dewatering of the bed.

372 One potential way to promote soft-bed sliding would be to increase the volume of  
373 meltwater reaching the bed. However, where the bed is composed of low to moderately permeable  
374 sediments this is more likely to overwhelm the rate at which these sediments can transmit large  
375 volumes of fluid. The direct result would be the development of a stable (channelized) subglacial  
376 drainage system. This highly efficient drainage system would rapidly remove any excess meltwater  
377 from the subglacial environment, leading to the dewatering of the bed. Furthermore several studies  
378 suggest that during periods of low flow, the lowering of the water levels within subglacial drainage  
379 channels leads to the development of a hydrostatic gradient towards these open conduits,  
380 promoting the dewatering of the sediments adjacent to the channel walls (Hubbard *et al.*, 1995;  
381 Boulton *et al.*, 2007a, b; Magnússon *et al.*, 2010).

382 An alternative approach to increasing the volume of meltwater reaching the base of glacier  
383 is to increase the pressure of the subglacial meltwater system. An increase in the effective pressure  
384 (ice overburden minus water pressure) would help drive water from the ice-bed interface into the  
385 bed, overcoming the limiting factor presented by the permeability of the till. However, if the  
386 pressure exceeds the shear strength of the sediment it will result in hydrofracturing of either the bed  
387 and/or overlying ice. Hydrofracture systems are increasingly being recognised in glacial  
388 environments and provide clear evidence for the movement of pressurised meltwater through  
389 subglacial to ice-marginal settings (Dionne and Shilts, 1974; Christiansen *et al.*, 1982; von Brunn and  
390 Talbot, 1986; Burbridge *et al.*, 1988; Dreimanis, 1992; Larsen and Mangerud, 1992; McCabe and  
391 Dardis, 1994; Dreimanis and Rappol, 1997; van der Meer *et al.*, 1999; Rijdsdijk *et al.*, 1999; Le Heron  
392 and Etienne, 2005; Boulton, 2006; Goździk and van Loon, 2007; van der Meer *et al.*, 2009; Phillips

393 and Merritt, 2008; Phillips *et al.*, 2013a; Phillips and Hughes, 2014). They record marked changes in  
394 hydrostatic pressure within the subglacial meltwater system, leading to brittle fracturing and  
395 penecontemporaneous liquefaction and the introduction of a sediment-fill, and can occur in both  
396 soft (sedimentary) and/or hard (bedrock) beds (see van der Meer *et al.*, 2009; Phillips *et al.*, 2013a).  
397 Due to the pressurised nature of the meltwater, the sediment-fill can be introduced from  
398 structurally above (downward injection) or below (upward injection) the developing hydrofracture  
399 system (Dreimanis, 1992; Rijdsdijk *et al.*, 1999; Le Heron and Etienne, 2005; Goździk and van Loon,  
400 2007; van der Meer *et al.*, 2009). Furthermore, it is becoming increasingly apparent that the  
401 introduction of pressurised meltwater can have a profound effect on subglacial to ice-marginal  
402 deformation. It can, for example, aid the development of water-lubricated detachments within the  
403 sediment pile (e.g. Phillips *et al.*, 2002; Benediktsson *et al.*, 2008; Vaughan-Hirsch and Phillips, 2016)  
404 and thereby promote rapid ice movement (e.g. Kjær *et al.*, 2006), and aid the initial detachment and  
405 transport of sediment and/or bedrock rafts (e.g. Moran *et al.*, 1980; Broster and Seaman, 1991;  
406 Phillips and Merritt, 2008; Burke *et al.*, 2009; Vaughan-Hirsh *et al.*, 2013). Several studies have  
407 shown that once formed, hydrofracture systems can be reactivated on multiple occasions (Phillips  
408 and Merritt, 2008; Phillips *et al.*, 2013a; Phillips and Hughes, 2014; Lee *et al.*, 2015) and as a result  
409 have the potential to profoundly influence subglacial drainage. The overpressurised states required  
410 to reactivate an existing hydrofracture system are likely to be much lower than those required  
411 during its initial formation, in effect forming the “pressure release valve” proposed by van der Meer  
412 *et al.* (2009). Consequently, the introduction of pressurised meltwater into the sediments beneath  
413 the ice as a trigger for bed deformation and/or soft-bed sliding will be controlled by their  
414 permeability and shear strength. Both of these factors will have a direct impact on the magnitude of  
415 the fluid pressures which can be achieved before the onset of hydrofracturing, leading to draining of  
416 the bed and depressurisation of the system.

#### 417 **4.2. Control 2: glacitectonism**

418 A second potential control on increasing the intergranular porewater pressure leading to  
419 liquefaction in subglacial sediments is glacitectonism. Compression resulting from folding and/or the  
420 stacking/imbrication of fault-bound slabs of sediment during thrusting can lead to a localised  
421 increase in overburden pressure. This in-turn can lead to an increase in porewater pressure and  
422 potential liquefaction in response to the glacitectonic thickening of the bed. However, the thrust  
423 planes or ductile shear zones responsible for this imbrication have the potential to act as fluid  
424 pathways, helping to transmit water through the deforming sediment pile (Benediktsson *et al.*, 2008;  
425 Lee and Phillips, 2008; Phillips *et al.*, 2008; Vaughan-Hirsch and Phillips, 2016). Migration of  
426 meltwater along these potentially laterally extensive glacitectonic structures is driven by the

427 hydropotential gradient, resulting from the increased overburden pressure and/or compression  
428 deeper within the deforming sequence. This could lead to the dewatering of the sediment and  
429 transition from initial ductile shearing to subsequent brittle deformation.

430 Importantly, thrusting and stacking of detached slabs of till is only likely to occur at the  
431 glacier margin where the ice is thinnest (Evans and Hiemstra, 2005; Hiemstra *et al.*, 2007; Lee *et al.*,  
432 2016; Vaughan-Hirsch and Phillips, 2016). Further up-ice, large-scale tectonic thickening of the bed is  
433 less likely as not only is this an area of low driving stress but also the process requires the glacier to  
434 be lifted vertically to overcome the relatively high overburden pressures and to provide the required  
435 accommodation space for the stacking (imbrication) of the detached thrust slices. Consequently, the  
436 thickening of the bed in response to large-scale glaciectonic thrusting is less likely to be a  
437 contributing factor to triggering liquefaction and soft-bed sliding.

#### 438 **4.3. Control 3: glacier related seismicity**

439 A third and potentially more important control on liquefaction, and thereby soft-bed sliding, which  
440 has yet to be considered by the glaciological community is the seismicity caused by icequakes or  
441 glacier quakes. Recent studies in modern glacial environments (e.g. Ekstrom *et al.*, 2003; Ekstrom *et*  
442 *al.*, 2006; Tsai and Ekstrom, 2007; Wiens *et al.*, 2008; Peng *et al.*, 2014; Lipovsky and Dunham, 2016;  
443 Podolskiy *et al.*, 2016) have demonstrated that modern glaciers are seismically active with icequakes  
444 occurring in response to movement on faults within the glacier or underlying bed, crevasse/fracture  
445 propagation, iceberg calving, seracs toppling in ice-falls, opening and closing of englacial drainage  
446 conduits and/or slip events at the ice base. These processes are an integral part of glacier flow and  
447 as such can occur along the entire length of the glacier and also throughout the year. Seismic events  
448 related to these processes are therefore continually releasing energy into the surrounding ice and  
449 underlying bed. Wiens *et al.*, (2008) have shown that these events can release over a prolonged  
450 period of time (e.g. up to 30 minutes) the same amount of energy as a moment magnitude 7  
451 earthquake. However, the seismic amplitudes are modest ( $M_s$  3.6–4.2) due to the long source  
452 duration of these events (Wiens *et al.*, 2008). The energy released from an ice-quake can also travel  
453 in all directions, and therefore migrate both up- and down-ice from its hypocentre (focus).  
454 Consequently the seismic effects of, for example, a large iceberg calving event at the glacier margin  
455 has the potential to have an impact several kilometres up-ice. Seismic signals can also be generated  
456 by slip initiation at the glacier bed (Wiens *et al.*, 2008; Walter *et al.*, 2011; Lipovsky and Dunham,  
457 2016).

458 The liquefaction of unconsolidated sediments as a result of the seismicity caused by  
459 earthquakes is well-known and represents a major geological hazard (Holzer *et al.*, 1989; Youd,

2003; Miwa *et al.*, 2006). Evidence of palaeoseismic induced liquefaction (seismites) has also been reported from the geological record (Obermeier, 1998; Menzies and Taylor, 2003; Green *et al.*, 2005; Obermeier *et al.*, 2005). Seismically induced liquefaction depends upon several factors, including earthquake moment magnitude (i.e. total energy released), shaking duration, peak ground motion, depth to groundwater table, susceptibility of sediments to liquefaction, and water saturation (Youd, 1978; Youd, 2003 and references therein). Liquefaction is typically observed associated with earthquakes of magnitude 5 or above. However, it can also occur in water-saturated sediments at much lower magnitudes, for example during the 1865 Barrow (UK) earthquake, a very shallow focus low moment magnitude (Mw 3) quake generated localised liquefaction and formation of sand volcanoes in the saturated tidal sands of Morecambe Bay (R. Musson pers. comm.). Importantly, this instability may remain after the initial event which triggered liquefaction has passed/dissipated with subsequent, smaller aftershocks potentially leading to further/renewed liquefaction of the superficial deposits even at lower magnitudes.

A direct link between glacier seismicity and the localised liquefaction of the soft, unconsolidated sediments within the bed has yet to be demonstrated in contemporary glacial environments. However, the magnitude and duration of icequakes reported in the literature (e.g. Ekstrom *et al.*, 2003) do compare favourably with earthquakes which are known to have induced liquefaction. Furthermore, the sediments forming the bed of a glacier meet the criteria required for seismically induced liquefaction, in particular: they are typically composed of unconsolidated, granular sediments which have the potential to undergo liquefaction; they can possess a high water content and are at, or near saturation; and the water table within subglacial environments is high or even perched, being constrained within the soft bed by the underlying less permeable bedrock and the overlying ice. Consequently, it is feasible that the energy released during the larger icequakes has the potential to result in liquefaction and sliding within the underlying soft-sediment bed. It is important to stress that seismically induced liquefaction of the bed would be localised in nature as a direct consequence of the spatial and temporal variation in sediment grain size, composition, porosity, permeability and water content. Furthermore, the consolidation of subglacial sediments is very variable. Subglacial sediments are typically consolidated, with lower consolidation ratios in actively deforming "slippery spots" within the bed (Clarke, 1987; Boulton and Dobbie, 1993; Tulaczyk *et al.*, 2000; Leeman *et al.*, 2016). Basal freeze-on can also further elevate consolidation ratios by removing water from the till (Christoffersen and Tulaczyk, 2003a, b) further adding to the localised nature of the potential for soft-bed sliding. The confining pressure exerted by the ice can also prevent dilation and/or liquefaction of the sediments within the bed, effectively applying a 'breaking mechanism' to glacier motion. Consequently, liquefaction and soft-bed sliding is likely to only occur

494 in response to icequakes over a certain magnitude, once again promoting a “stick-slip” style of  
495 glacier motion.

496

### 497 **5. Seismically induced soft-bed sliding in subglacial sediments?**

498 During an icequake the pulse of energy released passes through the ice and into the underlying  
499 water saturated sediments and has the potential to provide a ‘trigger’ for dilation and transient  
500 liquefaction, and soft-bed sliding (Figs. 13 and 14). On a granular scale this relatively short duration  
501 pulse of energy causes the individual clasts within the sediment to vibrate, modifying the packing of  
502 the grains and leading to the pressurisation of the intergranular porewater (Fig. 13). Seismicity will  
503 cause liquefaction if it results in the effective stress becoming zero or negative, so that porewater  
504 completely relieves the granular skeleton of its compressive stresses (Zhang and Campbell, 1992; Xu  
505 and Yu, 1997). The effect of this sudden increase in PWP is to reduce the number of grain to grain  
506 contacts, allowing the individual clasts to move (slide or rotate) past one another. The net effect is to  
507 reduce sediment shear strength, leading to dilation and thereby allowing soft-bed sliding to occur.  
508 This seismically induced ‘vibrating’ effect would propagate away from the focus of the ice-quake as a  
509 pulse or series of pulses (i.e. shear waves or ‘S-waves’). Thus, if the porewater pressure anomaly is  
510 sufficiently large, areas of the subglacial bed would initially undergo localised soft-bed sliding,  
511 followed by stabilisation outwards away from the icequake focus as a result of dewatering. Youd  
512 (2003) describes how the oscillating ground motion caused during an earthquake results in repeated  
513 reversals in the direction of shear releasing the effects of dilative arrest and resulting in repeated  
514 episodes of liquefaction and flow deformation as well as the arrest process. If applicable to the  
515 subglacial environment, this cyclic liquefaction (Youd, 2003) would potentially aid in maintaining  
516 soft-bed sliding during the duration of the icequake (potentially up to several minutes). However,  
517 dilative arrest (Youd, 2003) will result in the collapse and increased packing of the sediment  
518 (compaction) in effect switching off soft-bed sliding.

519 Due to the highly-heterogeneous nature of the sediments beneath glaciers, liquefaction  
520 leading to soft-bed sliding will be localised in nature, probably occurring within discrete, laterally  
521 discontinuous patches or narrow zones in the order of only a few centimetres or even millimetres  
522 thick. As liquefaction operates only in materials already at very low values of effective stress, it is  
523 most likely to take place only in glacier sub-marginal settings and hence its process-form signatures  
524 are indicative of glacier sub-marginal tills. The accompanying dilation will lead to a temporary  
525 increase in the connectivity between intergranular pore spaces within the sediment and therefore  
526 the permeability of the bed, enabling the transmission of porewater through the till (Fig. 13). This in



527 turn could facilitate the migration of flow deformation (soft-bed sliding) through the TMZ (Fig. 14).  
528 The amount of forward movement accommodated/achieved during an individual icequake induced  
529 'slip event' is likely to be relatively small. However, this displacement may, in itself, trigger further  
530 smaller seismic events within the bed or at the ice-bed interface (see Fig. 14), and thereby help to  
531 maintain soft-bed sliding after the initial seismic trigger has passed. As soon as the energy released  
532 by the icequake has been dissipated (probably taking only a few minutes), the fall in intergranular  
533 PWP and increase in sediment shear strength will result in the cessation of flow deformation, and  
534 hence forward movement will stop.

535         Spatial variation in, for example, ice thickness will lead to the variation in the magnitude of  
536 the overburden pressure being exerted on the underlying bed. The resultant hydrostatic pressure  
537 gradients will facilitate or even promote the displacement (mobilisation) of the liquefied sediment  
538 and its injection into relatively lower pressure areas within the bed (Fig. 14). As a result, flow  
539 deformation and soft-bed sliding would migrate through the bed (labelled 1 to 4 on Fig. 14). The  
540 positive buoyancy of liquefied sediments means that migration will occur both laterally and  
541 vertically, with the fluidised sediment preferentially migrating upwards through the bed where it will  
542 be confined at, or close to the ice-bed interface (Fig. 14; also see Fig. 2). This may lead to the  
543 effective dewatering of the structurally lower parts of the bed and an increase in the height of the  
544 water table toward the base of the glacier. Over time the net result will be for forward motion of the  
545 glacier due to soft-bed sliding, preferentially concentrated within the upper part of the bed (Fig. 14).  
546 The presence of a less permeable or more cohesive (i.e. clay-rich) layer or even an overridden  
547 (buried) permafrost layer within the bed, however, may impair the upward migration of the  
548 liquefied sediment, trapping it at a lower structural level and leading to forward motion being  
549 accommodated at this deeper level (Fig. 14).

## 550 **6. Feedback mechanism leading to glacier motion**

551 In reality glacier movement due to soft-bed sliding will be controlled by subglacial PWP, glacier  
552 seismic activity and deformation (Fig. 15a). The interplay between these factors is thought to lead to  
553 a feedback mechanism which helps maintain glacier motion (Fig. 15b). The cycle begins with an  
554 icequake associated with ice deformation, potentially leading to localised liquefaction of the  
555 underlying sediments, triggering soft-bed sliding within the bed. This forward movement leads to  
556 further extensional deformation (crevassing) within the ice and continued seismic activity, which in  
557 turn triggers further sliding and the cycle starts again (Fig. 15b). Importantly, ice deformation and  
558 the associated seismicity is a relatively continuous process that occurs throughout the year, enabling  
559 forward motion of the glacier to be maintained. In addition, seasonal increases in meltwater  
560 productivity can potentially facilitate movement by increasing the saturation of the bed, leading to

561 either increasing amounts of soft-bed sliding and/or basal sliding. However, dewatering of the bed,  
562 either due to the development of a stable subglacial drainage system and/or hydrofracturing, will  
563 disrupt this feedback loop and “switch off” forward movement.

564 Fast flowing glaciers and ice streams are characteristically highly crevassed (see Benn and  
565 Evans, 2010 and references therein) and are therefore likely to be more seismically active, leading to  
566 an increase in the rate at which they pass through the feedback loop (Fig. 15b). Large-scale (decadal)  
567 fluctuations in subglacial hydrogeology (Clarke, 2005) may promote a periodicity within this  
568 feedback mechanism potentially leading to surge-type behaviour. Alternatively, if conditions  
569 conducive to soft-bed sliding and basal sliding are maintained then the repeated “cycling” of the  
570 feedback loop has the potential to result in fast ice flow and ice streaming. Tidal modulation of  
571 subglacial stresses and stick-slip motion has also been proposed for tidewater or floating glacier  
572 snouts by Bindschadler *et al.* (2003a, b) and Walker *et al.* (2013). Such external controls on stick-slip  
573 motion, and indeed on icequake activity, are likely to play a more dominant role than those  
574 operating under thicker ice, where basal driving stress predominantly exceeds sediment strength so  
575 that deformation is a continuous uninterrupted process (e.g. Schofield and Wroth, 1968; Iverson *et*  
576 *al.*, 1998; Tulaczyk *et al.*, 2000a; Damsgaard *et al.*, 2013, 2015). In contrast, the sticky spots  
577 identified on ice stream beds represent the very few places where till strength is sufficiently high  
578 enough to exceed driving stress (e.g. Alley, 1993; Joughin *et al.*, 2004) and hence arrest deformation.  
579 The higher effective pressures beneath such areas of thicker ice make it unlikely that liquefaction  
580 could operate in the subglacial deforming till mosaic. But the existence of materials already at low  
581 values of effective stress for at least part of the time in glacier sub-marginal settings make this a  
582 prime location for the operation of liquefaction in response to glacier seismicity (cf. Zhang and  
583 Campbell, 1992; Xu and Yu, 1997) and hence its process-form signatures are likely indicative of  
584 glacier sub-marginal tills.

## 585 **7. Conclusions**

586 This paper provides a review of the theoretical models of glacier forward motion involving  
587 deformation of the soft-sediments within the underlying bed. The results of several detailed  
588 microstructural studies clearly demonstrate that this deformation results in the development of a  
589 range of ductile and brittle structures as these potentially water-saturated sediments accommodate  
590 the shearing being applied by the overriding glacier. The geometry of the clast microfabrics  
591 developed within matrix of these polydeformed subglacial traction tills are consistent with the  
592 development of Riedel shears within a subhorizontal or very gently dipping shear zone located  
593 within the bed of the overriding ice. Furthermore, these studies also reveal that tills may also  
594 contain evidence of having undergone repeated phases of liquefaction prior to a final phase of solid-

595 state shear deformation as this subglacial shear zone begins to lock up. Liquefaction within the bed  
596 is short-lived and results in the lowering of the shear strength of the till. This leads to the formation  
597 of spatially and temporally restricted “transient mobile zones” within subglacial traction tills,  
598 effectively resulting in decoupling within the glacier bed, likely concentrated in glacier sub-marginal  
599 zones where materials are at low values of effective stress. This process is referred to as “soft-bed  
600 sliding” and forms part of a continuum with bed deformation and basal sliding that facilitate glacier  
601 movement. The spatial and temporal variations in the physical properties of subglacial traction tills  
602 means that the dominant mechanism responsible for their forward motion will also vary across the  
603 bed (spatial) and will change over time (temporal). Rather than being a continuous uninterrupted  
604 process, the generally accepted view is that glacier motion occurs in a series of ‘stick-slip’ events.  
605 Consequently it is essential for there to be a specific control built into the glacier system which  
606 enables forward motion to take place. The individual slip events resulting from liquefaction and soft-  
607 bed sliding are relatively short-lived, but over time allow the glacier to move forward without  
608 becoming unstable. Three potential controls are proposed: (i) the introduction of pressurised  
609 meltwater into the bed; (ii) the pressurisation of pore water already present within the till as a result  
610 of subglacial deformation; and (iii) the periodic liquefaction of water-saturated subglacial traction  
611 tills in response to glacier seismic activity (icequakes). In reality soft-bed sliding is likely to result as a  
612 consequence of the interplay between deformation, meltwater content/pressure and glacier seismic  
613 activity, and leading to a cyclic feedback mechanism that promotes the continued forward motion of  
614 the overriding ice mass.

## 615 **Acknowledgements**

616 The authors would like to thank various colleagues for numerous discussions on the nature of glacier  
617 bed deformation over the years, in particular Clive Auton, Jon Merritt, John Hiemstra, Simon Carr,  
618 Andrew Finlayson, Jez Everest, Ívar Örn Benediktsson, Ewelina Lipka, Kurt Kjaer, John Menzies,  
619 Johannes Brumme, Włodzimierz Narloch and Mark Tarplee. Keith Westhead, Alan Stephenson and  
620 Dee Flight are thanked for their comments on an earlier draft of this paper. John Fletcher (BGS,  
621 Keyworth, UK) is thanked for his expertise in making the thin sections. ERP and JRL publish with the  
622 permission of the Executive Director of the British Geological Survey, Natural Environmental  
623 Research Council. The constructive critique of Anders Damsgaard is greatly appreciated and made a  
624 significant contribution to our refinement of this paper.

625

626 **References**

- 627 Abou-Sayed, A.S., Sinha, K.P., Clifton, R.J., 1984. Evaluation of the influence of in-situ reservoir  
628 conditions in the geometry of hydraulic fractures using a 3-D simulator: Part 1 – Technical approach.  
629 Society of Petroleum Engineers, Conference Paper 12877. Unconventional Gas Recovery Symposium,  
630 Pittsburgh, PA, 433–438.
- 631 Alley, R.B., 1989a. Water pressure coupling of sliding and bed deformation: 1. Water system. Journal  
632 of Glaciology 35, 108–118.
- 633 Alley, R.B., 1989b. Water pressure coupling of sliding and bed deformation: II. Velocity-depth  
634 profiles. Journal of Glaciology 35,119–129.
- 635 Alley, R.B., 1993. In search of ice stream sticky spots. Journal of Glaciology 39, 447–454.
- 636 Alley, R.B., Blankenship, D.D., Bentley, C.R., Rooney, S.T., 1986. Deformation of till beneath ice  
637 stream B, West Antarctica. Nature 322, 57–59.
- 638 Alley, R.B., Blankenship, D.D., Bentley, C.R., Rooney, S.T., 1987a. Till beneath ice stream B: 3. Till  
639 deformation: evidence and implications. Journal of Geophysical Research 92, 8921–8929.
- 640 Alley, R.B., Blankenship, D.D., Rooney, S.T., Bentley, C.R., 1987b. Till beneath ice stream B: 4. A  
641 coupled ice-till flow model. Journal of Geophysical Research 92, 8931–8940.
- 642 Andrews, L.C., Catania, G.A., Hoffman, M.J., Gulley, J.D., Lüthi, M.P., Ryser, C., Hawley, R.L.,  
643 Neumann, T.A. 2014. Direct observations of evolving subglacial drainage beneath the Greenland Ice  
644 Sheet. Nature 514, 80–83. doi:10.1038/nature13796.
- 645 Auton, C.A., Firth, C.R., Merritt, J.W., 1990. Beaully to Nairn: field Guide. Quaternary Research  
646 Association, London 149.
- 647 Merritt, J.W., Auton, C.A., Phillips, E. 2017. The Quaternary of around Nairn and the Inverness Firth:  
648 Field Guide. Quaternary Research Association, London.
- 649 Baroni, C., Fasano, F. 2006. Micromorphological evidence of warm-based glacier deposition from the  
650 Ricker Hills Tillite (Victoria Land, Antarctica). Quaternary Science Reviews. 25, 976-992.
- 651 Bartholomaeus, T.C., Anderson, R.S., Anderson, S.P. 2008. Response of glacier basal motion to  
652 transient water storage. Nature Geoscience 1, 33-37.

653 Benediktsson, I.O., Möller, P., Ingólfsson, O., van der Meer, J.J.M., Kjær, K.H., Krüger, J., 2008.  
654 Instantaneous end moraine and sediment wedge formation during the 1890 glacier surge of  
655 Brúarjökull, Iceland. *Quaternary Science Reviews* 27, 209–234.

656 Benn, D.I., Evans, D.J.A., 1996. The interpretation and classification of subglacially-deformed  
657 materials. *Quaternary Science Reviews* 15, 23–52.

658 Benn, D.I., Evans, D.J.A., 2010. *Glaciers and Glaciation*. Hodder, London.

659 Bindschadler, R.A., Vornberger, P.L., King, M.A., Padman, L., 2003. Tidally driven stick-slip motion in  
660 the mouth of Whillans Ice Stream, Antarctica. *Annals of Glaciology* 36, 263–272.

661 Blake, E.W., 1992. The deforming bed beneath a surge-type glacier: measurements of mechanical  
662 and electrical properties. Unpublished PhD thesis, University of British Columbia.

663 Blake, E.W., Clarke, G.K.C., Gerin, M.C., 1992. Tools for examining subglacial bed deformation.  
664 *Journal of Glaciology* 38, 388–396.

665 Blankenship, D.D., Bentley, C.R., Rooney, S.T., Alley, R.B., 1986. Seismic measurements reveal a  
666 saturated porous layer beneath an active Antarctic ice stream. *Nature* 322, 54–57.

667 Blankenship, D.D., Bentley, C.R., Rooney, S.T., Alley, R.B., 1987. Till beneath ice stream B: 1.  
668 Properties derived from seismic travel-times. *Journal of Geophysical Research* 92, 8903–8911.

669 Boulton, G.S., 1979. Processes of glacier erosion on different substrata. *Journal of Glaciology* 23, 15–  
670 38.

671 Boulton, G.S., 1986. A paradigm shift in glaciology? *Nature* 322, 18.

672 Boulton, G.S., 1996a. Theory of glacial erosion, transport and deposition as a consequence of  
673 subglacial sediment deformation. *Journal of Glaciology* 42, 43–62.

674 Boulton, G.S., 1996b. The origin of till sequences by subglacial sediment deformation beneath mid-  
675 latitude ice sheets. *Annals of Glaciology* 22, 75–84.

676 Boulton, G.S., 2006. Glaciers and their coupling with hydraulic and sedimentary processes. In Knight,  
677 P. G. (ed.) *Glacier Science and Environmental Change*, 3–22. Blackwell, Oxford.

678 Boulton, G.S., Dobbie, K.E., 1998. Slow flow of granular aggregates: the deformation of sediments  
679 beneath glaciers. *Philosophical Transactions of the Royal Society of London. A* 356, 2713–2745.

- 680 Boulton, G.S., Hindmarsh, R.C.A., 1987. Sediment deformation beneath glaciers: rheology and  
681 geological consequences. *Journal of Geophysical Research* 92, 9059–9082.
- 682 Boulton, G.S., Jones, A.S., 1979. Stability of temperate ice sheets resting on beds of deformable  
683 sediment. *Journal of Glaciology* 24, 29–43.
- 684 Boulton, G.S., Dent, D.L., Morris, E.M., 1974. Subglacial shearing and crushing, and the role of water  
685 pressures in tills from southeast Iceland. *Geografiska Annaler* 56A, 135–145.
- 686 Boulton, G.S., Dobbie, K.E., Zatsepin, S., 2001. Sediment deformation beneath glaciers and its  
687 coupling to the subglacial hydraulic system. *Quaternary International* 86, 3–28.
- 688 Boulton, G.S., Lunn, R., Vidstrand, P., Zatsepin, S., 2007a. Subglacial drainage by groundwater-  
689 channel coupling and the origin of esker systems: Part I – glaciological observations. *Quaternary  
690 Science Reviews* 26, 1067–1090.
- 691 Boulton, G.S., Lunn, R., Vidstrand, P., Zatsepin, S., 2007b. Subglacial drainage by groundwater-  
692 channel coupling and the origin of esker systems: Part II – theory and simulation of a modern  
693 system. *Quaternary Science Reviews* 26, 1091–1105.
- 694 Boyce, J.I., Eyles, N., 2000. Architectural element analysis applied to glacial deposits: internal  
695 geometry of a late Pleistocene till sheet, Ontario, Canada. *Bulletin of the Geological Society of  
696 America* 112, 98–118.
- 697 Broster, B.E., Seaman, A.A., 1991. Glacigenic rafting of weathered granite: Charlie Lake, New  
698 Brunswick. *Canadian Journal of Earth Sciences* 28, 649–654.
- 699 Brown, N.E., Hallet, B., Booth, D.B., 1987. Rapid soft bed sliding of the Puget glacial lobe. *Journal of  
700 Geophysical Research* 92, 8985–8997.
- 701 Burbridge, G.H., French, H.M., Rust, B.R., 1988. Water escape fissures resembling ice wedge casts in  
702 late Quaternary subaqueous outwash near St. Lazare, Quebec, Canada. *Boreas* 17, 33–40.
- 703 Burke, H., Phillips, E.R., Lee, J.R., Wilkinson, I.P., 2009. Imbricate thrust stack model for the formation  
704 of glaciotectionic rafts: an example from the Middle Pleistocene of north Norfolk, UK. *Boreas* 38,  
705 620–637.
- 706 Christiansen, E.A., Gendzwil, D.J., Meenely, W.A., 1982. Howe Lake: a hydrodynamic blowout  
707 structure. *Canadian Journal of Earth Sciences* 19, 1122–1139.

- 708 Christoffersen, P., Tulaczyk, S. 2003a. Response of subglacial sediments to basal freeze-on 1. Theory  
709 and comparison to observations from beneath the West Antarctic Ice Sheet. *Journal of Geophysical*  
710 *Research: Solid Earth* 108.B4.
- 711 Christoffersen, P., Tulaczyk, S. 2003b. Signature of palaeo-ice-stream stagnation: till consolidation  
712 induced by basal freeze-on. *Boreas* 32, 114–129.
- 713 Clark, C. D., Tulaczyk, S. M., Stokes, C. R., Canals, M., 2003. A groove-ploughing theory for the  
714 production of mega-scale glacial lineations, and implications for ice-stream mechanics. *Journal of*  
715 *Glaciology* 49, 240–256.
- 716 Clarke, G.K.C., 1987. Subglacial till: a physical framework for its properties and processes. *Journal of*  
717 *Geophysical Research* 92, 9023–9036.
- 718 Clarke, G.K.C., 2005. Subglacial processes. *Annual Review of Earth and Planetary Sciences* 33, 247–  
719 276.
- 720 Clark, P.U., Hansel, A.K., 1989. Clast ploughing, lodgement and glacier sliding over a soft glacier bed.  
721 *Boreas* 18, 201–207.
- 722 Damsgaard, A., Egholm, D.L., Piotrowski, J.A., Tulaczyk, S., Larsen, N.K., Tylmann, K., 2013. Discrete  
723 element modelling of subglacial sediment deformation. *Journal of Geophysical Research: Earth*  
724 *Surface* 118, 2230–2242.
- 725 Damsgaard, A., Egholm D.L., Piotrowski J.A., Tulaczyk S., Larsen N.K., Brædstrup C.F., 2015. A new  
726 methodology to simulate subglacial deformation of water-saturated granular material. *The*  
727 *Cryosphere* 9, 2183–2200. doi: 10.5194/tc-9-2183-2015.
- 728 Damsgaard, A., Egholm, D. L., Beem, L. H., Tulaczyk, S., Larsen, N.K., Piotrowski, J.A., Siegfried, M.R.  
729 2016. Ice flow dynamics forced by water pressure variations in subglacial granular beds. *Geophysics*  
730 *Research Letters* 43. doi: 10.1002/2016gl071579.
- 731 Denis, M., Guiraud, M., Konaté, M., Buoncristiani, J.-F., 2010. Subglacial deformation and water-  
732 pressure cycles as a key for understanding ice stream dynamics: evidence from the Late Ordovician  
733 succession of the Djado Basin (Niger). *International Journal of Earth Science (Geol Rundsch)* 99,  
734 1399-1425.
- 735 Dionne, J.C., Shilts, W.W. 1974. A Pleistocene clastic dike, Upper Chaudière Valley, Quebec. *Canadian*  
736 *Journal of Earth Sciences* 11, 1594–1605.

- 737 Dreimanis, A., 1992. Downward injected till wedges and upward injected till dykes. *Sveriges*  
738 *Geologiska Undersøgelse, Series Ca 81*, 91–96.
- 739 Dreimanis, A., Rappol, M., 1997. Late Wisconsinan sub-glacial clastic intrusive sheets along Lake Erie  
740 bluffs, at Bradville, Ontario, Canada. *Sedimentary Geology* 111, 225–248.
- 741 Ekstrom, G., Nettles, M., Abers, G.A. 2003. Glacial earthquakes. *Science* 302, 622–624.
- 742 Ekstrom, G., Nettles, M., Tsai, V.C., 2006. Seasonality and increasing frequency of Greenland glacial  
743 earthquakes. *Science* 311, 1756–1758.
- 744 Engelhardt, H.F., Kamb, B., 1998. Sliding velocity of Ice Stream B. *Journal of Glaciology* 44, 223–230.
- 745 Evans, D.J.A., Hiemstra, J.F., 2005. Till deposition by glacier submarginal, incremental thickening.  
746 *Earth Surface Processes and Landforms* 30, 1633-1662.
- 747 Evans, D.J.A., Phillips, E.R., Hiemstra, J.F., Auton, C.A., 2006. Subglacial till: formation, sedimentary  
748 characteristics and classification. *Earth-Science Reviews* 78, 115-176.
- 749 Fischer, U.H., Clarke, G.K.C., 1997. Stick-slip sliding behaviour at the base of a glacier. *Annals of*  
750 *Glaciology* 24, 390-396.
- 751 Fischer, U.H., Clarke, G.K.C., Blatter, H., 1999. Evidence for temporally varying ‘sticky spots’ at the  
752 base of Trapridge Glacier, Yukon Territory, Canada. *Journal of Glaciology* 45, 352-360.
- 753 Fischer, U., Porter, P.R., Schuler, T., Evans, A.J., Guðmundsson, G. H., 2001. Hydraulic and mechanical  
754 properties of glacial sediments beneath Unteraargletscher, Switzerland: implications for glacier basal  
755 motion. *Hydrological Processes* 15, 3525–3540.
- 756 Fuller, S., Murray, T., 2000. Evidence against pervasive bed deformation during the surge of an  
757 Icelandic glacier. In: Maltman, A.J., Hubbard, B., Hambrey, M.J. (Eds.), *Deformation of Glacial*  
758 *Materials*. Geological Society, London, Special Publications 176, pp. 203–216.
- 759 Goździk, J., van Loon, A.J., 2007. The origin of a giant downward directed clastic dyke in a kame  
760 (Belchatow mine, central Poland). *Sedimentary Geology* 193, 71–79.
- 761 Green, S.M., Obermeier, S.F., Olson, S.M., 2005. Engineering geologic and geotechnical analysis of  
762 paleoseismic shaking using liquefaction effects: field examples. *Engineering Geology* 76, 263–293.
- 763 Holzer, T.L., Hanks, T.C., Youd, T.L., 1989. Dynamics of Liquefaction during the 1987 Superstition  
764 Hills, California, Earthquake. *Science* 244, 56-59.



- 765 Hiemstra, J.F., van der Meer, J.J.M., 1997. Pore-water controlled grain fracturing as an indicator for  
766 subglacial shearing in tills. *Journal of Glaciology* 43, 446-454.
- 767 Hiemstra, J.F., Rijdsdijk, K.F., 2003. Observing artificially induced strain: implications for subglacial  
768 deformation. *Journal of Quaternary Science* 18, 373–383.
- 769 Hiemstra, J.F., Rijdsdijk, K.F., Evans, D.J.A., van der Meer, J.J.M., 2005. Integrated micro- and macro-  
770 scale analyses of Last Glacial maximum Irish Sea diamicts from Abermaw and Treath y Mwnt, Wales,  
771 UK. *Boreas* 34, 61-74.
- 772 Hiemstra, J.F., Evans, D.J.A., Cofaigh, C.Ó., 2007. The role of glacitectonic rafting and comminution in  
773 the production of subglacial tills: Examples from southwest Ireland and Antarctica. *Boreas* 36, 386-  
774 399.
- 775 Hindmarsh, R.C.A., 1996. Sliding of till over bedrock: scratching, polishing, comminution and  
776 kinematic wave theory. *Annals of Glaciology* 22, 41–48.
- 777 Hindmarsh, R.C.A., 1997. Deforming beds: viscous and plastic scales of deformation. *Quaternary*  
778 *Science Reviews* 16, 1039–1056.
- 779 Hoffmann, K., Piotrowski, J.A., 2001. Till melange at Amsdorf, central Germany: sediment erosion,  
780 transport and deposition in a complex, soft-bedded subglacial system. *Sedimentary Geology* 140,  
781 215–234.
- 782 Hooke, R. LeB., 1984. On the role of mechanical energy in maintaining subglacial water conduits at  
783 atmospheric pressure. *J. Glaciology* 30, 180–187. doi:10.3198/1984JoG30-105-180-187.
- 784 Hooke, R. LeB., Hanson, B., Iverson, N.R., Jansson, P., Fischer, U.H. 1997. Rheology of till beneath  
785 Storglaciären, Sweden. *Journal of Glaciology* 43.143, 172–179. doi:10.3198/1997JoG43-143-172-179.
- 786 Hooyer, T.S., Iverson, N.R., 2000. Diffusive mixing between shearing granular layers: constraints on  
787 bed deformation from till contacts. *Journal of Glaciology* 46, 641–651.
- 788 Hubbard, B., Sharp, M.J., Willis, I.C., Nielsen, M.K., Smart, C.C., 1995. Borehole water level variations  
789 and the structure of the subglacial hydrogeological system of the Haut Glacier d’Arolla, Valais,  
790 Switzerland. *Journal of Glaciology* 39, 572– 583.
- 791 Humphrey, N., Kamb, B., Fahnestock, M., Engelhardt, H., 1993. Characteristics of the bed of the  
792 lower Columbia Glacier, Alaska. *Journal of Geophysical Research* 98, 837–846.

793 Iken, A., Bindschadler, R.A. 1986. Combined measurements of subglacial water pressure and surface  
794 velocity of Findelengletscher, Switzerland: conclusions about drainage system and sliding  
795 mechanism. *Journal of Glaciology* 32 (110), 101-119.

796 Iken, A., Röthlisberger, H., Flotron, A., Haeblerli, W. 1983. The uplift of Unteraargletscher at the  
797 beginning of the melt season – a consequence of water storage at the bed? *Journal of Glaciology*, 29  
798 (101), 28-47.

799 Iverson, N.R., 1999. Coupling between a glacier and a soft bed: II. Model results. *Journal of*  
800 *Glaciology* 45, 41–53.

801 Iverson, N.R., 2010. Shear resistance and continuity of subglacial till: hydrology rules. *Journal of*  
802 *Glaciology* 56, 1104-1114.

803 Iverson, N.R., Hooyer T.S., Baker R.W., 1998. Ring-shear studies of till deformation: Coulomb-plastic  
804 behaviour and distributed strain in glacier beds. *Journal of Glaciology* 148, 634–642.

805 Iverson, N.R., Jansson, P., Hooke, R. Le B., 1994. In situ measurements of the strength of deforming  
806 subglacial till. *Journal of Glaciology* 40, 497–503.

807 Iverson, N.R., Hanson, B., Hooke, R. LeB., Jansson, P., 1995. Flow mechanism of glaciers on soft beds.  
808 *Science* 267, 80–81.

809 Joughin, I., MacAyeal, D.R., Tulaczyk, S. 2004. Basal shear stress of the Ross ice streams from control  
810 method inversions. *Journal of Geophysical Research: Solid Earth* 109.B9.

811 Kavanaugh, J.L., Clarke, G.K.C., 2006. Discrimination of the flow law for subglacial sediment using in  
812 situ measurements and an interpretation model. *Journal of Geophysical Research*, 111, F01002,  
813 doi:10.1029/2005JF000346.

814 Khatwa, A., Tulaczyk, S., 2001. Microstructural interpretations of modern and Pleistocene  
815 subglacially deformed sediments: the relative role of parent material and subglacial processes.  
816 *Journal of Quaternary Science* 16, 507-517.

817 Kilfeather, A.A., van der Meer, J.J.M. 2008. Pore size, shape and connectivity in tills and their  
818 relationship to deformation processes. *Quaternary Science Reviews* 27, 250–266.

819 Kjær, K.H., Larsen, E., van der Meer, J.J.M., Ingólfsson, Ó., Krüger, J., Benediktsson, I.O., Knudsen, C.  
820 G., Schomacker, A., 2006. Subglacial decoupling at the sediment/bedrock interface: a new  
821 mechanism for rapid flowing ice. *Quaternary Science Reviews* 25, 2704–2712.

- 822 Lachniet, M.S., Larson, G.J., Lawson, D.E., Evenson, E.B., Alley, R.B., 2001. Microstructures of  
823 sediment flow deposits and subglacial sediments: a comparison. *Boreas* 30, 254–262.
- 824 Larsen, E., Mangerud, J., 1992. Subglacially formed clastic dykes. *Sveriges Geologiska Undersökning,*  
825 *Series Ca* 81, 163–170.
- 826 Larsen, N.K., Piotrowski, J.A., Kronborg, C., 2004. A multiproxy study of a basal till: a time-  
827 transgressive accretion and deformation hypothesis. *Journal of Quaternary Science* 19, 9–21.
- 828 Larsen, N.K., Piotrowski, J.A., Christiansen, F., 2006. Microstructures and micro-shears as proxy for  
829 strain in subglacial diamicts: implications for basal till formation. *Geology* 34, 889-892.
- 830 Larsen, N.K., Piotrowski, J.A., Menzies, J., 2007. Microstructural evidence of low-strain, time  
831 transgressive subglacial deformation. *Journal of Quaternary Science* 22, 593-608.
- 832 Lee, J.R., Phillips, E.R., 2008. Progressive soft sediment deformation within a subglacial shear zone –  
833 a hybrid mosaic-pervasive deformation model for Middle Pleistocene glaciotectionised sediments  
834 from eastern England. *Quaternary Science Reviews* 27, 1350-1362.
- 835 Lee, J.R., Wakefield, O.J.W., Phillips, E., Hughes, L., 2015. Sedimentary and structural evolution of a  
836 relict subglacial to subaerial drainage system and its hydrogeological implications: an example from  
837 Anglesey, north Wales, UK. *Quaternary Science Reviews* 109, 88-110.
- 838 Lee, J.R., Phillips, E., Rose, J., Vaughan Hirsch, D., 2016. The Middle Pleistocene glacial evolution of  
839 northern East Anglia, UK: a dynamic tectonostratigraphic–parasequence approach. *Journal of*  
840 *Quaternary Science* 32, 231-260.
- 841 Leeman, J.R., Saffer, D.M., Scuderi, M.M., Marone, C. 2016. Laboratory observations of slow  
842 earthquakes and the spectrum of tectonic fault slip modes. *Nature Communications* 7, 11104.  
843 doi:10.1038/ncomms11104.
- 844 Le Heron, D.P., Etienne, J.L., 2005. A complex subglacial clastic dyke swarm, Sólheimajökull, southern  
845 Iceland. *Sedimentary Geology* 181, 25–37.
- 846 Lipovsky, B.P., Dunham, E.M., 2016. Tremor during ice-stream stick slip. *The Cryosphere*, 10, 385–  
847 399.
- 848 Magnússon, E., Björnsson, H., Rott, H., Pálsson, F., 2010. Reduced glacier sliding caused by persistent  
849 drainage from a subglacial lake. *The Cryosphere* 4, 13–20.

- 850 McCabe, A.M., Dardis, G.F., 1994. Glaciotectonically induced water-through flow structures in a Late  
851 Pleistocene drumlin, Kanrawer, County Galway, western Ireland. *Sedimentary Geology* 91, 173–190.
- 852 Menzies, J., 2000. Micromorphological analyses of microfabrics and microstructures indicative of  
853 deformation processes in glacial sediments. In: A.J. Maltman, B. Hubbard, M.J. Hambrey (eds.).  
854 *Deformation of glacial materials*. Geological Society of London, Special Publication 176, 245-257.
- 855 Menzies, J., Maltman, A.J., 1992. Microstructures in diamictos - evidence of subglacial bed  
856 conditions. *Geomorphology* 6, 27-40.
- 857 Menzies, J., Taylor, J.M., 2003. Seismically induced soft-sediment microstructures (seismites) from  
858 Meileour, western Strathmore, Scotland. *Boreas* 32, 314-327.
- 859 Menzies, J., Zaniewski, K., Dreger, D., 1997. Evidence from microstructures of deformable bed  
860 conditions within drumlins, Chimney Bluffs, New York State. *Sedimentary Geology* 111, 161-175.
- 861 Menzies, J., van der Meer, J.J.M., Rose, J., 2006. Till – a glacial "tectomict", a microscopic  
862 examination of a till's internal architecture. *Geomorphology* 75, 172-200.
- 863 Meriano, M., Eyles, N., 2009. Quantitative assessment of the hydraulic role of subglaciofluvial  
864 interbeds in promoting deposition of deformation till (Northern Till, Ontario). *Quaternary Science*  
865 *Reviews* 28, 608-620.
- 866 Miwa, S., Ikedaa, T., Satob, T., 2006. Damage process of pile foundation in liquefied ground during  
867 strong ground motion. *Soil Dynamics and Earthquake Engineering* 26, 325–336.
- 868 Moran, S.R., Clayton, L., Hooke, R.L., Fenton, M.M., Andriashek, L.D., 1980. Glacier-bed landforms of  
869 the prairie region of North America. *Journal of Glaciology* 25, 457–476.
- 870 Moore, P.L., Iverson, N.R. 2002. Slow episodic shear of granular materials regulated by dilatant  
871 strengthening. *Geology* 30, 843–846.
- 872 Murray, T., 1997. Assessing the paradigm shift: deformable glacier beds. *Quaternary Science Reviews*  
873 16, 995–1016.
- 874 Narloch, W., Piotrowski, J.A., Wysota, W., Larsen, N.K., Menzies, J., 2012. The signature of strain  
875 magnitude in tills associated with the Vistula Ice Stream of the Scandinavian Ice Sheet, central  
876 Poland. *Quaternary Science Reviews* 57, 105-120.

877 Narloch, W., Wysota, W., Piotrowski, J.A., 2013. Sedimentological record of subglacial conditions and  
878 ice sheet dynamics of the Vistula Ice Stream (north-central Poland) during the Last Glaciation.  
879 *Sedimentary Geology* 293, 30-44.

880 Neudorf, C.M., Brennand, T.A., Lian, O.B., 2013. Till-forming processes beneath parts of the  
881 Cordilleran Ice Sheet, British Columbia, Canada: macroscale and microscale evidence and a new  
882 statistical technique for analysing microstructure data. *Boreas*, 10.1111/bor.12009. ISSN 0300-9483.

883 Nienow, P.W., Hubbard, A.L., Hubbard, B.P., Chandler, D.M., Mair, D.W.F., Sharp, M.J., Willis, I.C.,  
884 2005. Hydrological controls on diurnal ice flow variability in valley glaciers. *Journal of Geophysical*  
885 *Research* 110 doi:10.1029/2003JF000112.

886 Obermeier, S.F., 1998. Liquefaction evidence for strong earthquakes of Holocene and latest  
887 Pleistocene ages in the states of Indiana and Illinois, USA. *Engineering Geology* 50, 227–254.

888 Obermeier, S.F., Olson, S.M., Green, R.A., 2005. Field occurrences of liquefaction-induced features: a  
889 primer for engineering geologic analysis of paleoseismic shaking. *Engineering Geology* 76, 209–234.

890 Passchier, C.W., Trouw, R.A.J., 1996. *Microtectonics*. Springer.

891 Peng, Z., Walter, J.I., Aster, R.C., Nyblade, A., Wiens, D.A., Anandakrishnan, S., Antarctic icequakes  
892 triggered by the 2010 Maule earthquake in Chile. *Nature Geoscience* 7, 677-681.

893 Phillips, E.R., 2006. Micromorphology of a debris flow deposit: evidence of basal shearing,  
894 hydrofracturing, liquefaction and rotational deformation during emplacement. *Quaternary Science*  
895 *Reviews* 25, 720-738.

896 Phillips, E.R., Auton, C.A., 2000. Micromorphological evidence for polyphase deformation of  
897 glaciolacustrine sediments from Strathspey, Scotland. In: Maltman, A.J., Hubbard, B., Hambrey, M.J.  
898 (eds.). *Deformation of glacial materials*. The Geological Society of London, Special Publication 176,  
899 279-291.

900 Phillips, E., Merritt, J., 2008. Evidence for multiphase water-escape during rafting of shelly marine  
901 sediments at Clava, Inverness-shire, NE Scotland. *Quaternary Science Reviews* 27, 988–1011.

902 Phillips, E., Hughes, L., 2014. Hydrofracturing in response to the development of an overpressurised  
903 subglacial meltwater system during drumlin formation: an example from Anglesey, NW Wales.  
904 *Proceedings of the Geologists' Association* 125, 296–311.

905 Phillips, E.R., Evans, D.J.A., Auton, C.A. 2002: Polyphase deformation at an oscillating ice margin  
906 following the Loch Lomond Readvance, central Scotland, UK. *Sedimentary Geology* 149, 157–182.

907 Phillips, E., Merritt, J.W., Auton, C.A., Gollledge, N.R., 2007. Microstructures developed in subglacially  
908 and proglacially deformed sediments: faults, folds and fabrics, and the influence of water on the  
909 style of deformation. *Quaternary Science Reviews* 26, 1499-1528.

910 Phillips, E.R., Lee, J.R., Burke, H. F., 2008. Progressive proglacial to subglacial deformation and  
911 syntectonic sedimentation at the margins of the Mid-Pleistocene British ice sheet: evidence from  
912 north Norfolk, UK. *Quaternary Science Reviews* 27, 1848–1871

913 Phillips, E.R., van der Meer, J.J.M., Ferguson, A., 2011. A new ‘microstructural mapping’  
914 methodology for the identification and analysis of microfabrics within glacial sediments. *Quaternary  
915 Science Reviews* 30, 2570-2596.

916 Phillips, E., Everest, J., Reeves, H., 2013a. Micromorphological evidence for subglacial multiphase  
917 sedimentation and deformation during overpressurized fluid flow associated with hydrofracturing.  
918 *Boreas* 42, 395–427.

919 Phillips, E., Lipka, E., van der Meer, J.J.M., 2013b. Micromorphological evidence of liquefaction,  
920 injection and sediment deposition during basal sliding of glaciers. *Quaternary Science Reviews* 81,  
921 114-137.

922 Piotrowski, J.A., Kraus, A.M., 1997. Response of sediment to ice sheet loading in northwestern  
923 Germany: effective stresses and glacier bed stability. *Journal of Glaciology* 43, 495–502.

924 Piotrowski, J.A., Tulaczyk, S., 1999. Subglacial conditions under the last ice sheet in northwest  
925 Germany: ice-bed separation and enhanced basal sliding? *Quaternary Science Reviews* 18, 737-751.

926 Piotrowski, J.A., Doring, U., Harder, A., Qadirie, R., Wenghofer, S., 1997. ‘Deforming bed conditions  
927 on the Danischer Wohld Peninsula, northern Germany’: Comments. *Boreas* 26, 73–77.

928 Piotrowski, J.A., Geletneky, J., Vater, R., 1999. Soft-bedded subglacial meltwater channel from the  
929 Welzow-Sud open-cast lignite mine, Lower Lusatia, eastern Germany. *Boreas* 28, 363–374.

930 Piotrowski, J.A., Mickelson, D.M., Tulaczyk, S., Krzyszowski, D., Junge, F.W., 2001. Were deforming  
931 bed beneath past ice sheets really widespread? *Quaternary International* 86, 139–150.

- 932 Piotrowski, J.A., Mickelson, D.M., Tulaczyk, S., Krzyszowski, D., Junge, F.W., 2002. Reply to comments  
933 by G.S. Boulton, K.E. Dobbie, S. Zatsepin on: deforming soft beds under ice sheets: how extensive  
934 were they? *Quaternary International* 97–98, 173–177.
- 935 Piotrowski, J.A., Larsen, N.K., Junge, F., 2004. Soft subglacial beds: a mosaic of deforming and stable  
936 spots. *Quaternary Science Reviews* 23, 993-1000.
- 937 Piotrowski, J.A., Larsen, N.K., Menzies, J., Wysota, W., 2006. Formation of subglacial till under  
938 transient bed conditions: deposition, deformation, and basal decoupling under a Weichselian ice  
939 sheet lobe, central Poland. *Sedimentology* 53, 83-106.
- 940 Podolskiy, E.A., Walter, F. 2016. Cryoseismology. *Reviews in Geophysics* 54, 708–758. doi:  
941 10.1002/2016rg000526.
- 942 Podolskiy, E.A., Sugiyama, S., Funk, M., Walter, F., Genco, R., Tsutaki, S., Minowa, M., Ripepe, M.,  
943 2016. Tide-modulated ice flow variations drive seismicity near the calving front of Bowdoin Glacier,  
944 Greenland. *Geophysical Research Letters* 43, 2036-2044.
- 945 Rijdsdijk, K.F., Owen, G., Warren, W.P., McCarroll, D., van der Meer, J.J.M., 1999. Clastic dykes in over-  
946 consolidated tills: evidence for subglacial hydrofracturing at Killiney Bay, eastern Ireland.  
947 *Sedimentary Geology* 129, 111–126.
- 948 Roberts, D.H., Hart, J.K., 2005. The deforming bed characteristics of a stratified till assemblage in  
949 north East Anglia, UK: investigating controls on sediment rheology and strain signatures. *Quaternary  
950 Science Reviews* 24, 123-140.
- 951 Rosier, S.H.R., Guðmundsson G.H., Green, J.A.M. 2015. Temporal variations in the flow of a large  
952 Antarctic ice-stream controlled by tidally induced changes in the subglacial water system. *The  
953 Cryosphere* 9, 2397–2429. doi:10.5194/tc-9-1649-2015.
- 954 Salamon, T. 2016. Subglacial conditions and Scandinavian Ice Sheet dynamics at the coarse-grained  
955 substratum of the fore-mountain area of southern Poland. *Quaternary Science Reviews* 151, 72–87.  
956 doi:10.1016/j.quascirev.2016.09.002.
- 957 Schofield, A.N., Wroth, P., 1968. *Critical State Soil Mechanics*. McGraw-Hill London.
- 958 Schoof, C., Rada, C.A., Wilson, N.J., Flowers, G.E., Hasselhoff, M. 2014. Oscillatory subglacial drainage  
959 in the absence of surface melt. *The Cryosphere* 7, 959–976. doi:10.5194/tc-8-959-2014.

960 Spagnolo, M., Phillips, E., Piotrowski, J.A., Rea, B.R., Clark, C.D., Stokes, C.R., Carr, S.J., Ely, J.C.,  
961 Ribolini, A., Wysota, W., Szuman, I., 2016. Ice stream motion facilitated by a shallow-deforming and  
962 accreting bed. *Nature Communications* DOI: 10.1038/ncomms10723

963 Stokes, C. R., Clark, C. D., Lian, O. B., Tulaczyk, S., 2007. Ice stream sticky spots: a review of their  
964 identification and influence beneath contemporary and palaeo-ice streams. *Earth Science Reviews*  
965 81, 217–249.

966 Tarplee, M.F.V., van der Meer, J.J.M, Davis, G.R., 2010. The 3D microscopic ‘signature’ of strain  
967 within glacial sediments revealed using X-ray computed microtomography. *Quaternary Science*  
968 *Reviews* 30, 3501-3532.

969 Tsai, V.C., Ekstrom, G. 2007. Analysis of glacial earthquakes. *Journal of Geophysical Research* 112,  
970 doi:10.1029/2006JF000596.

971 Thompson, J., Simons, M., Tsai, V.C. 2014. Modelling the elastic transmission of tidal stresses to  
972 great distances inland in channelized ice streams. *The Cryosphere* 8, 2007–2029. doi:10.5194/tc-8-  
973 2007-2014.

974 Truffer, M., Harrison, W.D., Echelmeyer, K.A. 2000. Glacier motion dominated by processes deep in  
975 underlying till. *Journal of Glaciology* 46, 213–221. doi:10.3189/172756500781832909.

976 Tulaczyk, S., 1999. Ice sliding over weak, fine-grained tills: dependence of ice-till interactions on till  
977 granulometry. In: Mickelson, D.M., Attig, J.W. (Eds.), *Glacial Processes: Past and Present*. Geological  
978 Society of America, Special Paper 337, 159–177.

979 Tulaczyk, S., Kamb, B., Engelhardt, H.F., 2000a. Basal mechanics of Ice Stream, B. I. Till mechanics.  
980 *Journal of Geophysical Research* 105, 463–481.

981 Tulaczyk, S., Kamb, B., Engelhardt, H.F., 2000b. Basal mechanics of Ice Stream, B: II. Plastic undrained  
982 bed model. *Journal of Geophysical Research* 105, 483–494.

983 Tulaczyk, S., Scherer, R.P., Clark, C.D., 2001. A ploughing model for the origin of weak tills beneath  
984 ice streams: a qualitative treatment. *Quaternary International* 86, 59–70.

985 van der Meer, J.J.M., 1979. Complex till sections in the western Swiss Plain. In: Ch. Schlüchter (ed.).  
986 *Moraines and varves*. A.A. Balkema, Rotterdam. 265-269.

987 van der Meer, J.J.M., 1982. The Fribourg area. A study in Quaternary Geology and soil development.  
988 PhD thesis, University of Amsterdam.



- 989 van der Meer, J.J.M., 1993. Microscopic evidence of subglacial deformation. *Quaternary Science*  
990 *Reviews* 12, 553-587.
- 991 van der Meer, J.J.M., 1997. Particle and aggregate mobility in till: microscopic evidence of subglacial  
992 processes. *Quaternary Science Reviews* 16, 827-831.
- 993 van der Meer, J.J.M., Menzies, J., Rose, J., 2003. Subglacial till, the deformable glacier bed.  
994 *Quaternary Science Reviews* 22, 1659-1685.
- 995 van der Meer, J.J.M., Kjær, K., Krüger, J. 1999: Subglacial water-escape structures, Slettjökull,  
996 Iceland. *Journal of Quaternary Science* 14, 191–205.
- 997 van der Meer, J.J.M., Kjær, K.H., Krüger, J., Rabassa, J., Kilfeather, A.A., 2009. Under pressure: clastic  
998 dykes in glacial settings. *Quaternary Science Reviews* 28, 708-720.
- 999 van der Wateren, F.M., Kluiving, S.J., Bartek, L.R., 2000. Kinematic indicators of subglacial shearing.  
1000 In: A.J. Maltman, B. Hubbard, M.J. Hambrey (eds.) *Deformation of glacial materials*. Geological  
1001 Society of London, Special Publication. 176, 259-278.
- 1002 Vaughan-Hirsch, D.P., Phillips, E., Lee, J.R., Hart, J.K., 2013. Micromorphological analysis of poly-  
1003 phase deformation associated with the transport and emplacement of glaciotectionic rafts at West  
1004 Runton, north Norfolk, UK. *Boreas* 42, 376–394.
- 1005 Vaughan-Hirsch, D., Phillips, E., 2016. Mid-Pleistocene thin-skinned glaciotectionic thrusting of the  
1006 Aberdeen Ground Formation, Central Graben region, central North Sea *Journal of Quaternary*  
1007 *Science* 32, 196-212.
- 1008 Walker, R.T., Parizek, B.R., Alley, R.B., Anandakrishnan, S., Riverman, K.L., Christianson, K. 2013. Ice-  
1009 shelf tidal flexure and subglacial pressure variations. *Earth and Planetary Science Letters* 361, 422–  
1010 428.
- 1011 Walter, J.I., Brodsky, E.E., Tulaczyk, S., Schwartz, S.Y., Pettersson, R., 2011. Transient slip events from  
1012 near-field seismic and geodetic data on a glacier fault, Whillans Ice Plain, West Antarctica. *Journal of*  
1013 *Geophysical Research* 116, F01021, doi:10.1029/2010JF001754.
- 1014 Werder, M.A., Hewitt I.J., Schoof, C.G., Flowers, G.E. 2013. Modelling channelized and distributed  
1015 subglacial drainage in two dimensions. *Journal of Geophysical Research: Earth Surface* 118, 2140–  
1016 2158. doi:10.1002/jgrf.20146.

- 1017 Wiens, D.A., Anandakrishnan, S., Winberry, J.P., King, M.A., 2008. Simultaneous teleseismic and  
1018 geodetic observations of the stick-slip motion of an Antarctic ice stream. *Nature* 453,  
1019 doi:10.1038/nature06990.
- 1020 Winberry, P.J., Anandakrishnan, S., Alley, R.B., Bindschadler, R.A., King, M.A. 2009. Basal mechanics  
1021 of ice streams: Insights from the stick-slip motion of Whillans Ice Stream, West Antarctica. *Journal of*  
1022 *Geophysical Research: Earth Surface* 114, F01016, doi:10.1029/2008JF001035.
- 1023 Winberry, J.P., Anandakrishnan, S., Wiens, D.A., Alley, R.B., Christianson, K. 2011. Dynamics of stick-  
1024 slip motion, Whillans Ice Stream, Antarctica. *Earth and Planetary Science Letters* 305, 283–289.  
1025 doi:10.1016/j.j.quaint.2012.08.1876.
- 1026 Youd, T.L., 1978. Major cause of earthquake damage is ground failure. *Civil Engineering* 48, 47-51.
- 1027 Youd, T.L., 2003. Liquefaction mechanisms and induced ground failure. *International Handbook of*  
1028 *earthquake and engineering seismology*, volume 81B, 1159-1173.
- 1029 Xu, B.H., Yu, A.B., 1997. Numerical simulation of the gas-solid flow in a fluidized bed by combining  
1030 discrete particle method with computational fluid dynamics. *Chemical Engineering Science* 52.16,  
1031 2785–2809.
- 1032 Zhang, Y., Campbell, C.S. 1992. The interface between fluid-like and solid-like behaviour in two-  
1033 dimensional granular flows. *Journal of Fluid Mechanics* 237, 541.

1034

## 1035 **Figures**

1036 **Fig. 1.** Diagram showing the zonation of a relatively homogeneous subglacially deforming till and its  
1037 relationship to “dilation”, displacement, sediment volume, shear strength, connectivity and pore  
1038 water pressure (after Evans *et al.*, 2006).

1039 **Fig. 2.** Diagram showing the compiled results of a detailed micromorphological and microstructural  
1040 study carried out on a series of subglacial traction tills exposed in the Nairn-Inverness area of NE  
1041 Scotland (see text for details).

1042 **Fig. 3.** Map showing the location of the Meads of St. John, Riereach Burn, Drynachan Burn, Dalcharn  
1043 Burn, Cothall, Easterton farm and ‘stream’ sites in the Nairn-Inverness area of NE Scotland. Also  
1044 shown are the generalized ice-movement directions within the Moray Firth Ice Stream and ice  
1045 flowing northwards from the Cairngorm plateau across Lochindorb and down the valley of the River  
1046 Findhorn.

1047 **Fig. 4.** Microstructural map of a polydeformed subglacial traction till (sample N7126), the sandstone-  
1048 rich Dalcharn Lower Till exposed in a river section at Dalcharn West [NH 8144 4528], NE Scotland  
1049 (after Phillips *et al.*, 2011).

1050 **Fig. 5.** Microstructural map of a polydeformed subglacial traction till (sample N7128), the basal grey-  
1051 brown metasandstone and granite-rich till exposed at Riereach Burn [NH 83903 43151], NE Scotland  
1052 (after Phillips *et al.*, 2011).

1053 **Fig. 6.** Microstructural map of a polydeformed subglacial traction till (sample N7129), the basal grey-  
1054 brown metasandstone and granite-rich till exposed at Riereach Burn [NH 83903 43151], NE Scotland  
1055 (after Phillips *et al.*, 2011).

1056 **Fig. 7.** Microstructural map of a polydeformed subglacial traction till (sample N7132), the basal grey-  
1057 brown metasandstone and granite-rich till exposed at Riereach Burn [NH 84503 44132], NE Scotland  
1058 (after Phillips *et al.*, 2011).

1059 **Fig. 8.** Microstructural map of a polydeformed subglacial traction till (sample N12278) exposed at  
1060 Cothall [NJ 04463 54103], NE Scotland.

1061 **Fig. 9.** Microstructural map of a polydeformed subglacial traction till (sample N12279) exposed at  
1062 Cothall [NJ 04463 54103], NE Scotland.

1063 **Fig. 10.** Microstructural map of a polydeformed subglacial traction till (sample N12280) exposed at  
1064 Nairn (stream) [NJ 04162 54102], NE Scotland.

1065 **Fig. 11.** Microstructural map of a polydeformed subglacial traction till (sample N12281) exposed at  
1066 Nairn (stream) [NJ 04162 54102], NE Scotland.

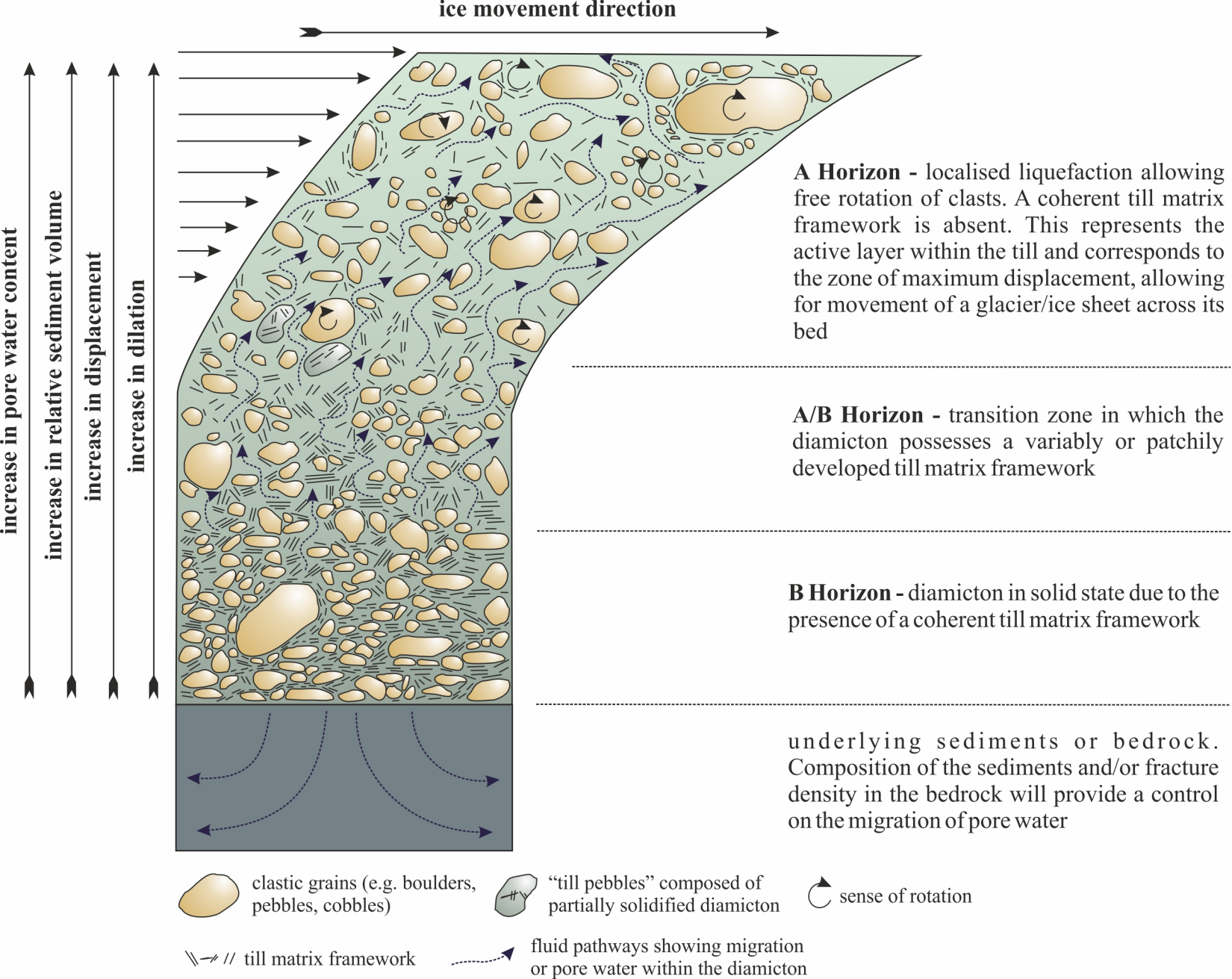
1067 **Fig. 12.** Diagram showing the microstructural maps constructed for a series of thin sections taken  
1068 from a thinly stratified till exposed at Galmis, Switzerland (Phillips *et al.*, 2013).

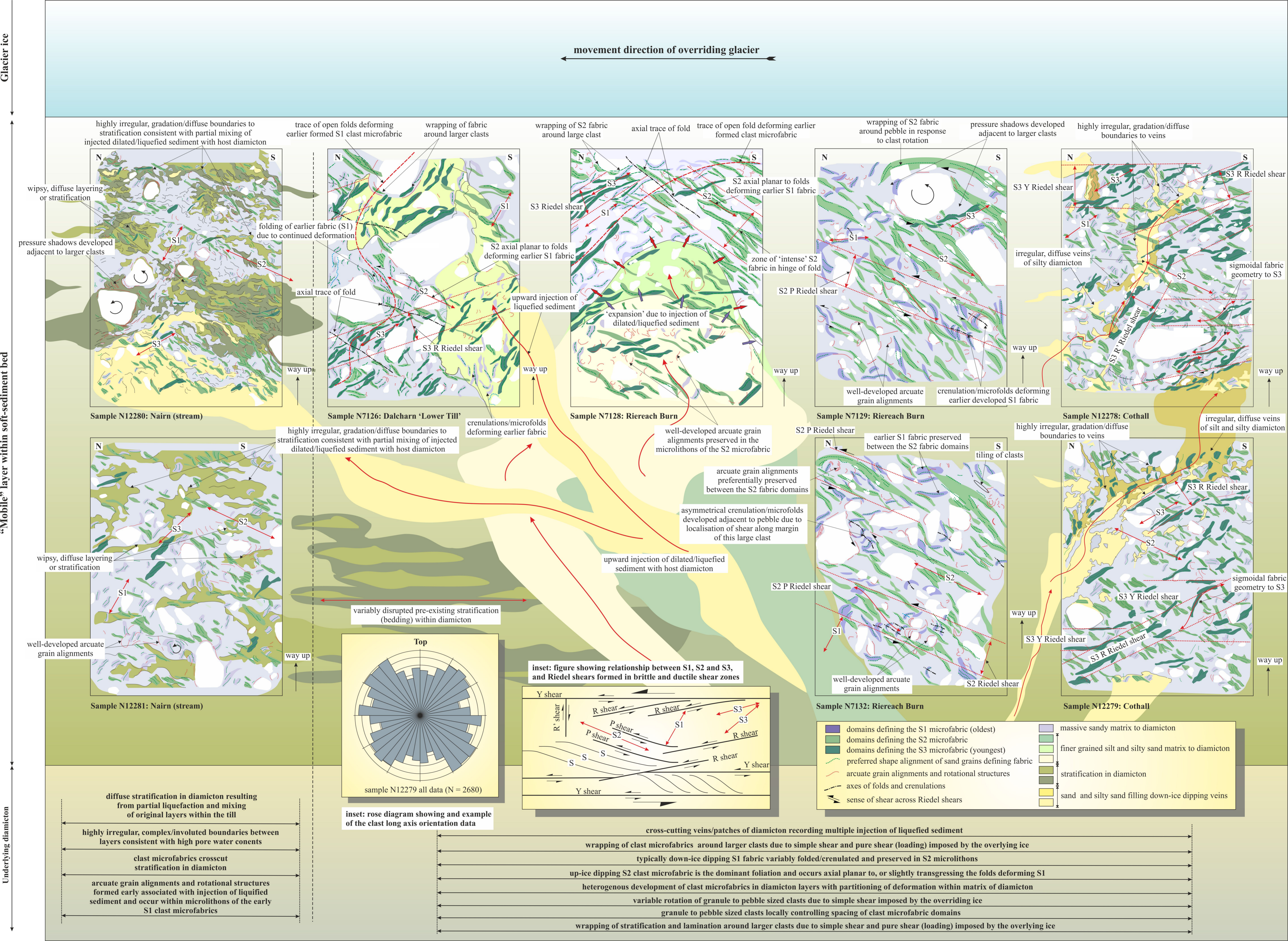
1069 **Fig. 13.** Diagram illustrating the effects of the seismic waves generated during an icequake on the  
1070 unconsolidated sediments within the bed (see text for details).

1071 **Fig. 14.** Diagram showing the proposed conceptual model leading to the development of a “transient  
1072 mobile zone” (TMZ) within the bed of glacier in response to an icequake (see text for details).

1073 **Fig. 15.** (a) Schematic ternary diagram showing the relative effects of deformation, increased  
1074 meltwater and ice quakes as potential triggers for soft-bed sliding versus bed deformation versus  
1075 basal sliding as the main mechanism for glacier motion; and (b) Flow-chart showing the proposed

1076 feedback mechanism responsible for promoting forward glacier motion as a result of soft-bed sliding  
1077 induced by icequake activity.



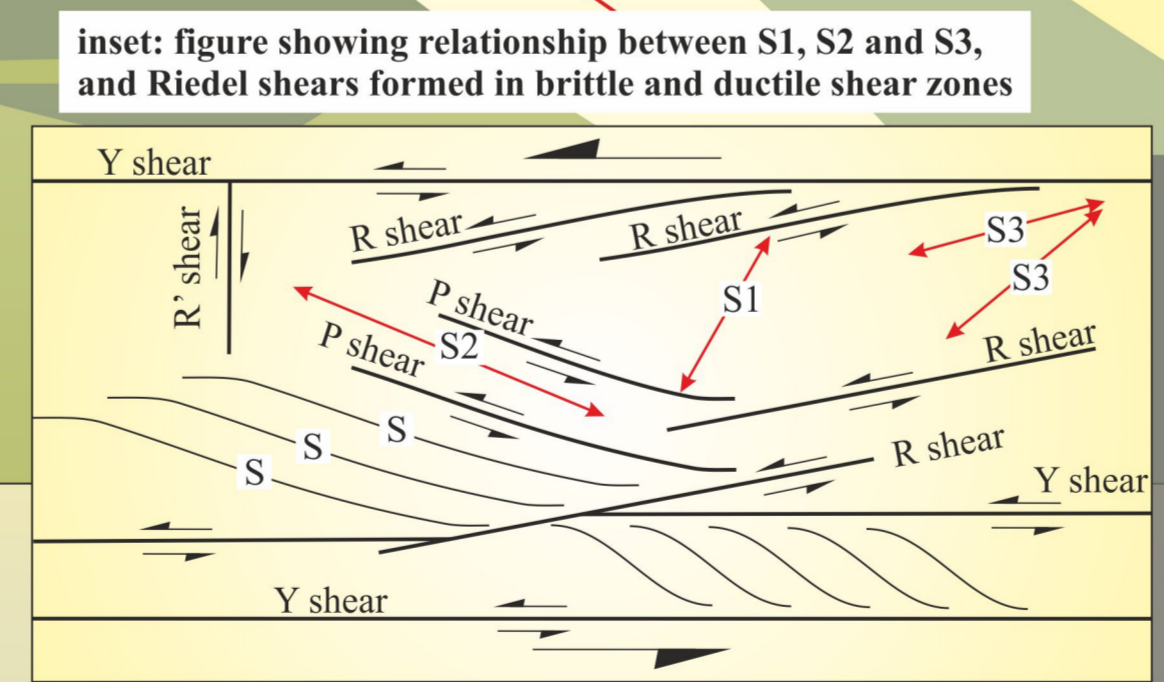
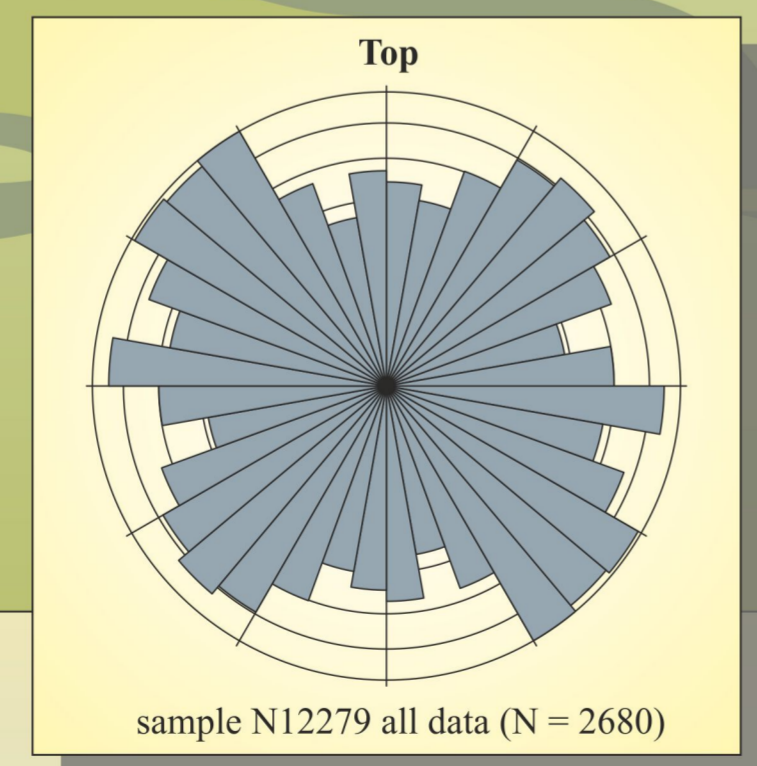
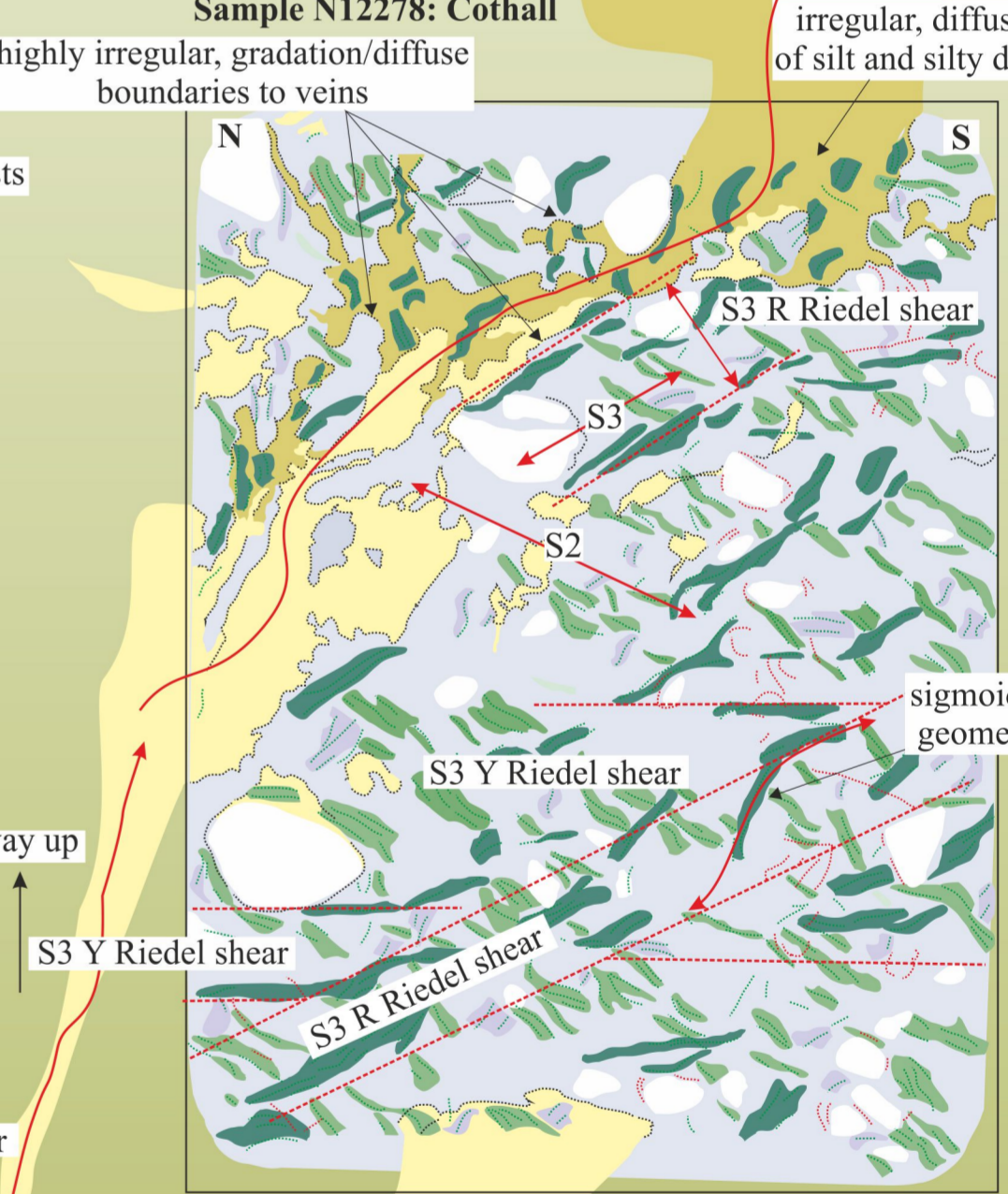
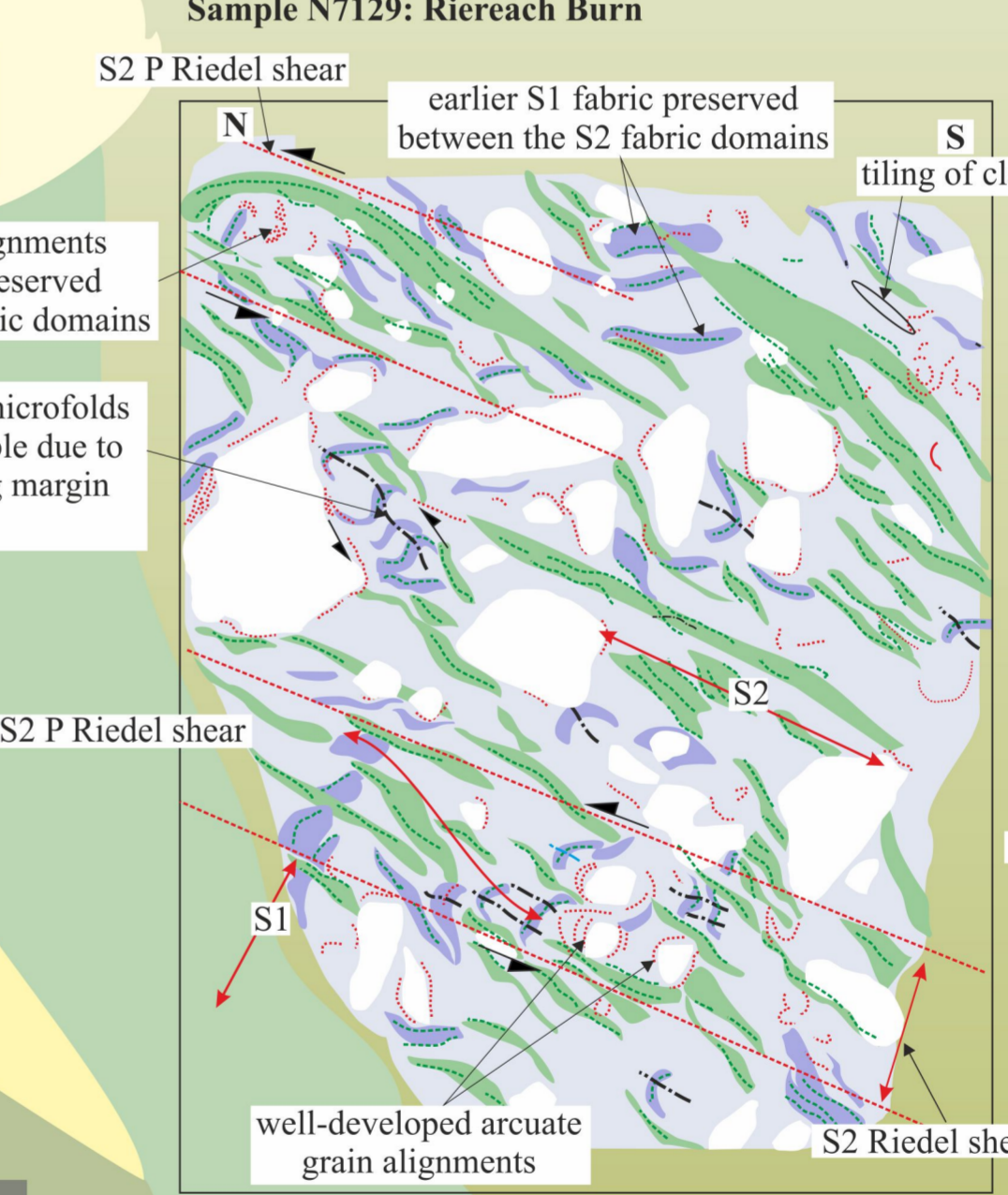
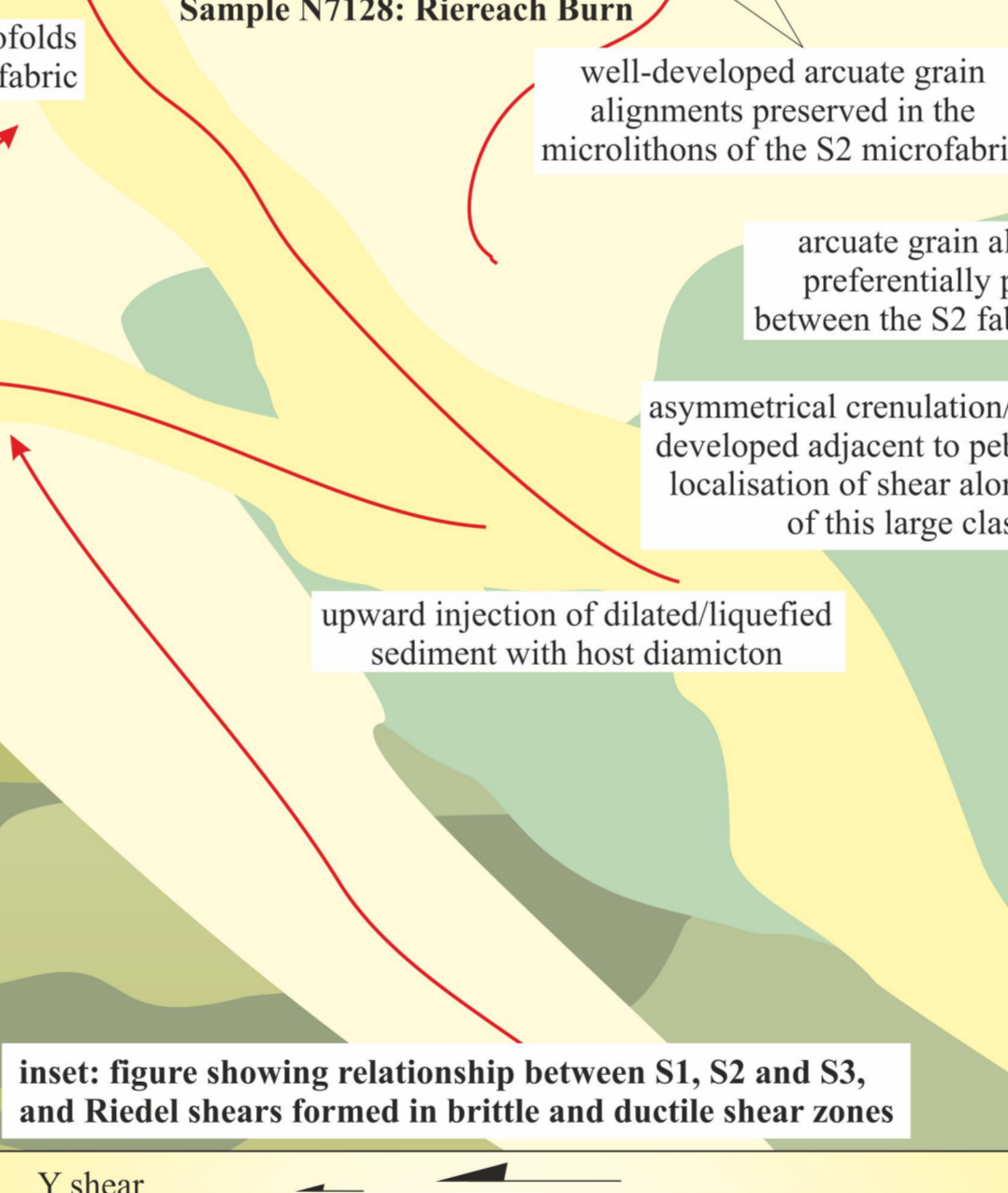
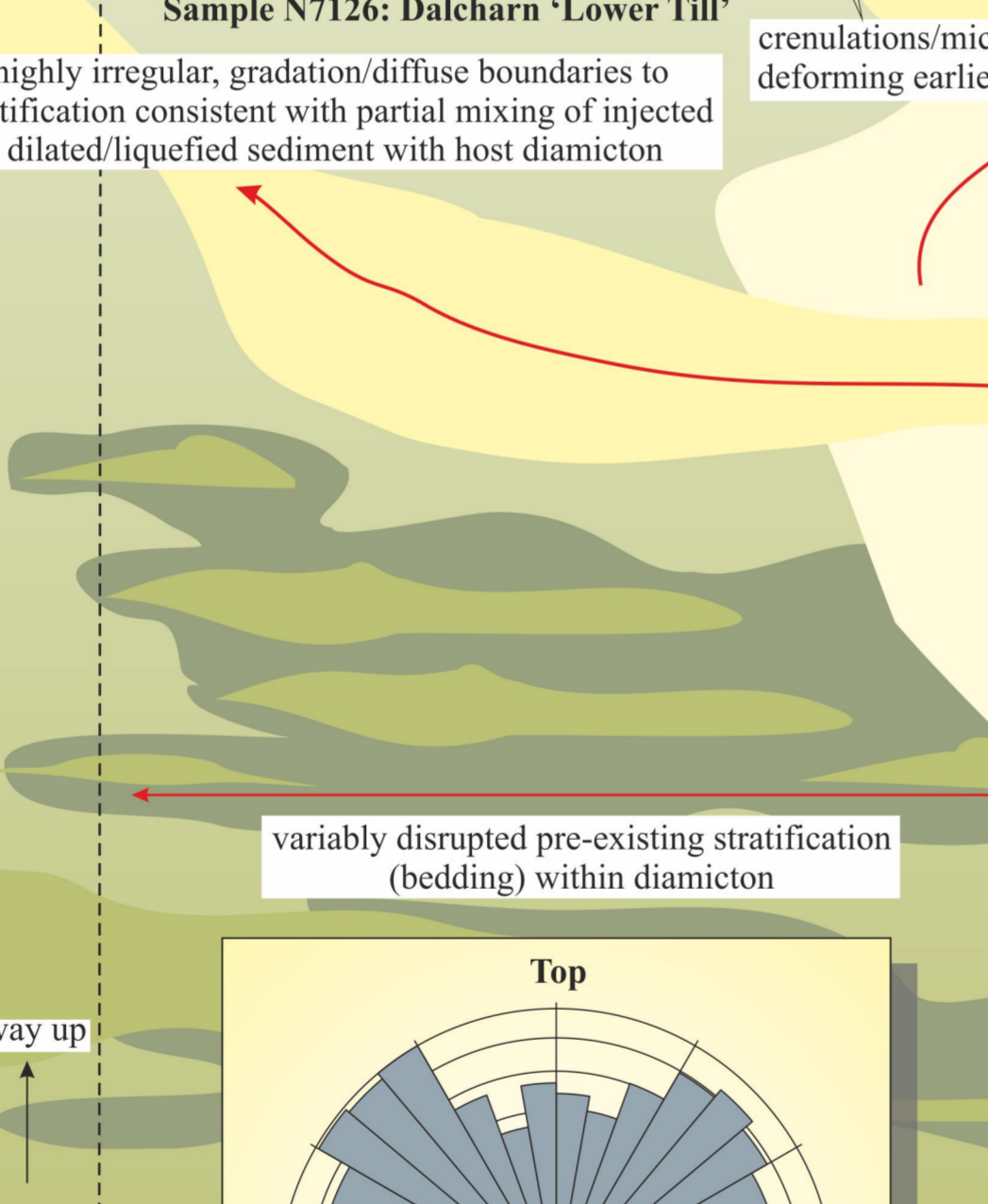
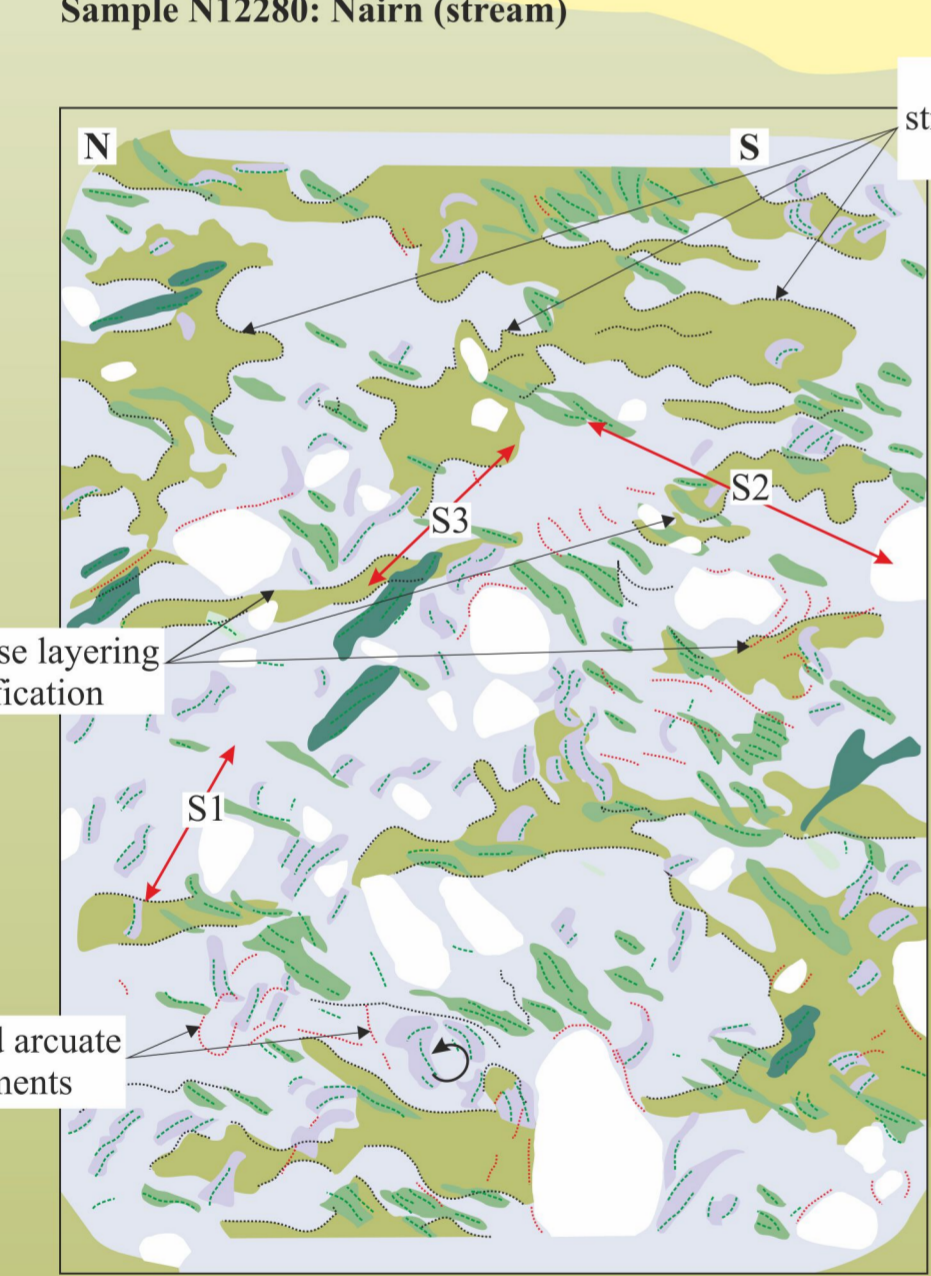
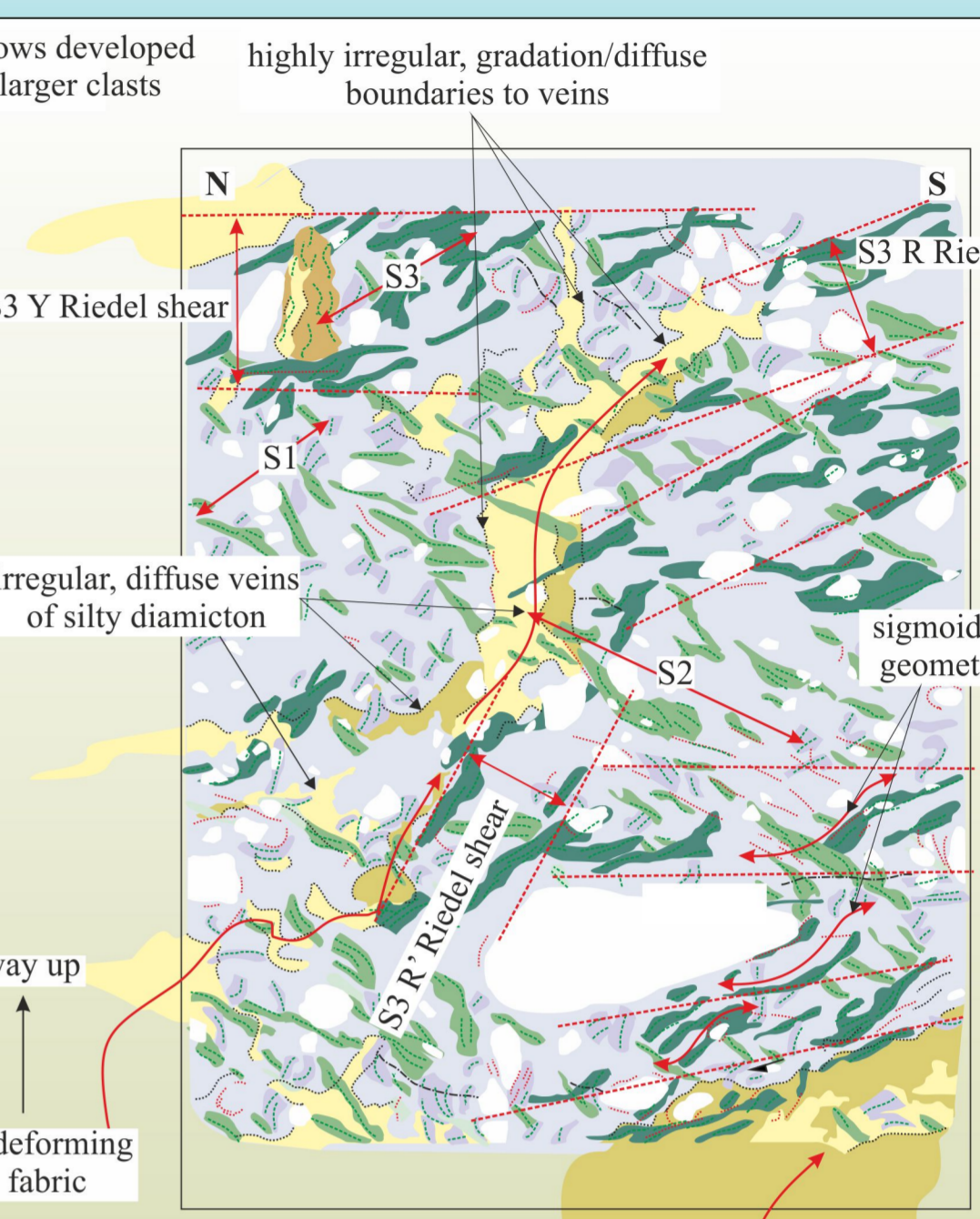
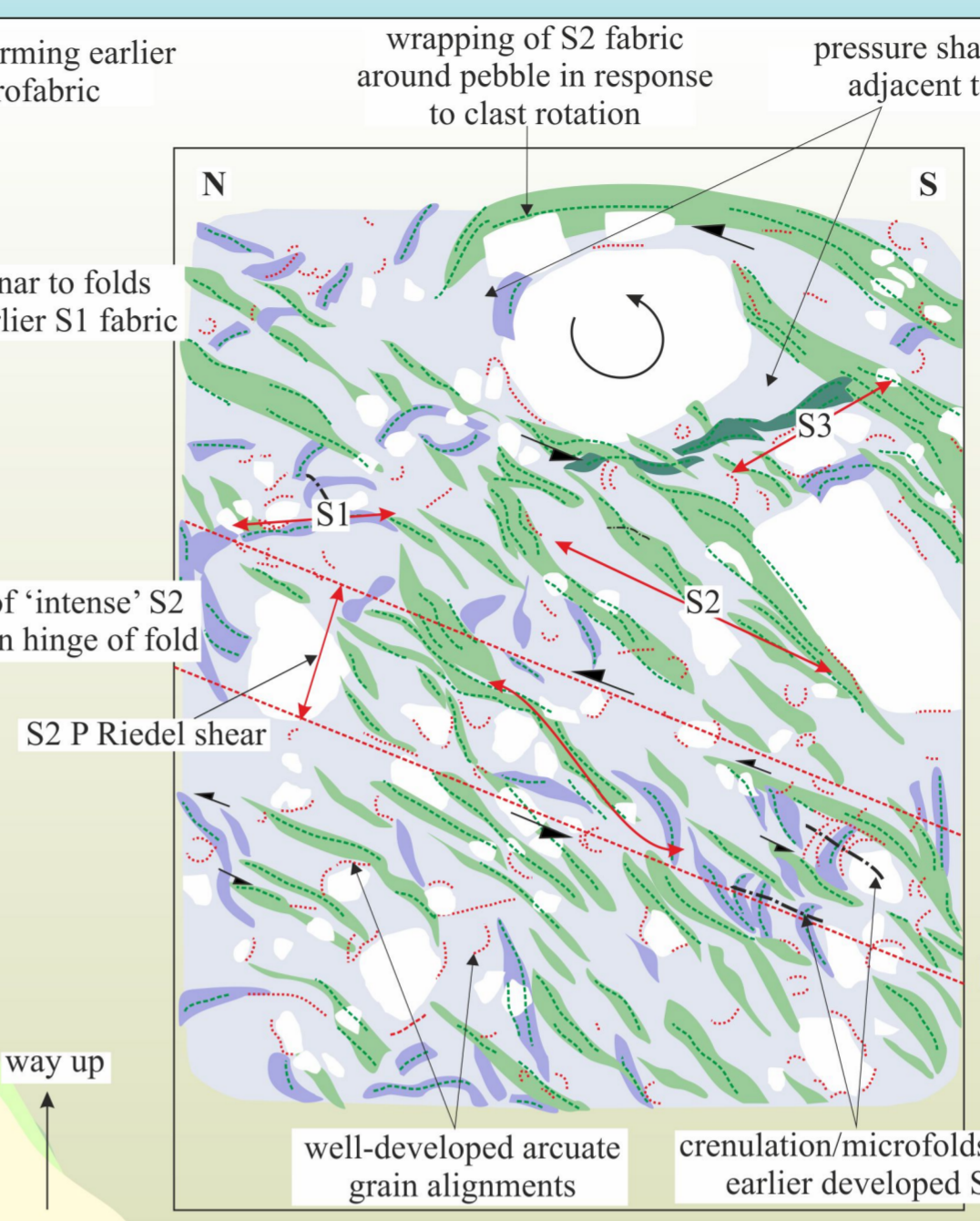
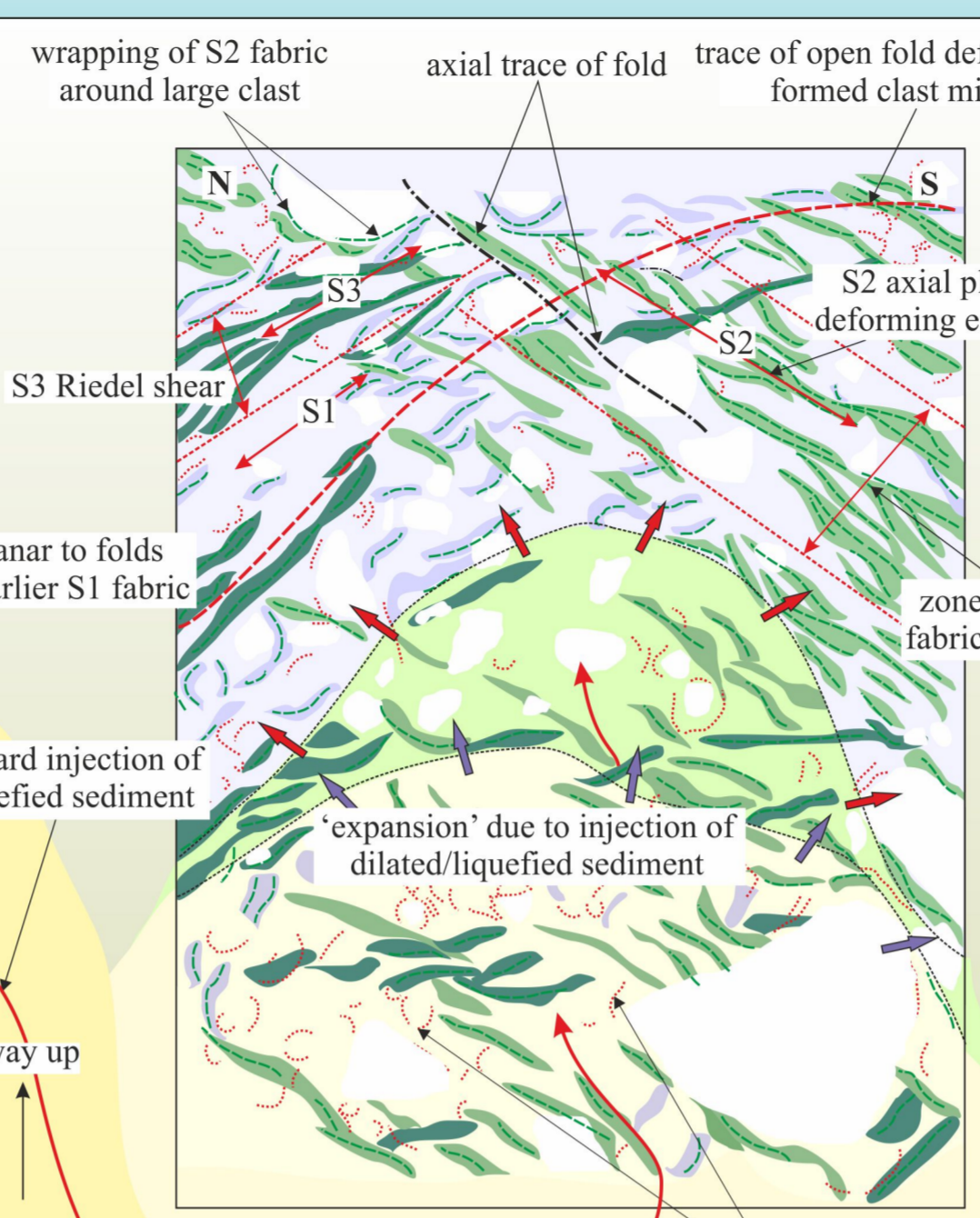
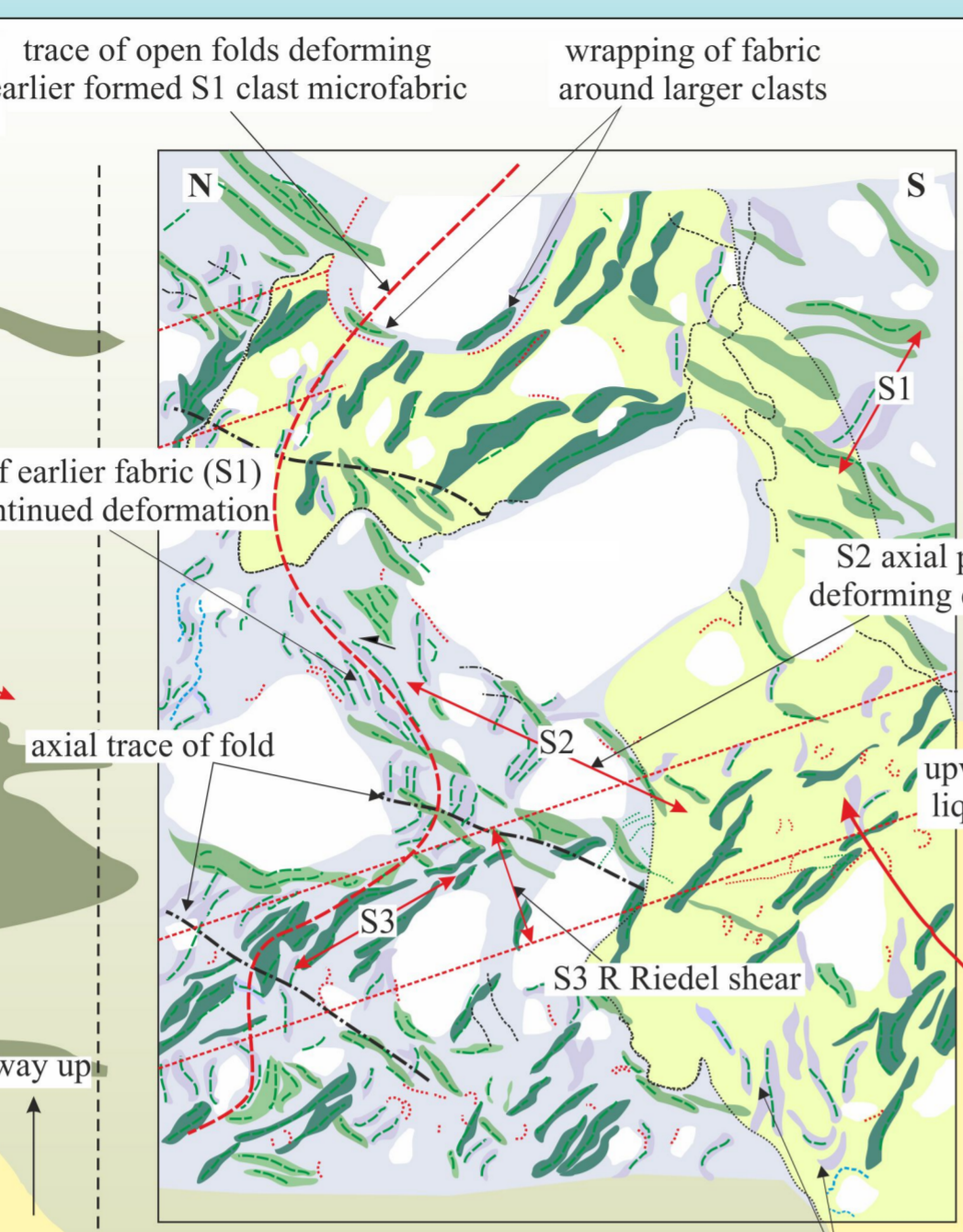
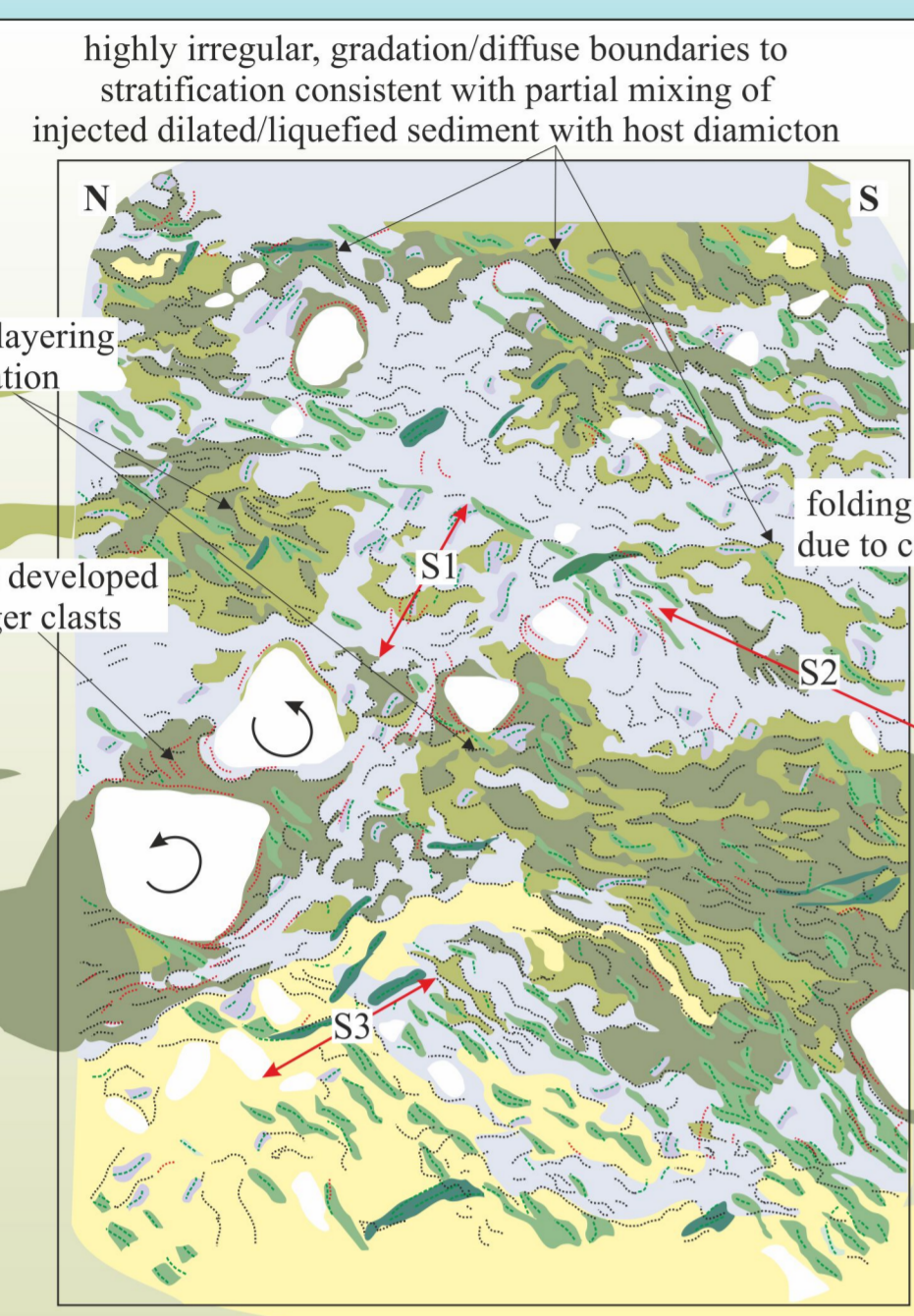


movement direction of overriding glacier

Glacier ice

“Mobile” layer within soft-sediment bed

Underlying diamicton



- domains defining the S1 microfabric (oldest)
- domains defining the S2 microfabric
- domains defining the S3 microfabric (youngest)
- preferred shape alignment of sand grains defining fabric
- arcuate grain alignments and rotational structures
- axes of folds and crenulations
- sense of shear across Riedel shears
- massive sandy matrix to diamicton
- finer grained silt and silty sand matrix to diamicton
- stratification in diamicton
- sand and silty sand filling down-ice dipping veins

diffuse stratification in diamicton resulting from partial liquefaction and mixing of original layers within the till

highly irregular, complex/involuted boundaries between layers consistent with high pore water contents

clast microfabrics crosscut stratification in diamicton

arcuate grain alignments and rotational structures formed early associated with injection of liquified sediment and occur within microlithons of the early S1 clast microfabrics

cross-cutting veins/patches of diamicton recording multiple injection of liquefied sediment

wrapping of clast microfabrics around larger clasts due to simple shear and pure shear (loading) imposed by the overlying ice

typically down-ice dipping S1 fabric variably folded/crenulated and preserved in S2 microlithons

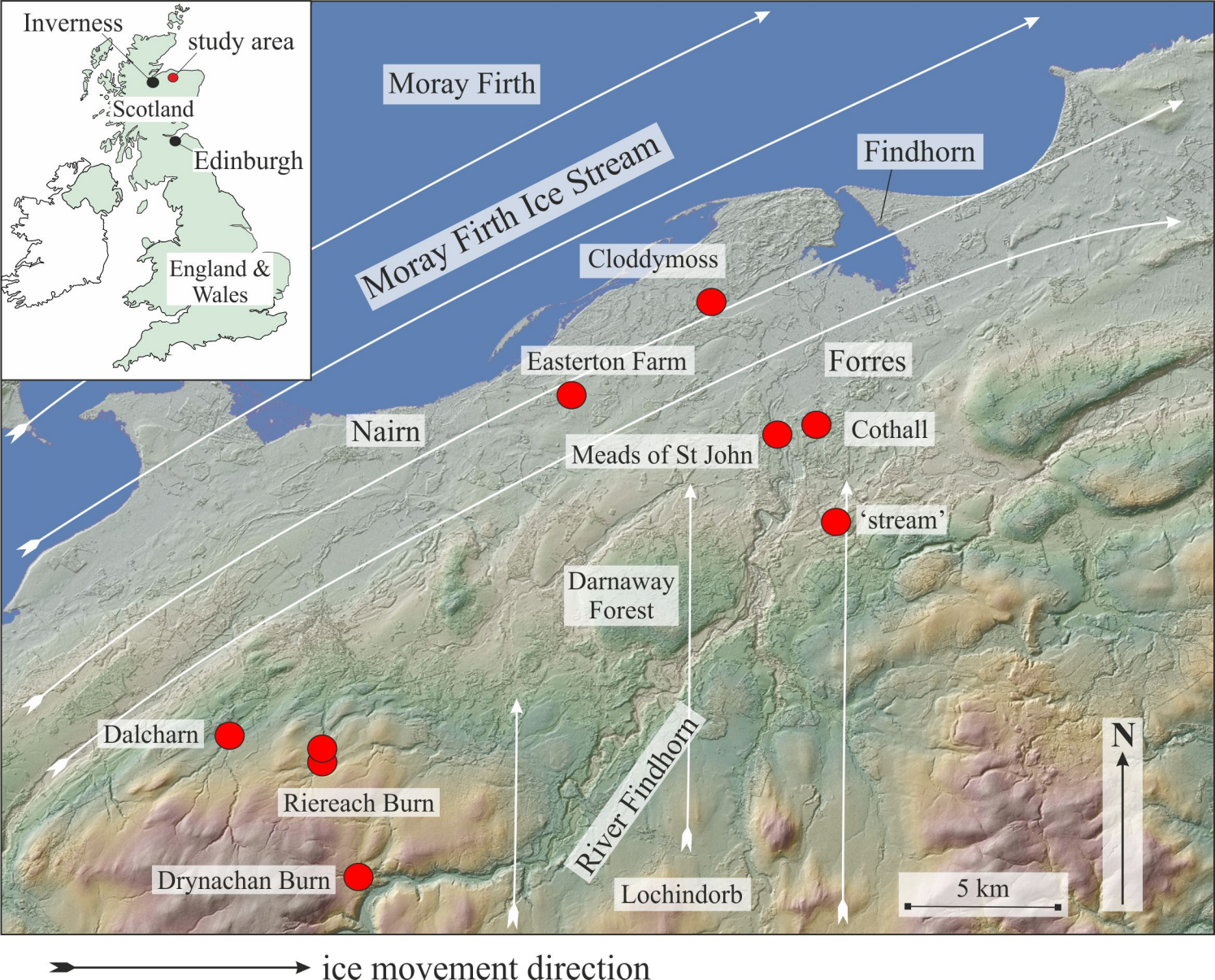
up-ice dipping S2 clast microfabric is the dominant foliation and occurs axial planar to, or slightly transgressing the folds deforming S1

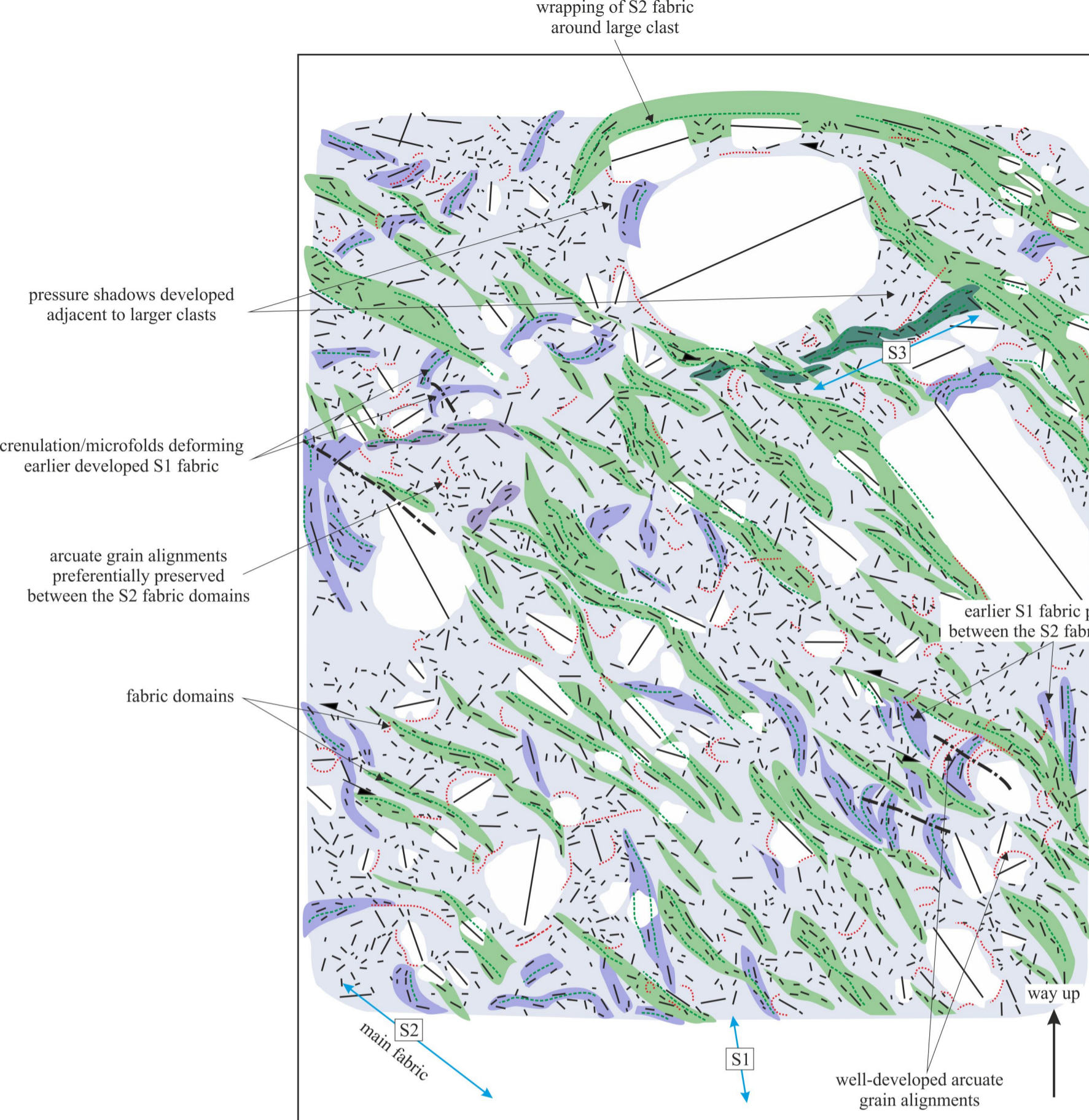
heterogenous development of clast microfabrics in diamicton layers with partitioning of deformation within matrix of diamicton

variable rotation of granule to pebble sized clasts due to simple shear imposed by the overriding ice

granule to pebble sized clasts locally controlling spacing of clast microfabric domains

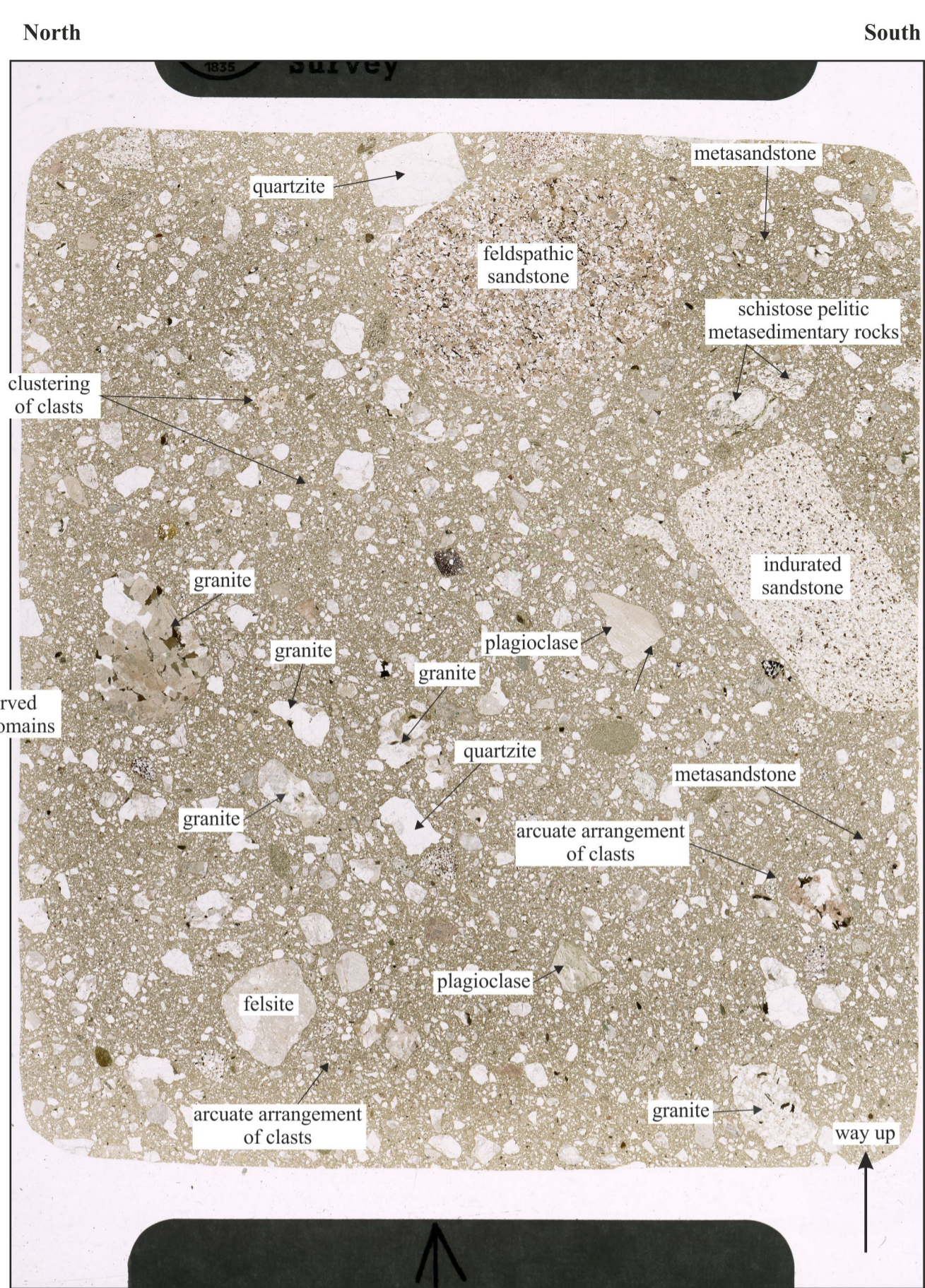
wrapping of stratification and lamination around larger clasts due to simple shear and pure shear (loading) imposed by the overlying ice





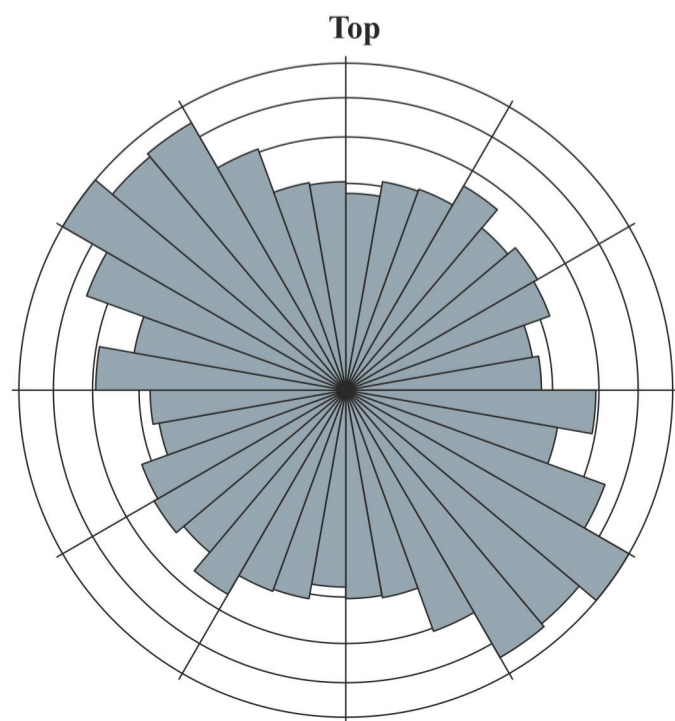
Sample N7129: Riereach Burn

10 mm



Sample N7129: Riereach Burn

10 mm

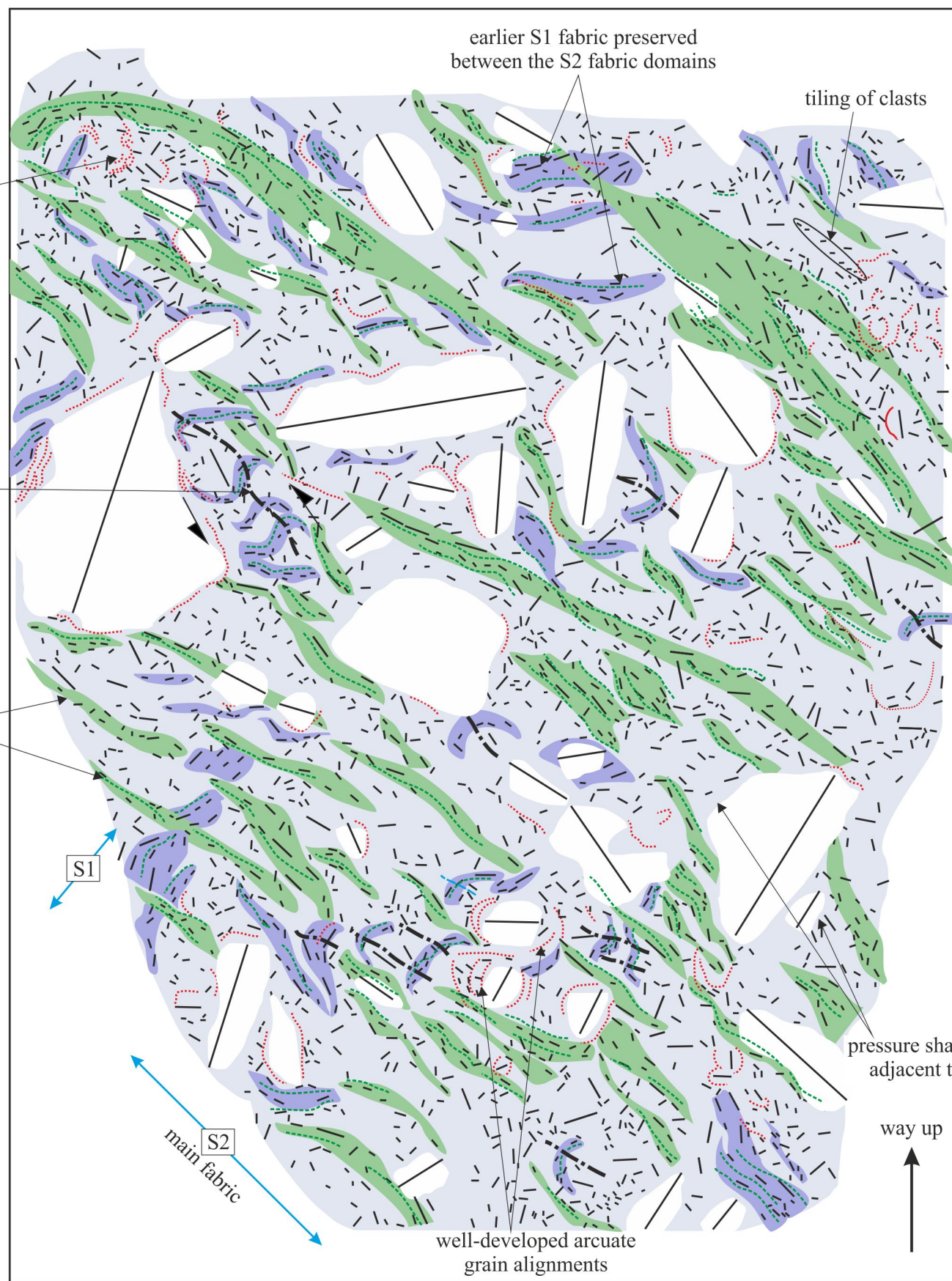


sample N7129 (N = 2214)

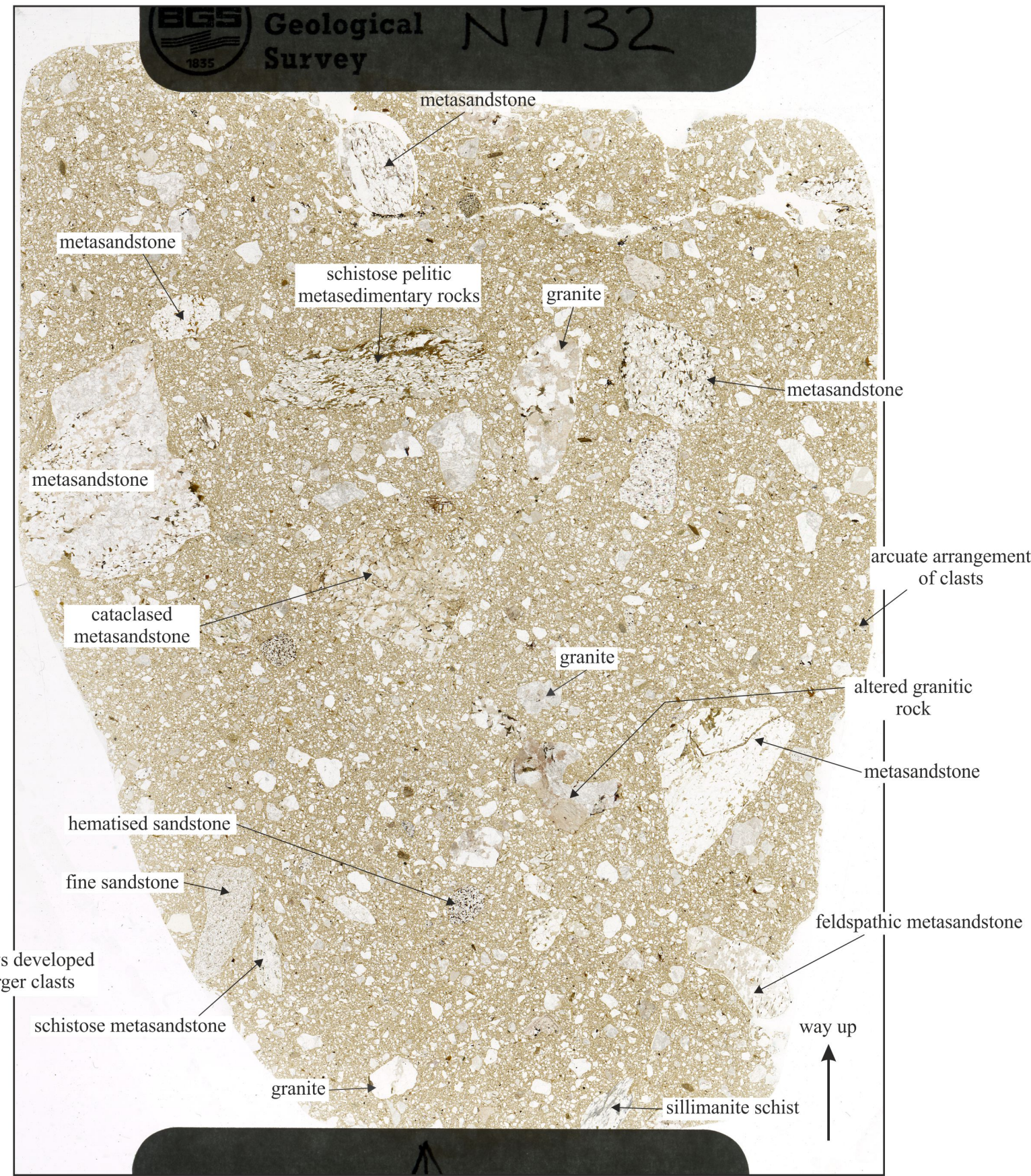
- microclast fabric defined by clast long axes
- axial traces of folds deforming earlier formed S1 clast microfabric
- axial surfaces of crenulations/microfolds
- arcuate to linear grain aggregates
- patchily developed boundary between dark and pale matrix
- trace of folds deforming earlier formed S1 clast microfabric
- domains defining the S1 microfabric (oldest)
- domains defining the S2 microfabric
- domains defining the S3 microfabric (youngest)

- S1 to n relative age of fabric(s)
- long axis of clasts
- sense of shear
- orientation of fabric(s)

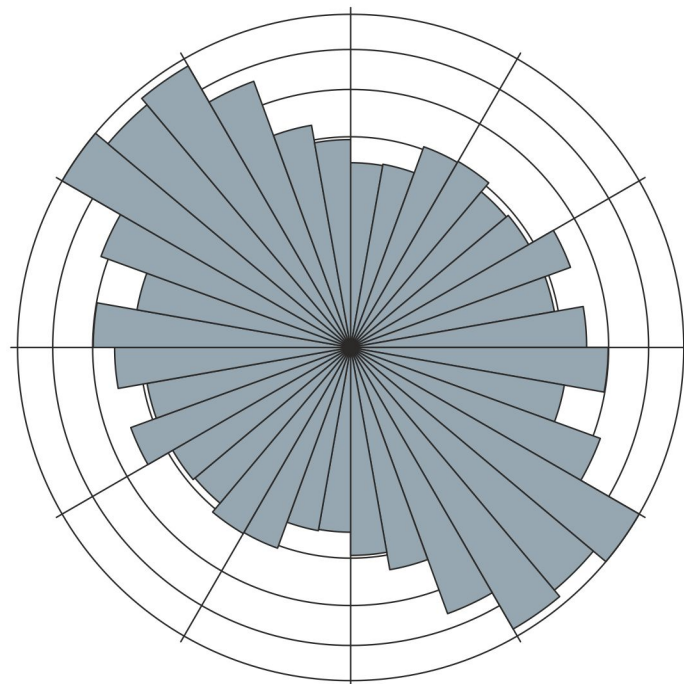




Sample N7132: Riereach Burn Top

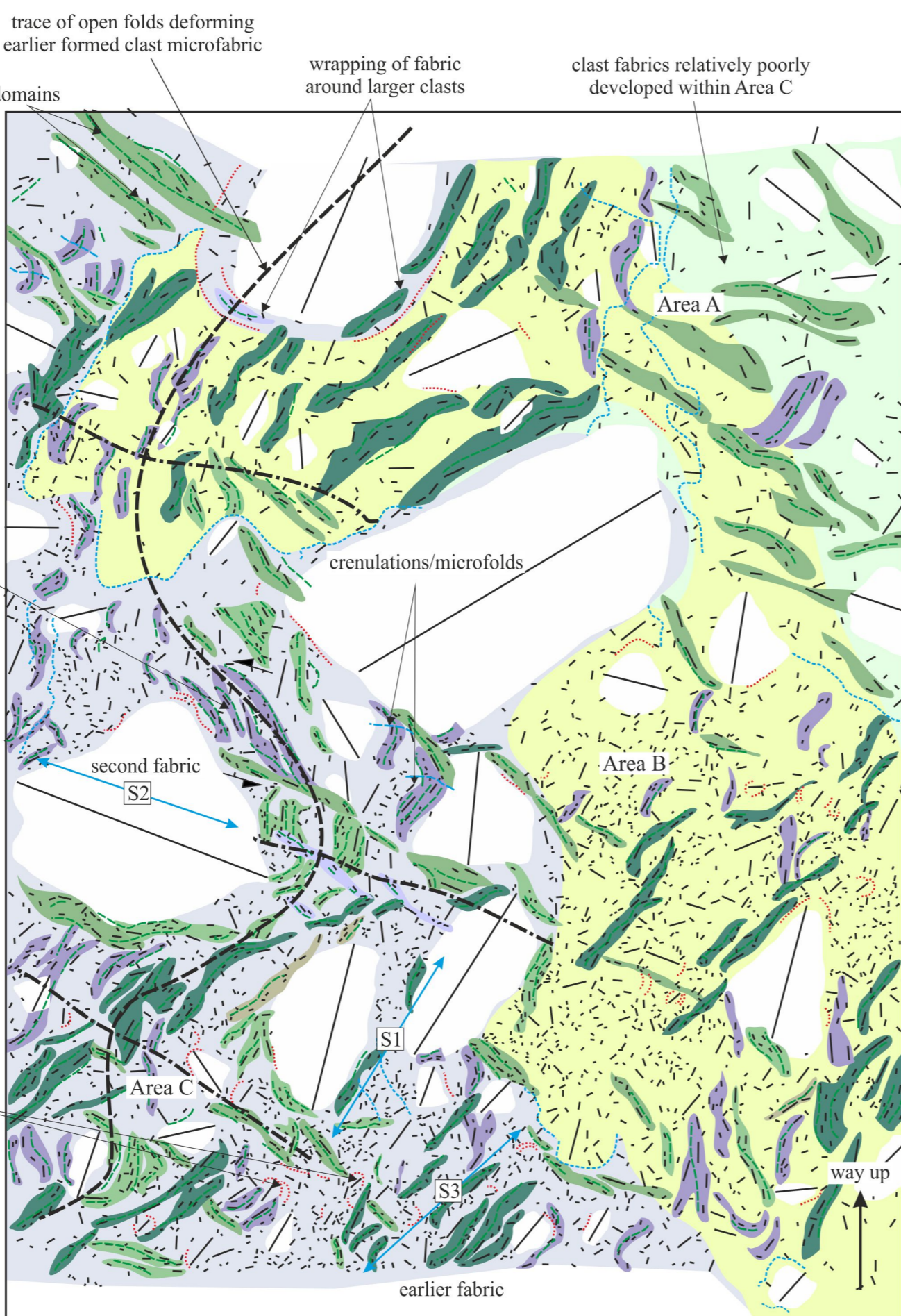
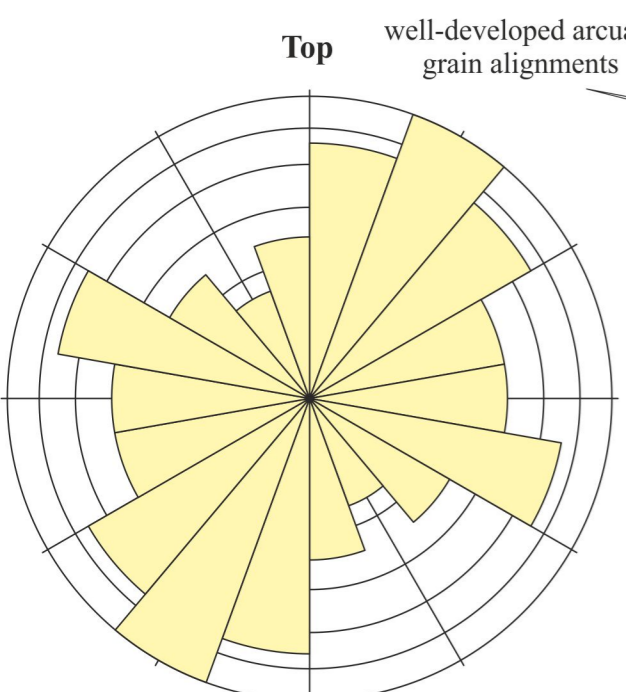
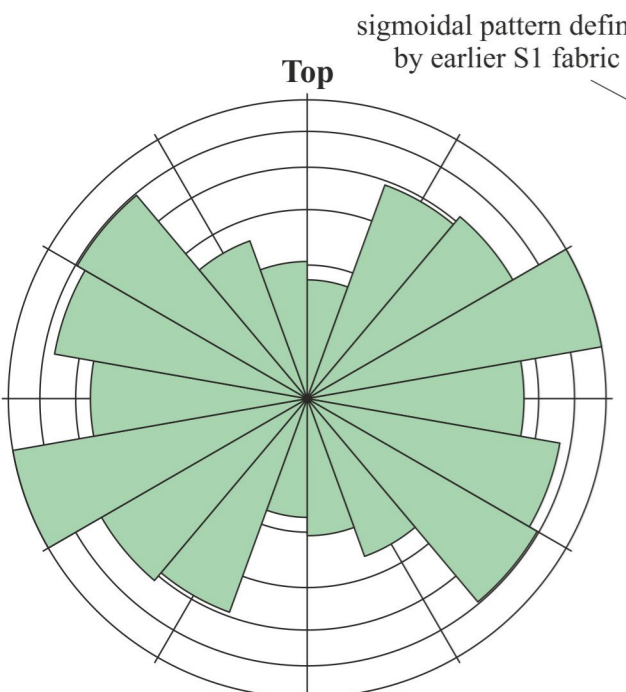
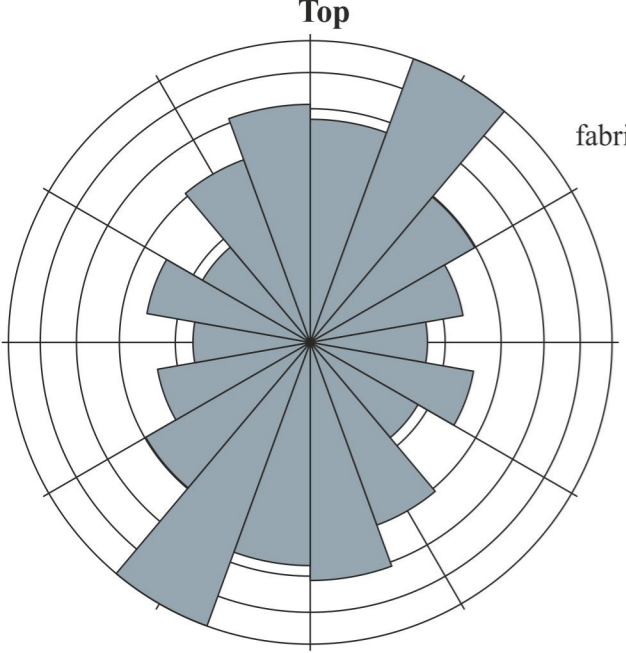


Sample N7132: Riereach Burn



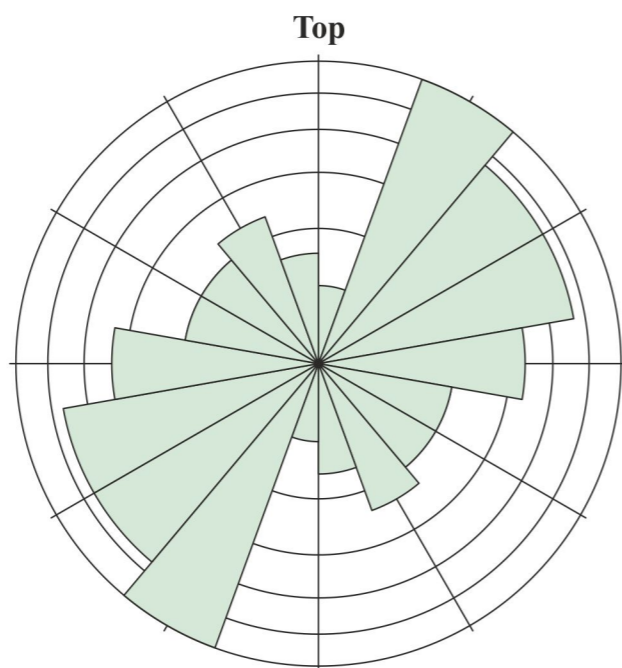
sample N7132 (N = 2233)

- microclast fabric defined by clast long axes
  - axial traces of folds deforming earlier formed S1 clast microfabric
  - axial surfaces of crenulations/microfolds
  - arcuate to linear grain aggregates
  - patchily developed boundary between dark and pale matrix
  - trace of folds deforming earlier formed S1 clast microfabric
  - domains defining the S1 microfabric (oldest)
  - domains defining the S2 microfabric
  - domains defining the S3 microfabric (youngest)
- S1 to n relative age of fabric(s)
- long axis of clasts
  - sense of shear
  - orientation of fabric(s)



Sample N7126: Dalcharn 'Lower Till'

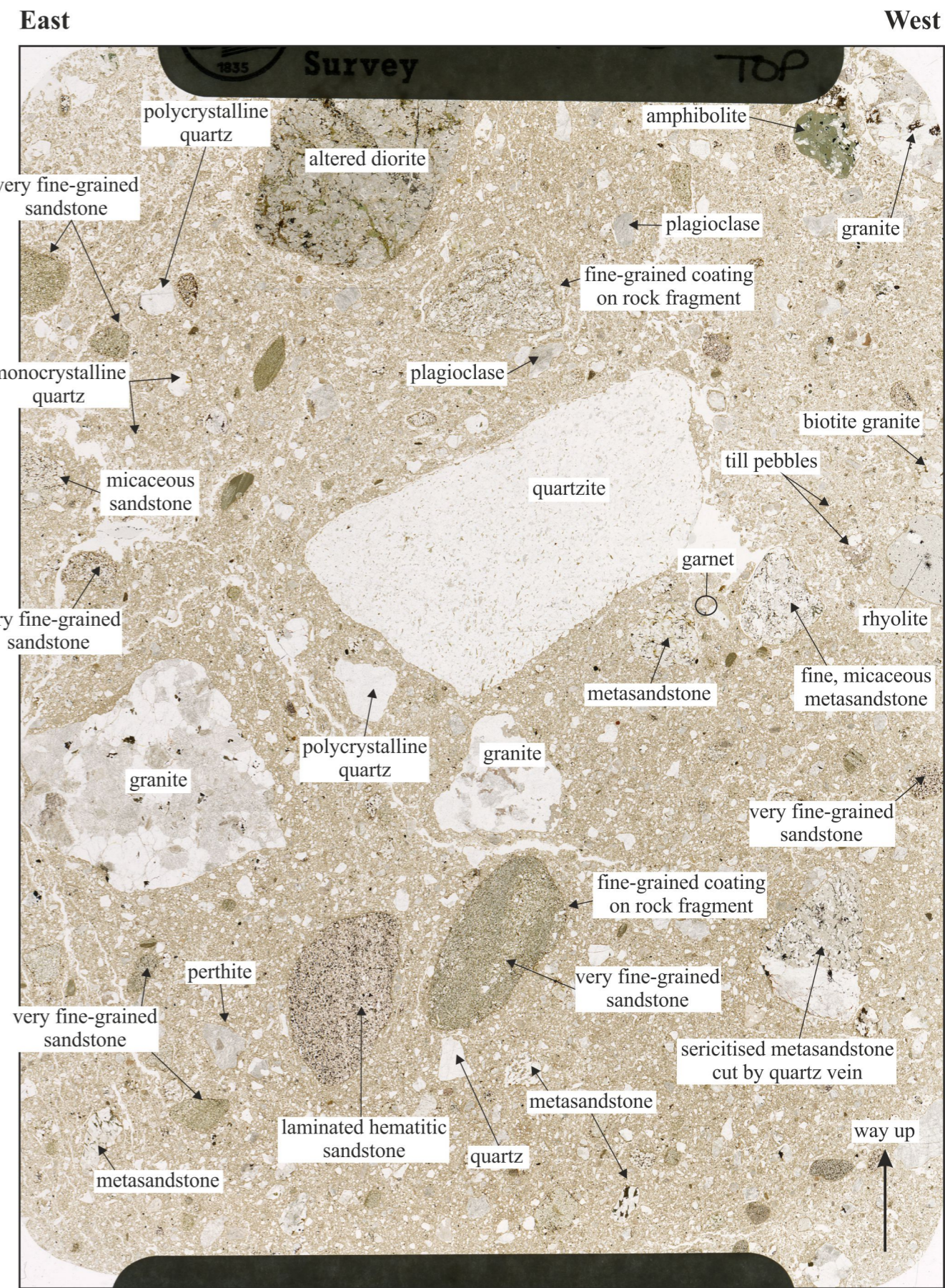
10 mm



- microclast fabric defined by clast long axes
- axial traces of folds deforming earlier formed S1 clast microfabric
- axial surfaces of crenulations/microfolds
- arcuate to linear grain aggregates
- patchily developed boundary between dark and pale matrix
- trace of folds deforming earlier formed S1 clast microfabric

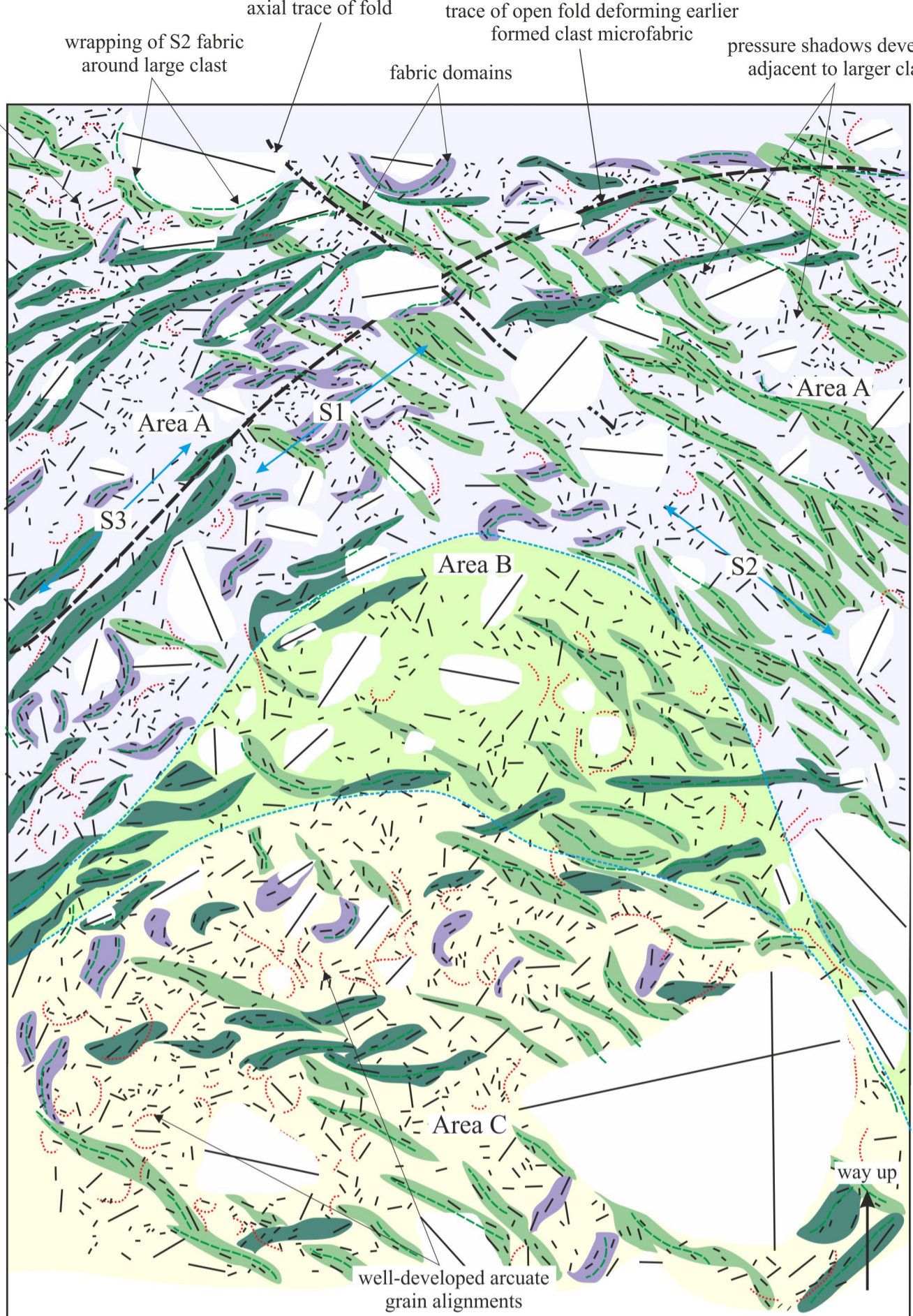
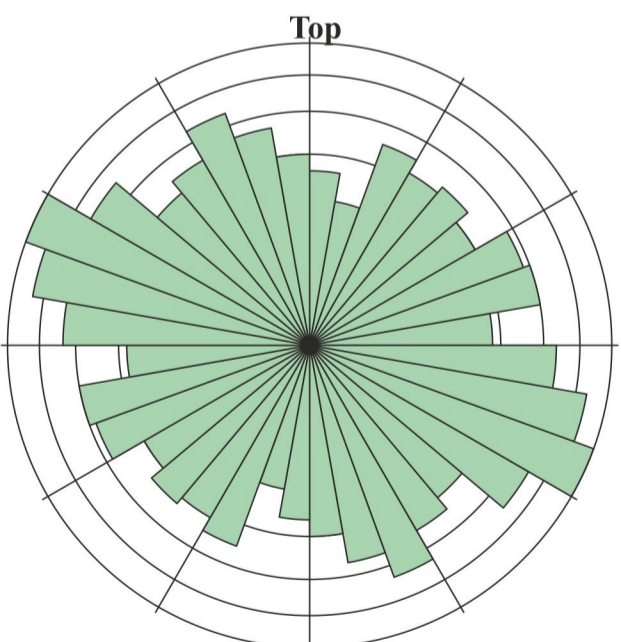
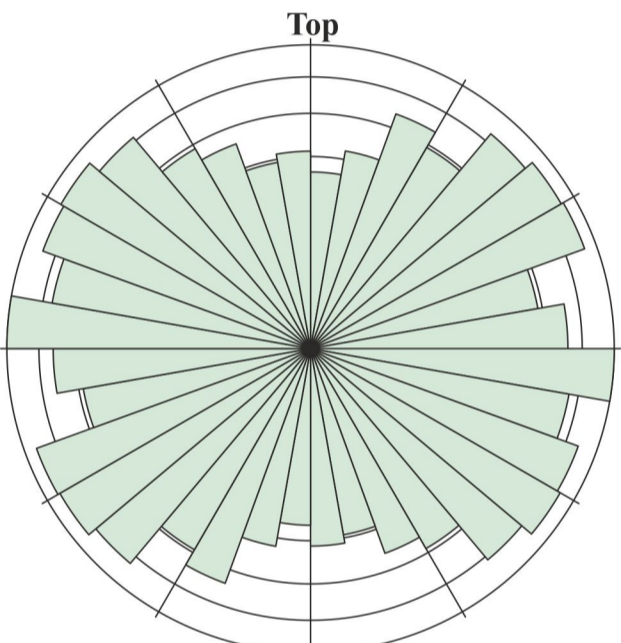
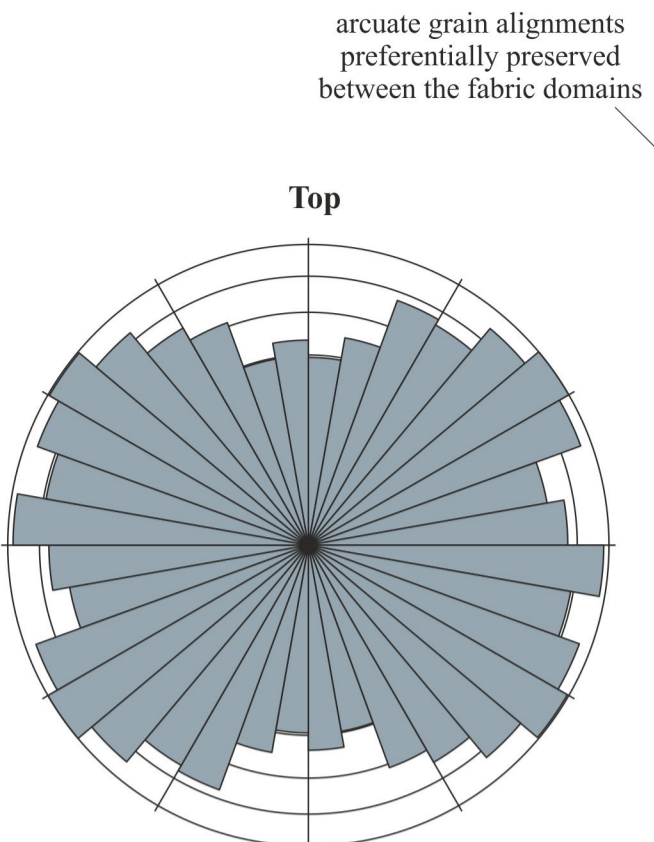
- domains defining the S1 microfabric (oldest)
- domains defining the S2 microfabric
- domains defining the S3 microfabric (youngest)

- S1 to n relative age of fabric(s)
- long axis of clasts
- sense of shear
- orientation of fabric(s)
- different phases of diamicton

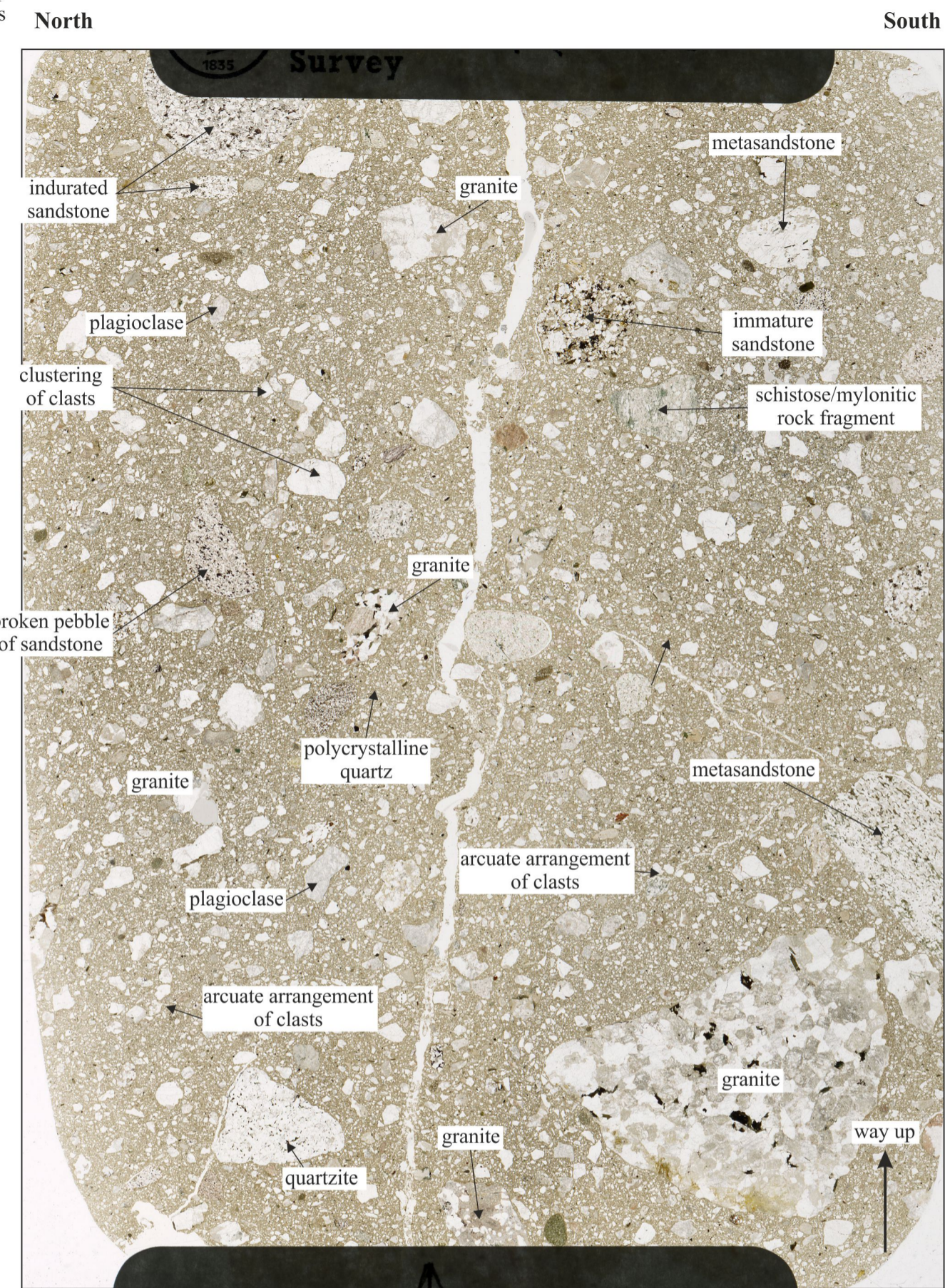
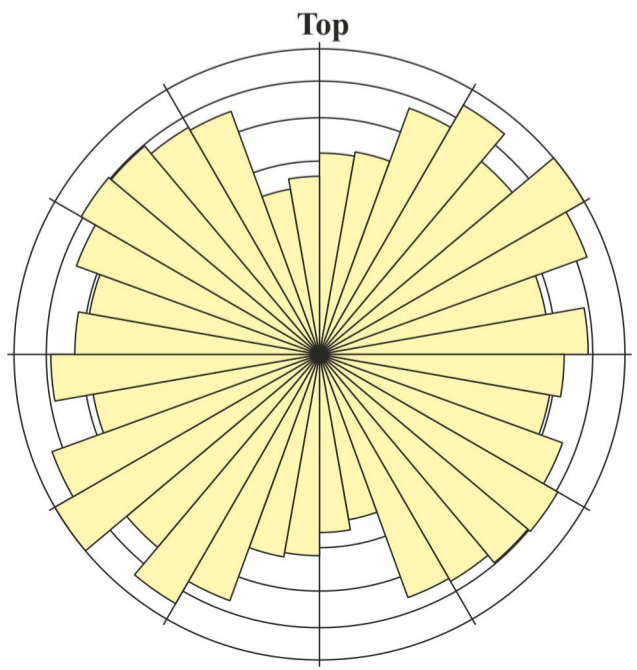


Sample N7126: Dalcharn 'Lower Till'

10 mm

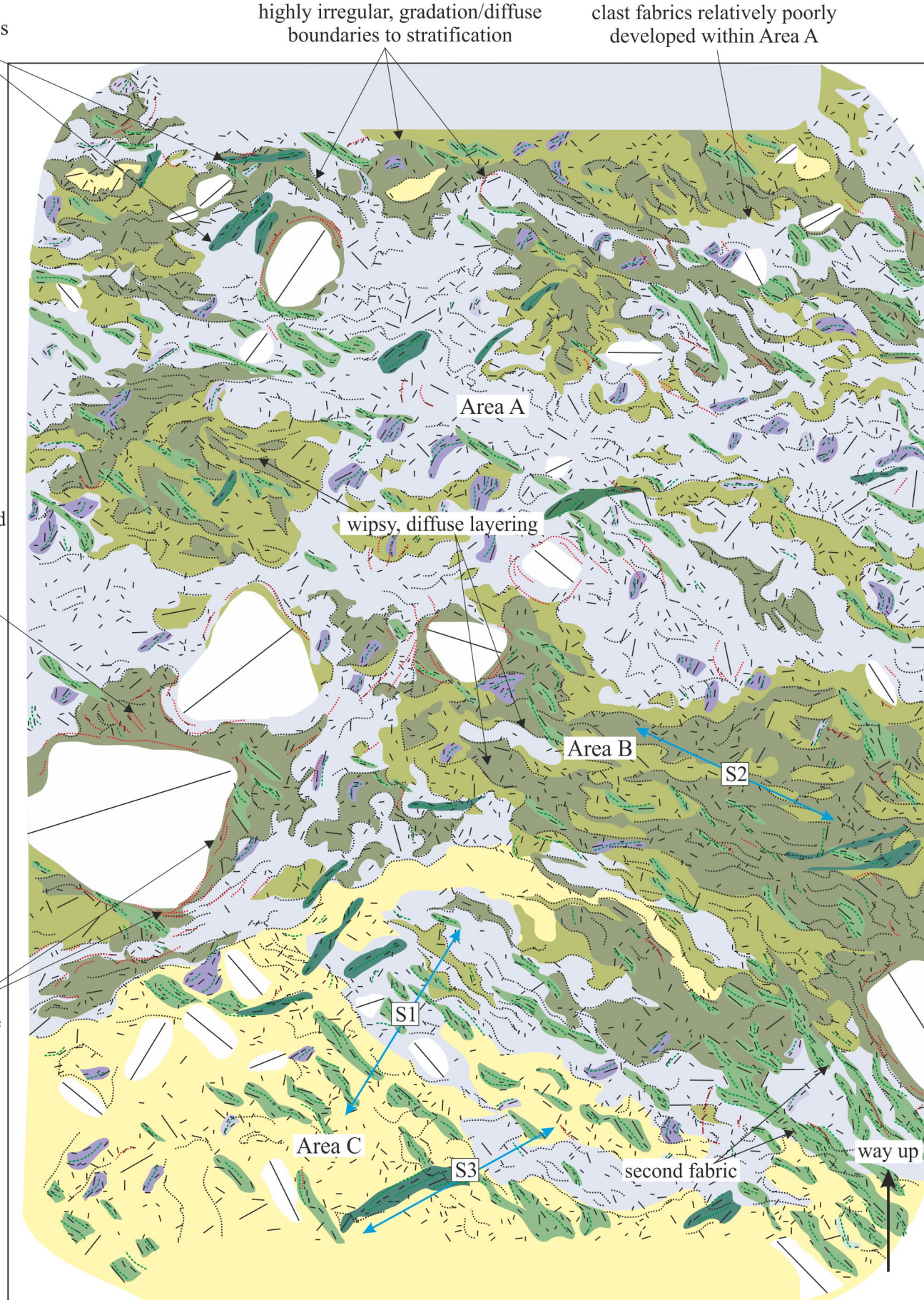
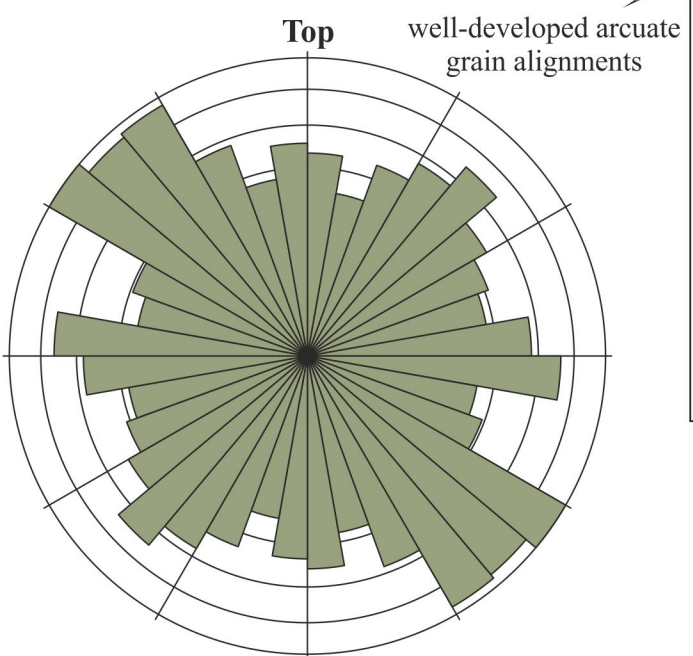
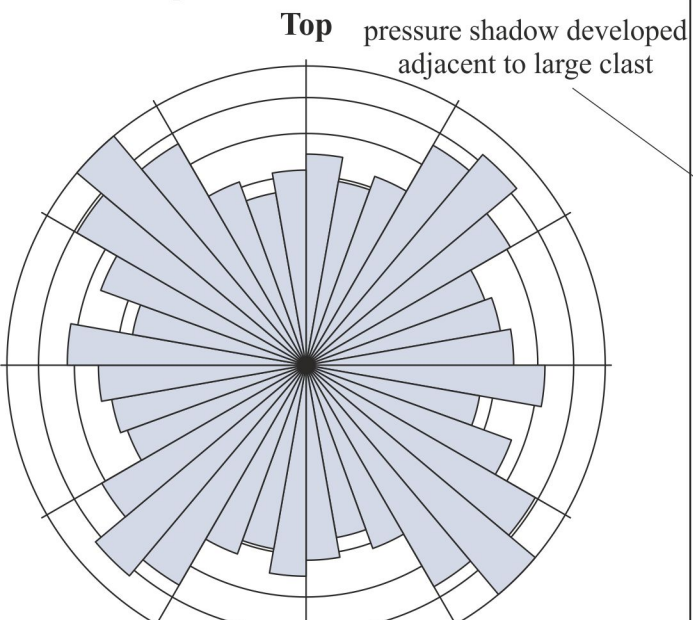
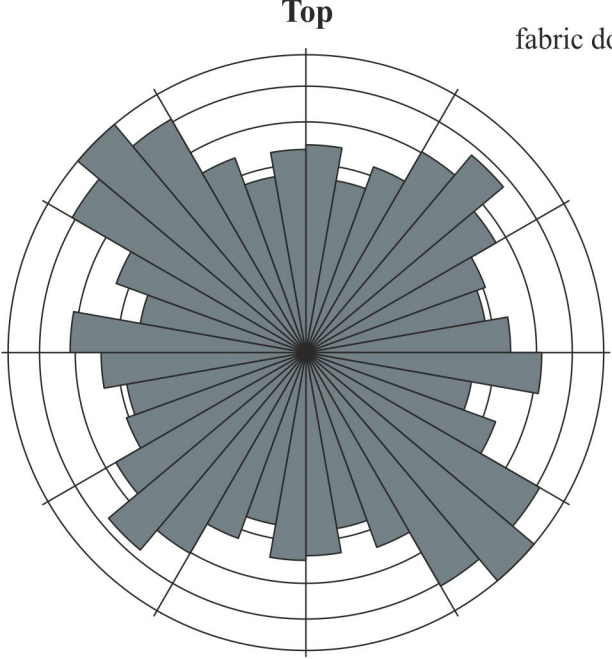


Sample N7128: Riereach Burn



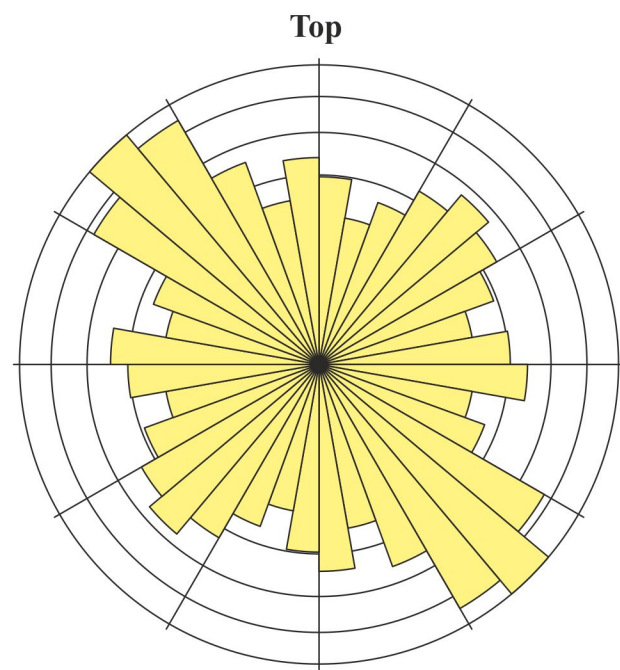
Sample N7128: Riereach Burn

- microclast fabric defined by clast long axes
  - axial traces of folds deforming earlier formed S1 clast microfabric
  - axial surfaces of crenulations/microfolds
  - arcuate to linear grain aggregates
  - patchily developed boundary between dark and pale matrix
  - trace of folds deforming earlier formed S1 clast microfabric
  - domains defining the S1 microfabric (oldest)
  - domains defining the S2 microfabric
  - domains defining the S3 microfabric (youngest)
- S1 to n relative age of fabric(s)
  - long axis of clasts
  - sense of shear
  - orientation of fabric(s)
  - different phases of diamicton



Sample N12280: Nairn (stream)

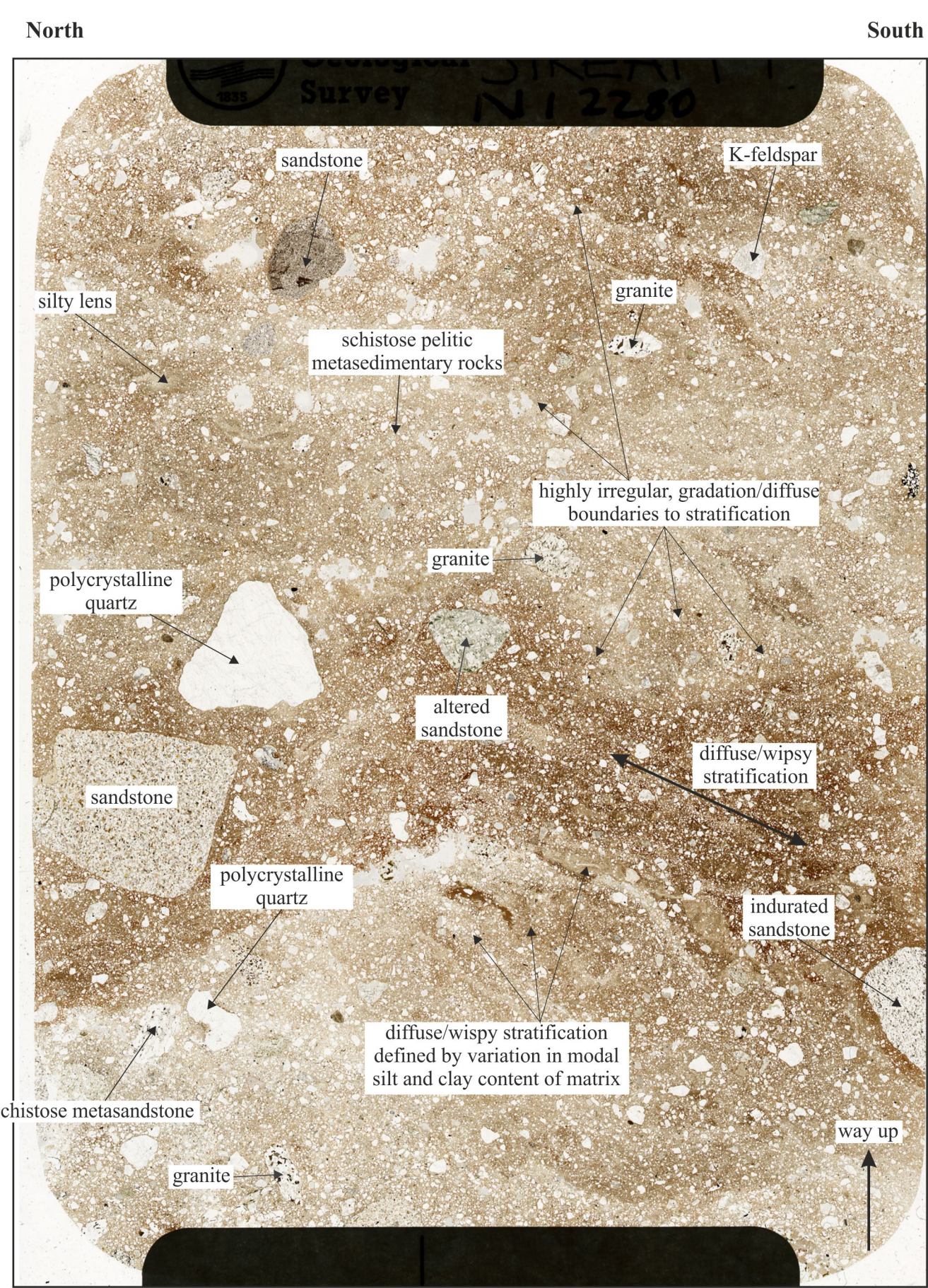
10 mm



sample N12280 area C (N = 1109)

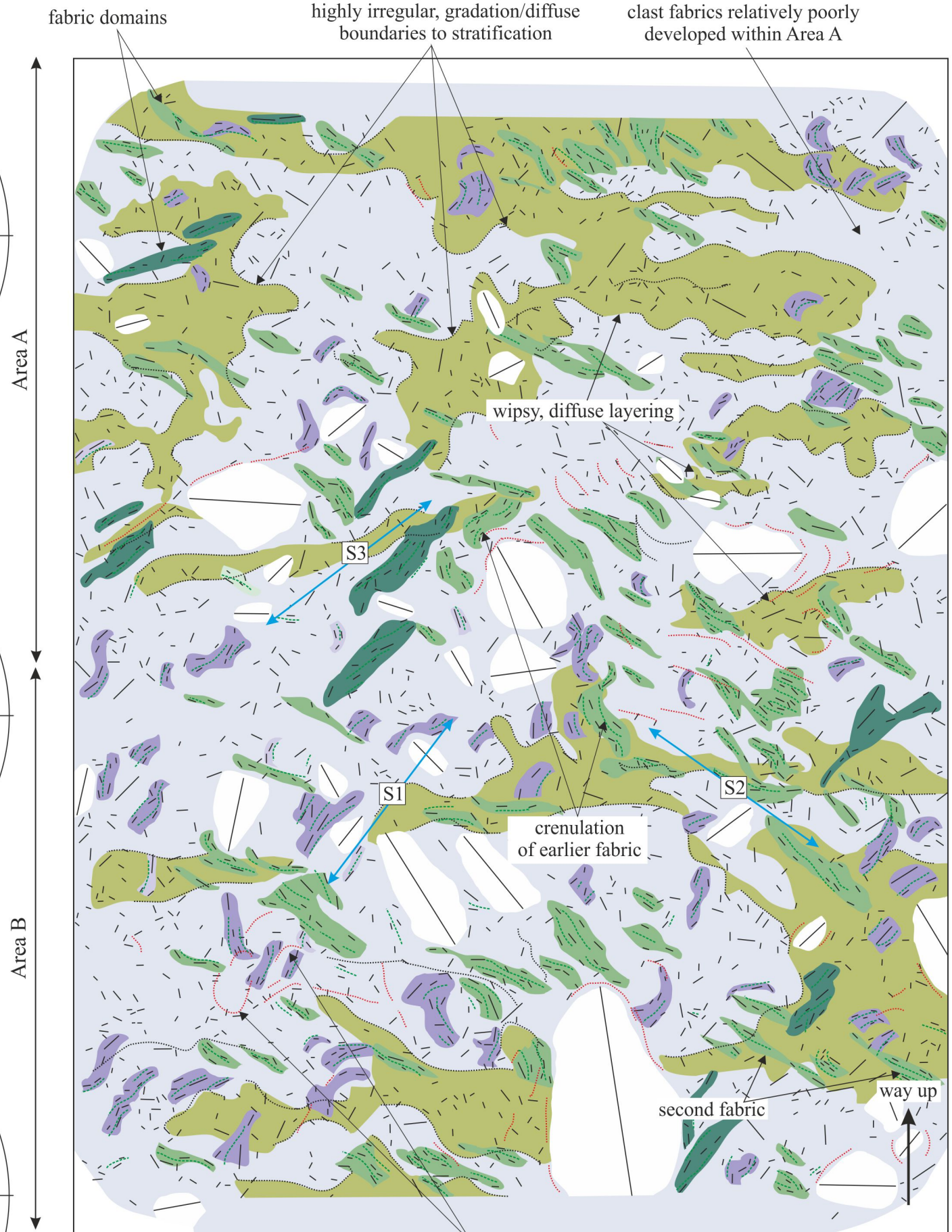
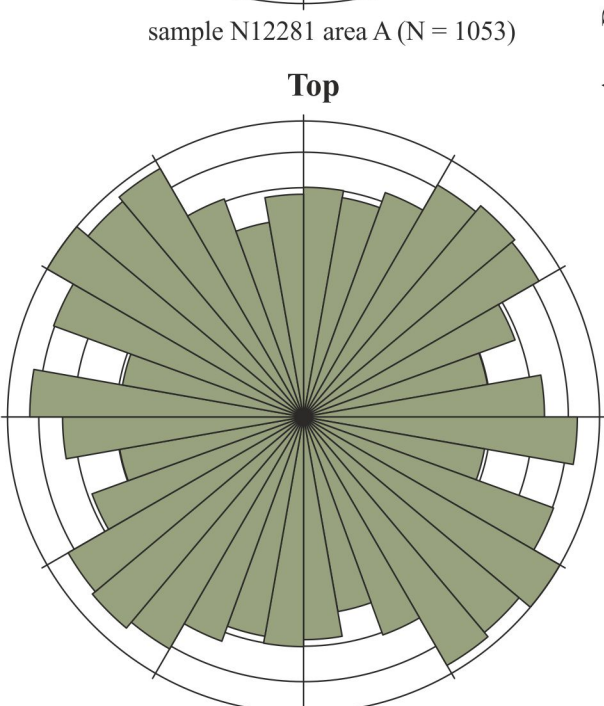
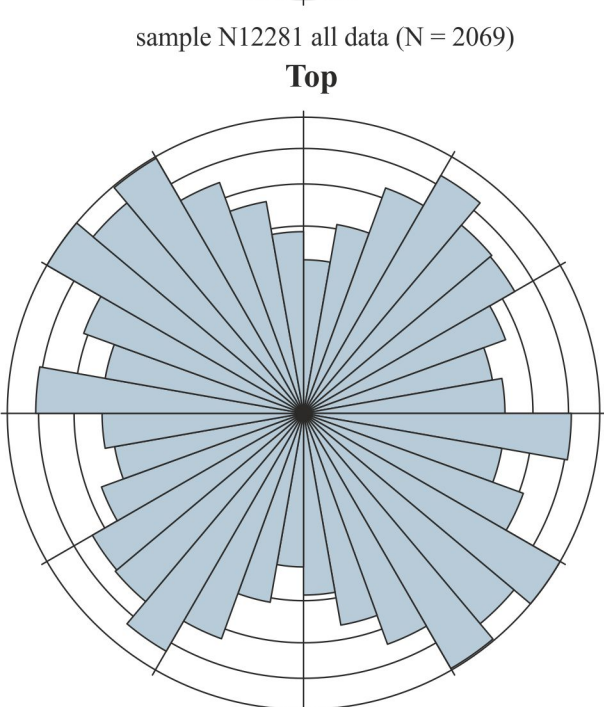
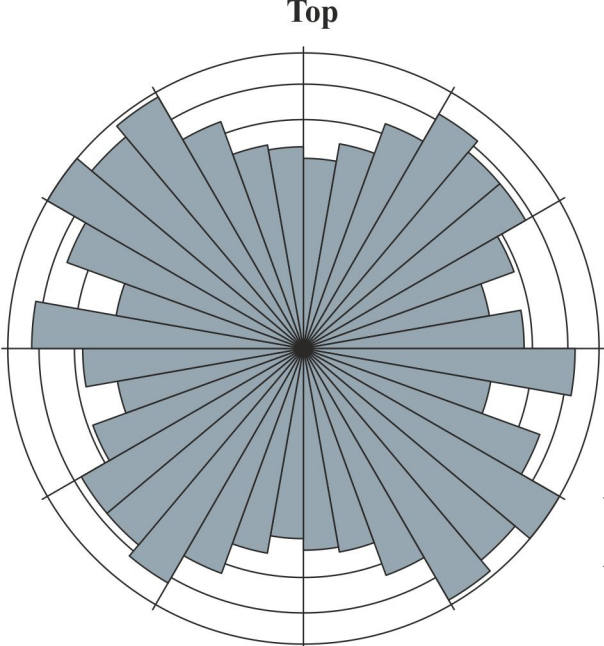
- microclast fabric defined by clast long axes
- axial traces of folds deforming earlier formed S1 clast microfabric
- axial surfaces of crenulations/microfolds
- arcuate to linear grain aggregates
- patchily developed boundary between dark and pale matrix
- trace of folds deforming earlier formed S1 clast microfabric
- domains defining the S1 microfabric (oldest)
- domains defining the S2 microfabric
- domains defining the S3 microfabric (youngest)

- S1 to n relative age of fabric(s)
- long axis of clasts
- sense of shear
- orientation of fabric(s)
- different phases of diamicton



Sample N12280: Nairn (stream)

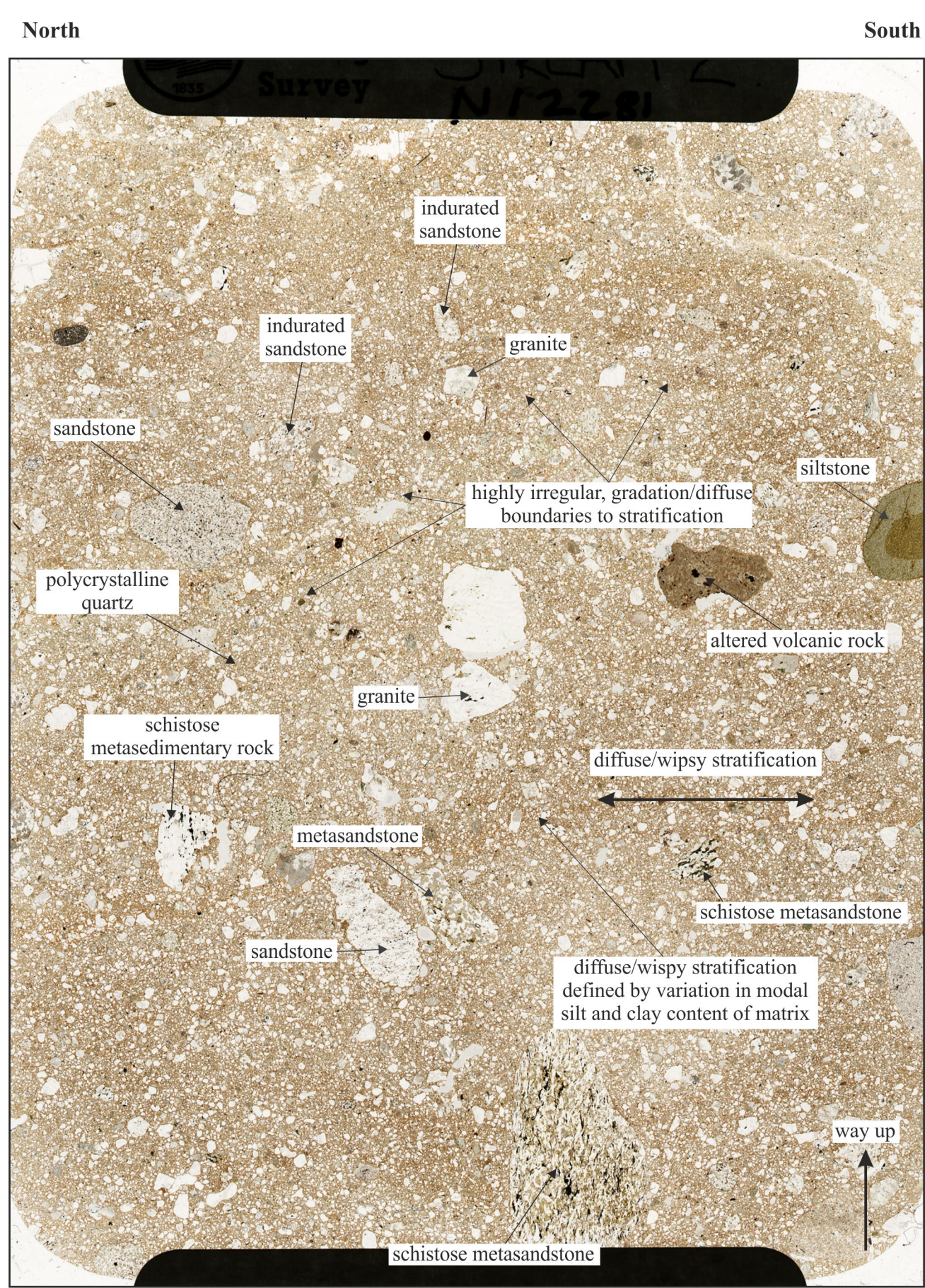
10 mm



**Sample N12281: Nairn (stream)** well-developed arcuate grain alignments

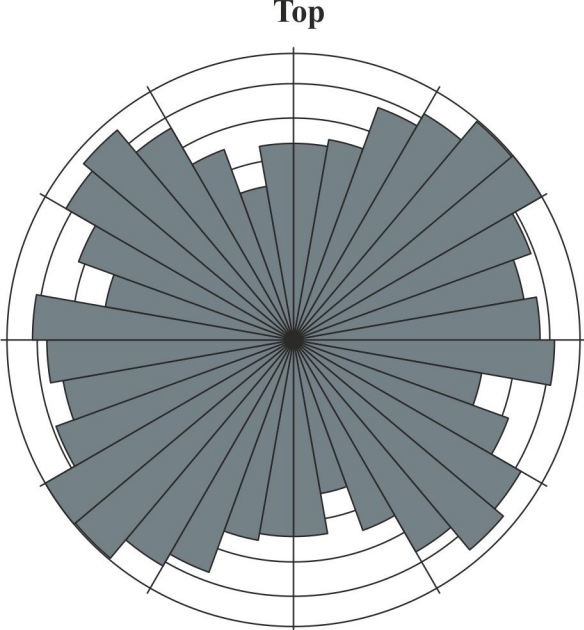
- domains defining the S1 microfabric (oldest)
- domains defining the S2 microfabric
- domains defining the S3 microfabric (youngest)
- different phases of diamicton

- microclast fabric defined by clast long axes
- axial traces of folds deforming earlier formed S1 clast microfabric
- axial surfaces of crenulations/microfolds
- arcuate to linear grain aggregates
- patchily developed boundary between dark and pale matrix
- trace of folds deforming earlier formed S1 clast microfabric

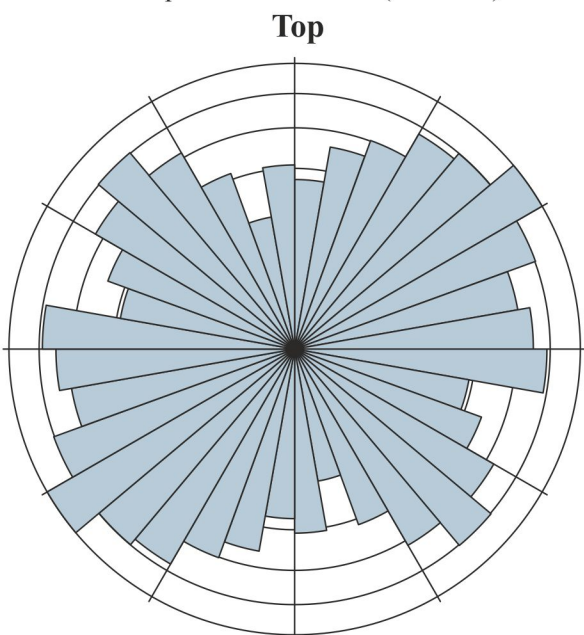


**Sample N12281: Nairn (stream)**

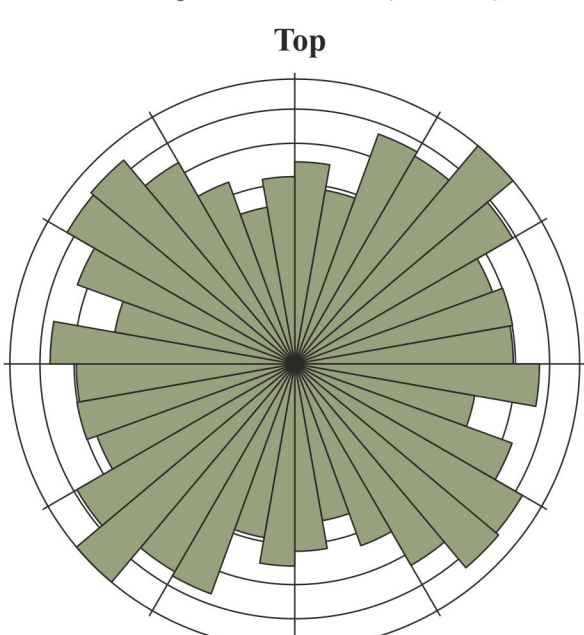
- S1 to n relative age of fabric(s)
- long axis of clasts
- sense of shear
- orientation of fabric(s)



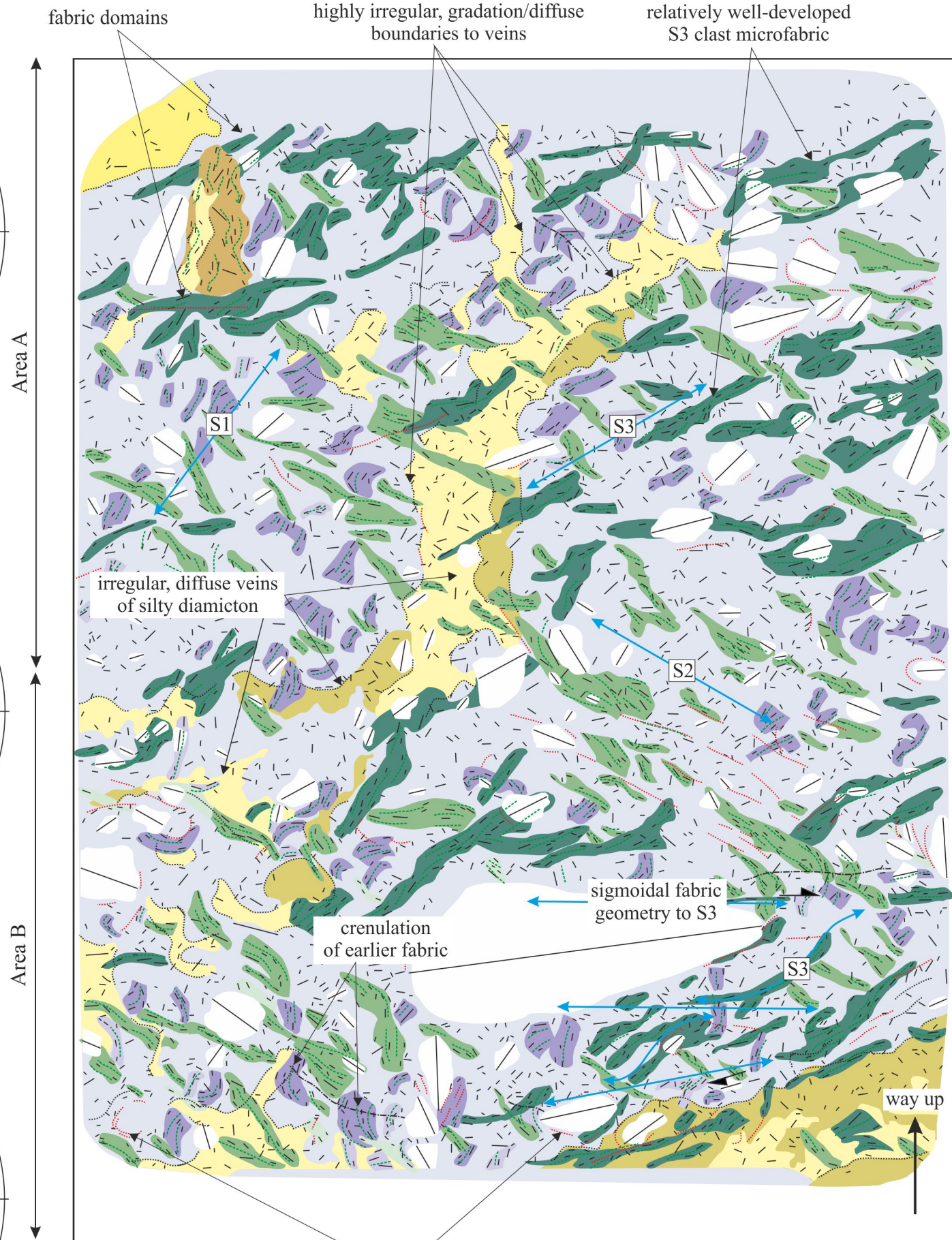
sample N12278 all data (N = 3344)



sample N12278 area A (N = 1741)



sample N12278 area B (N = 1587)



Sample N12278: Cothall

10 mm

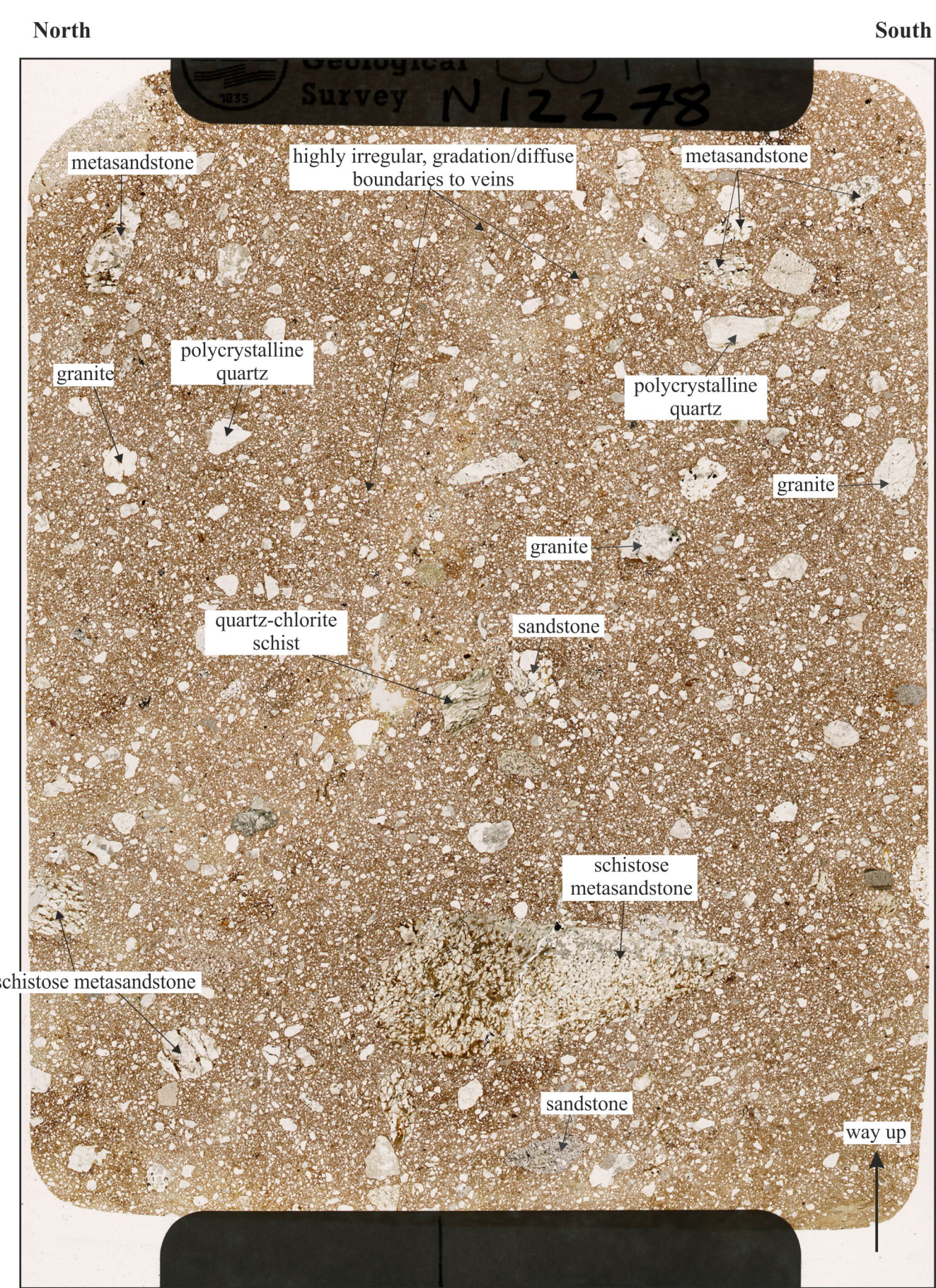
- domains defining the S1 microfabric (oldest)
- domains defining the S2 microfabric
- domains defining the S3 microfabric (youngest)
- sand and silt filling hydrofractures

well-developed arcuate grain alignments

- microclast fabric defined by clast long axes
- axial traces of folds deforming earlier formed S1 clast microfabric
- axial surfaces of crenulations/microfolds
- arcuate to linear grain aggregates
- patchily developed boundary between dark and pale matrix
- trace of folds deforming earlier formed S1 clast microfabric

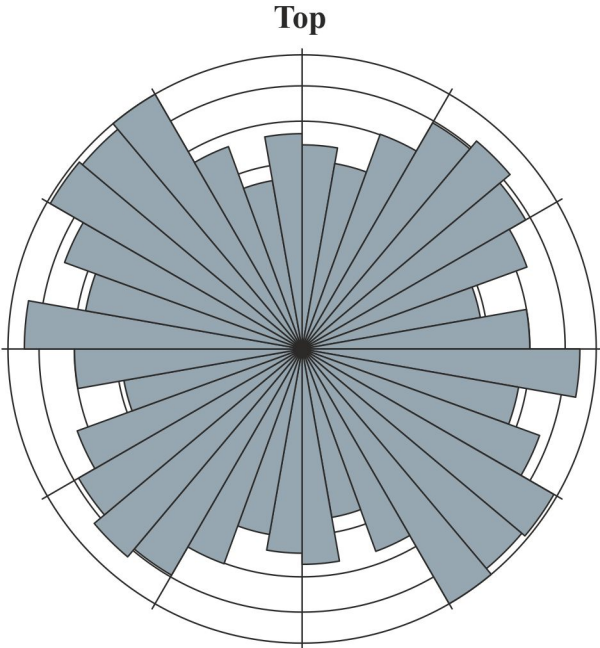
S1 to n relative age of fabric(s)

- long axis of clasts
- sense of shear
- orientation of fabric(s)

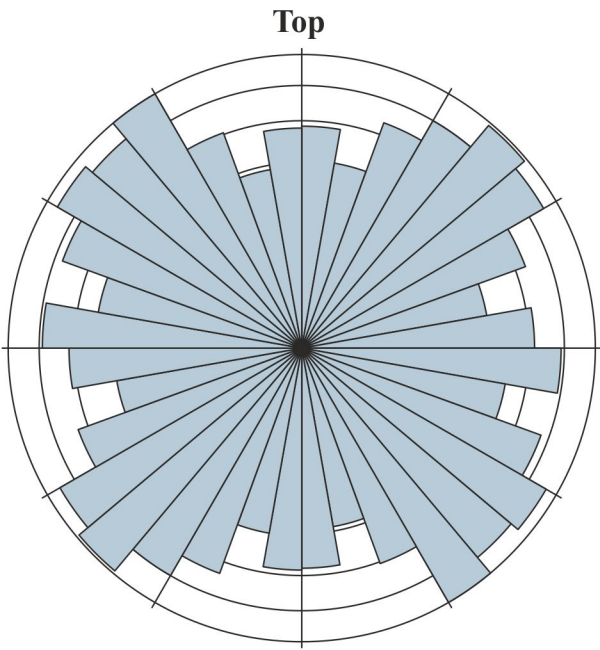


Sample N12278: Cothall

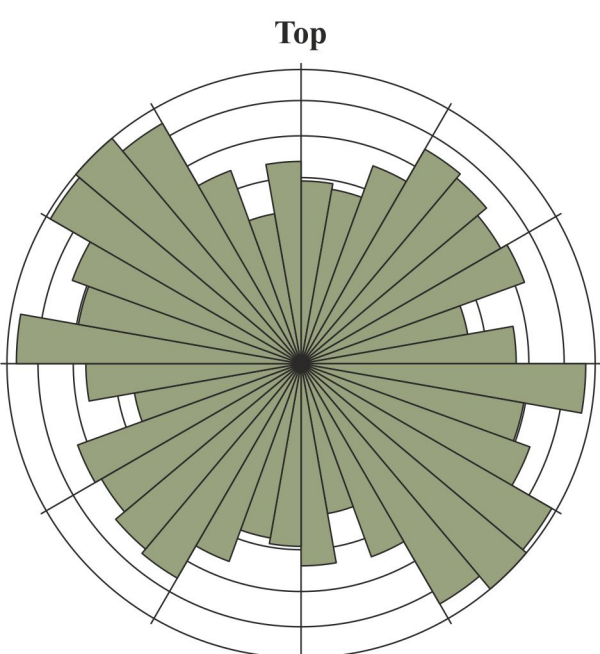
10 mm



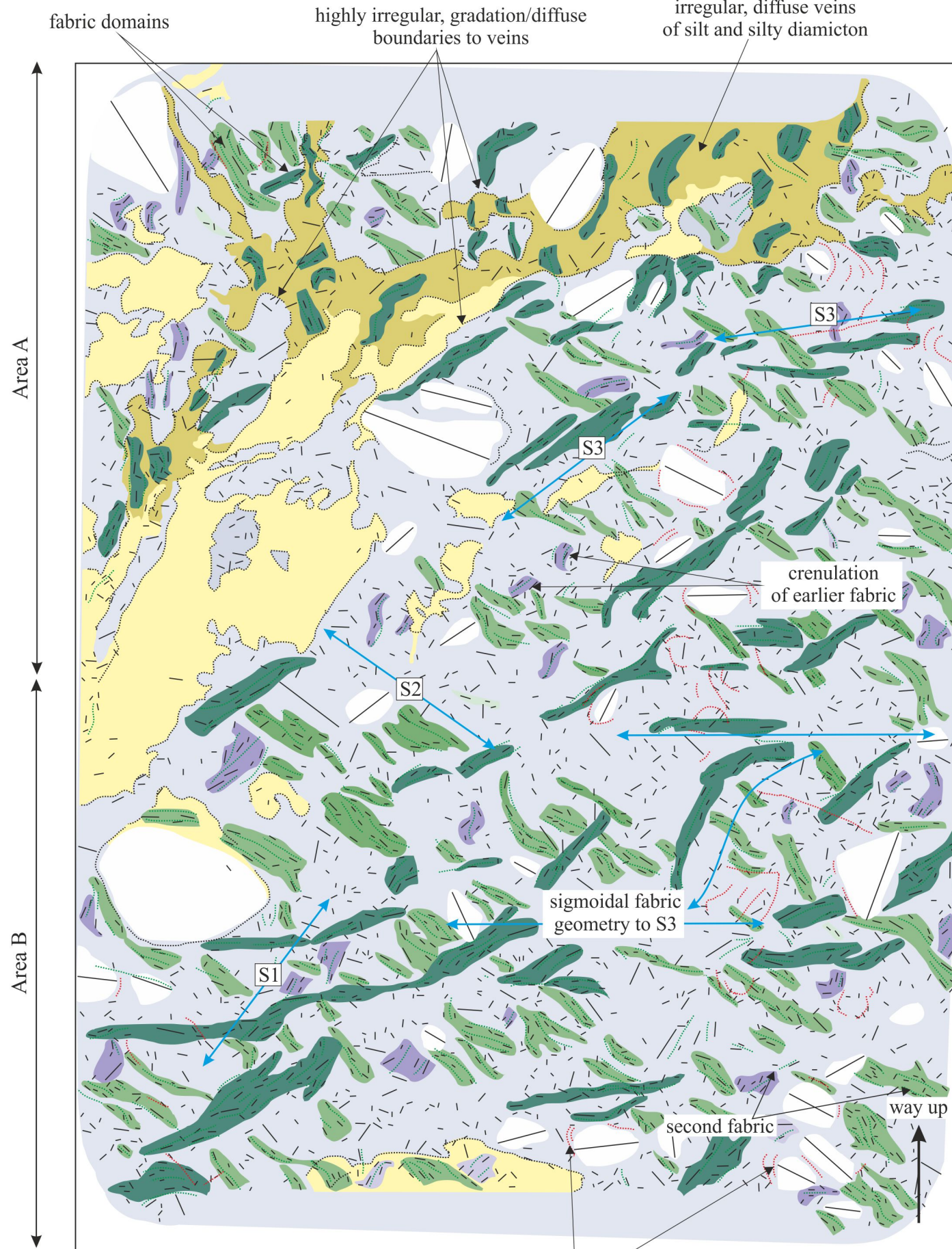
sample N12279 all data (N = 2680)



sample N12279 area A (N = 1302)



sample N12279 area B (N = 1407)



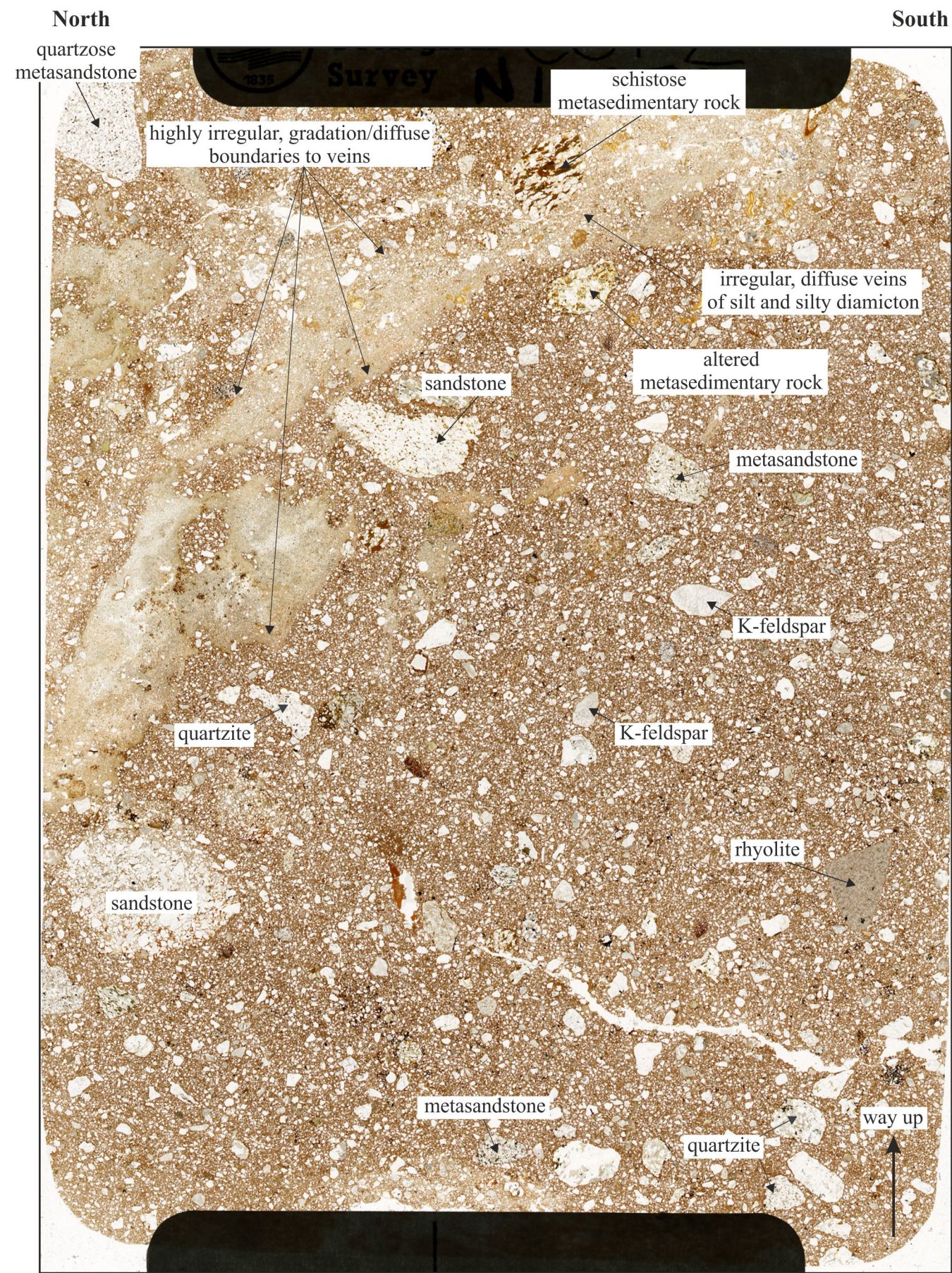
**Sample N12279: Cothall**

- domains defining the S1 microfabric (oldest)
- domains defining the S2 microfabric
- domains defining the S3 microfabric (youngest)
- sand and silt filling hydrofractures

well-developed arcuate grain alignments

10 mm

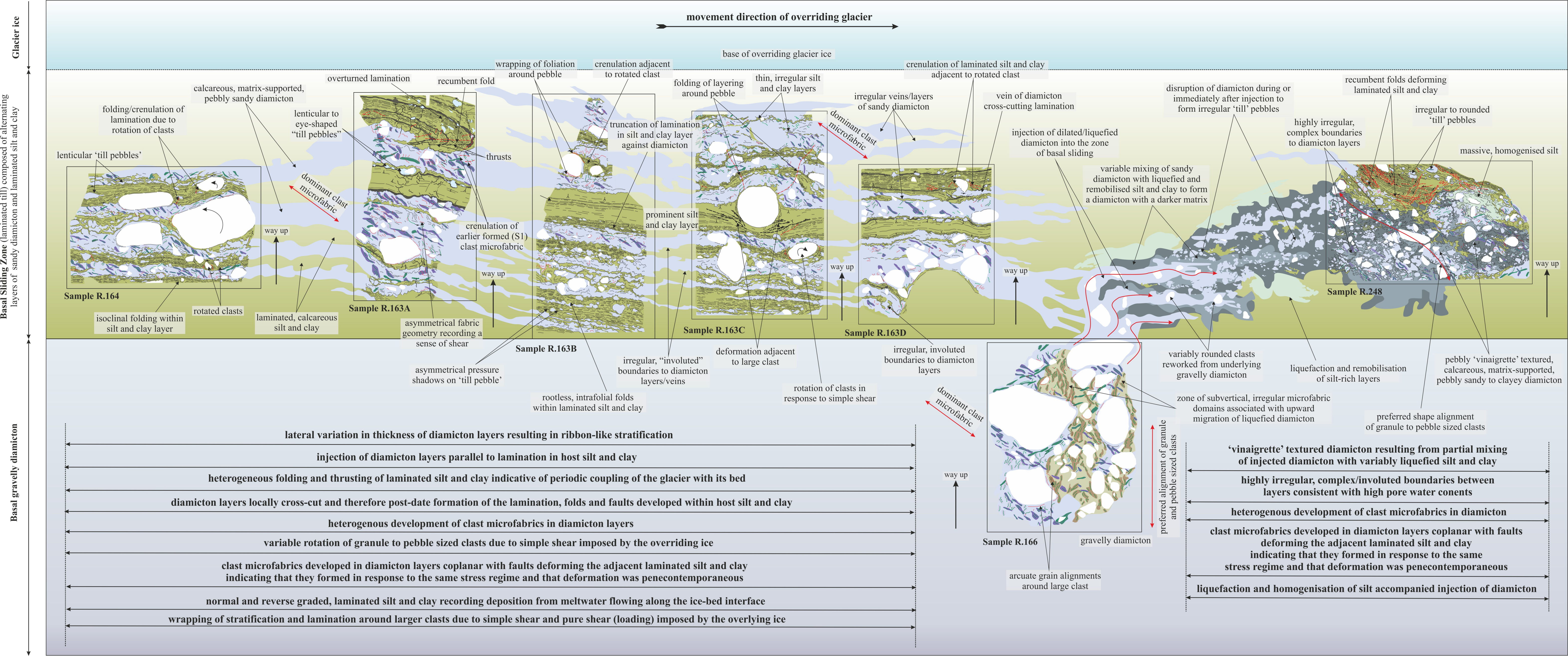
- microclast fabric defined by clast long axes
- axial traces of folds deforming earlier formed S1 clast microfabric
- axial surfaces of crenulations/microfolds
- arcuate to linear grain aggregates
- patchily developed boundary between dark and pale matrix
- trace of folds deforming earlier formed S1 clast microfabric



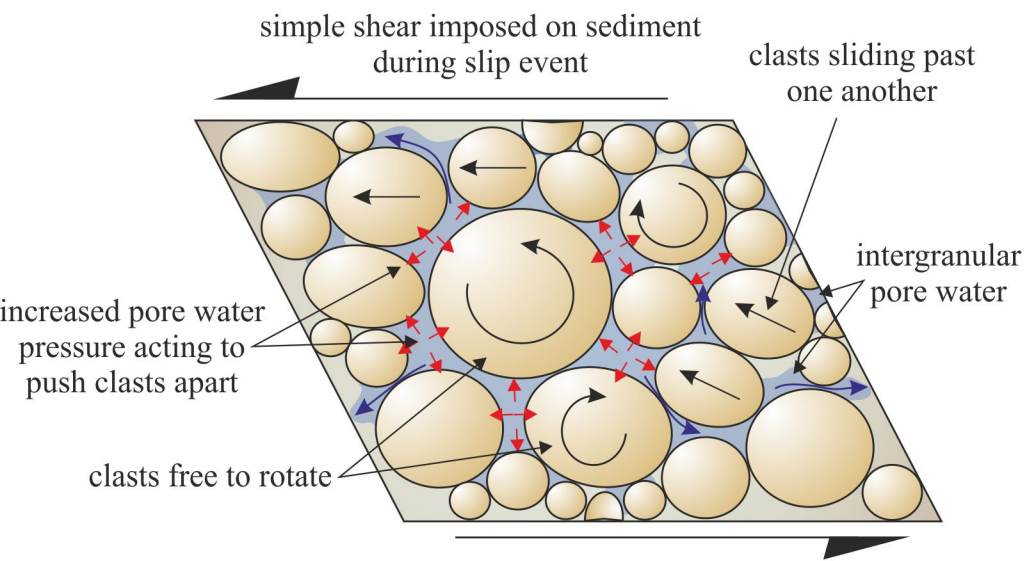
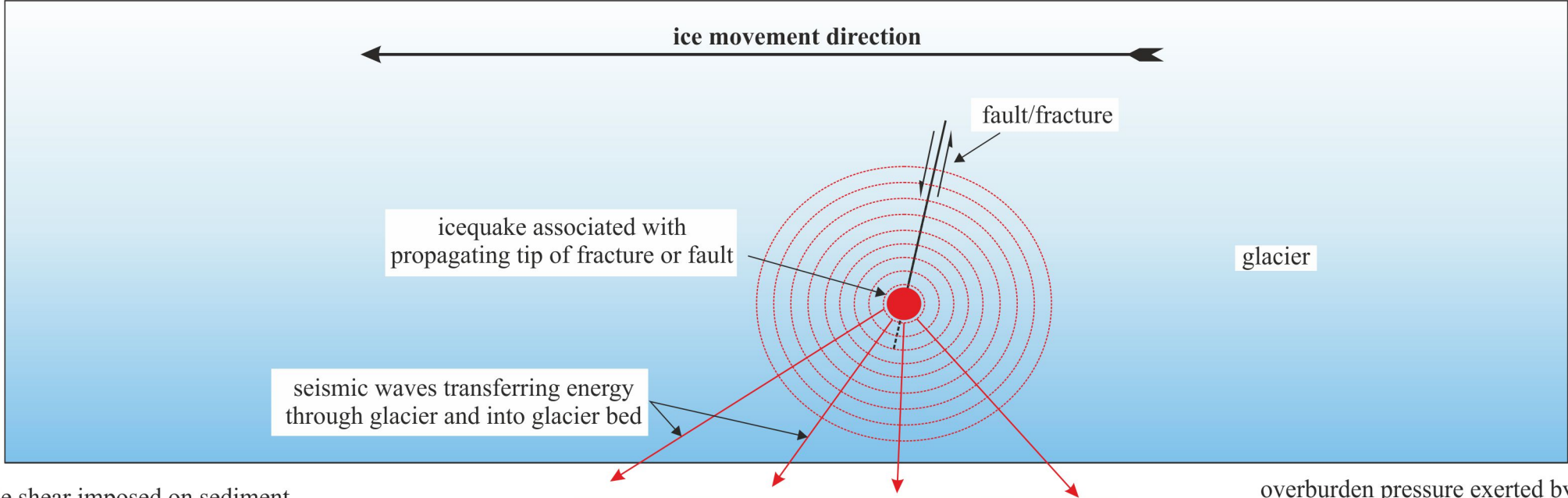
**Sample N12279: Cothall**

10 mm

- S1 to n relative age of fabric(s)
- long axis of clasts
- sense of shear
- orientation of fabric(s)

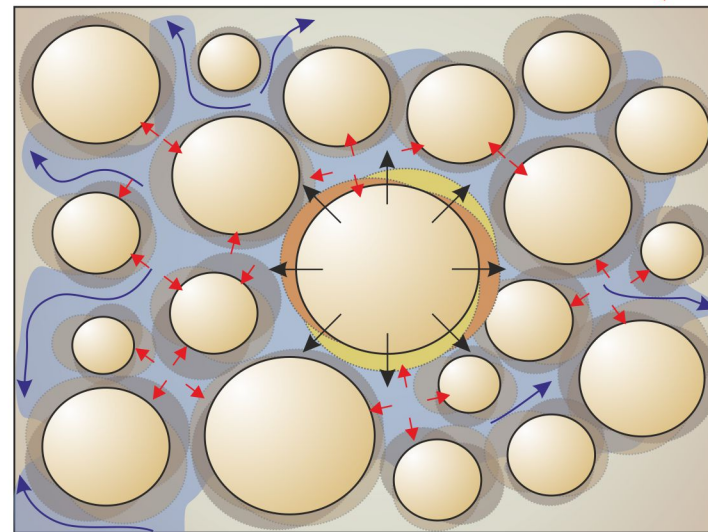




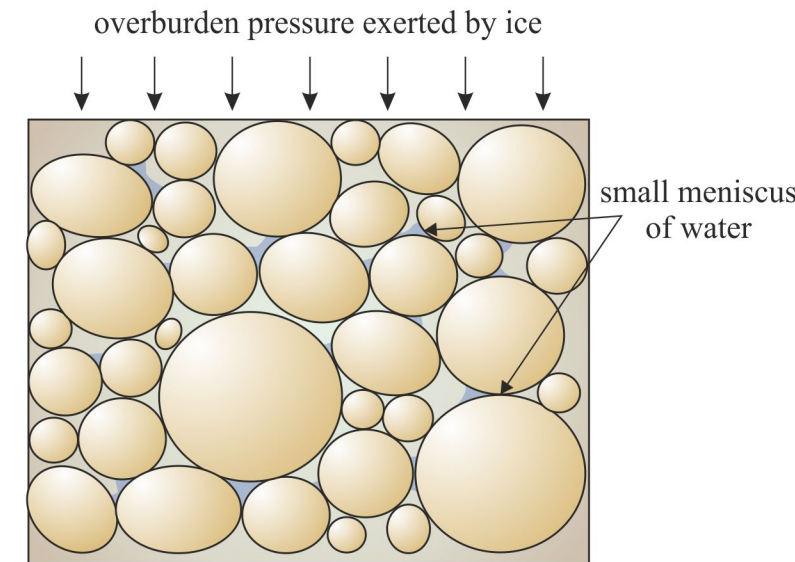


increased pore water pressure reducing grain to grain contacts, reducing sediment cohesion leading to weakening of bed, resulting in flow deformation accommodating forward motion (slip) of overriding glacier

**sediment at or near saturation  
= liquefaction  
= slippery spot initiation**

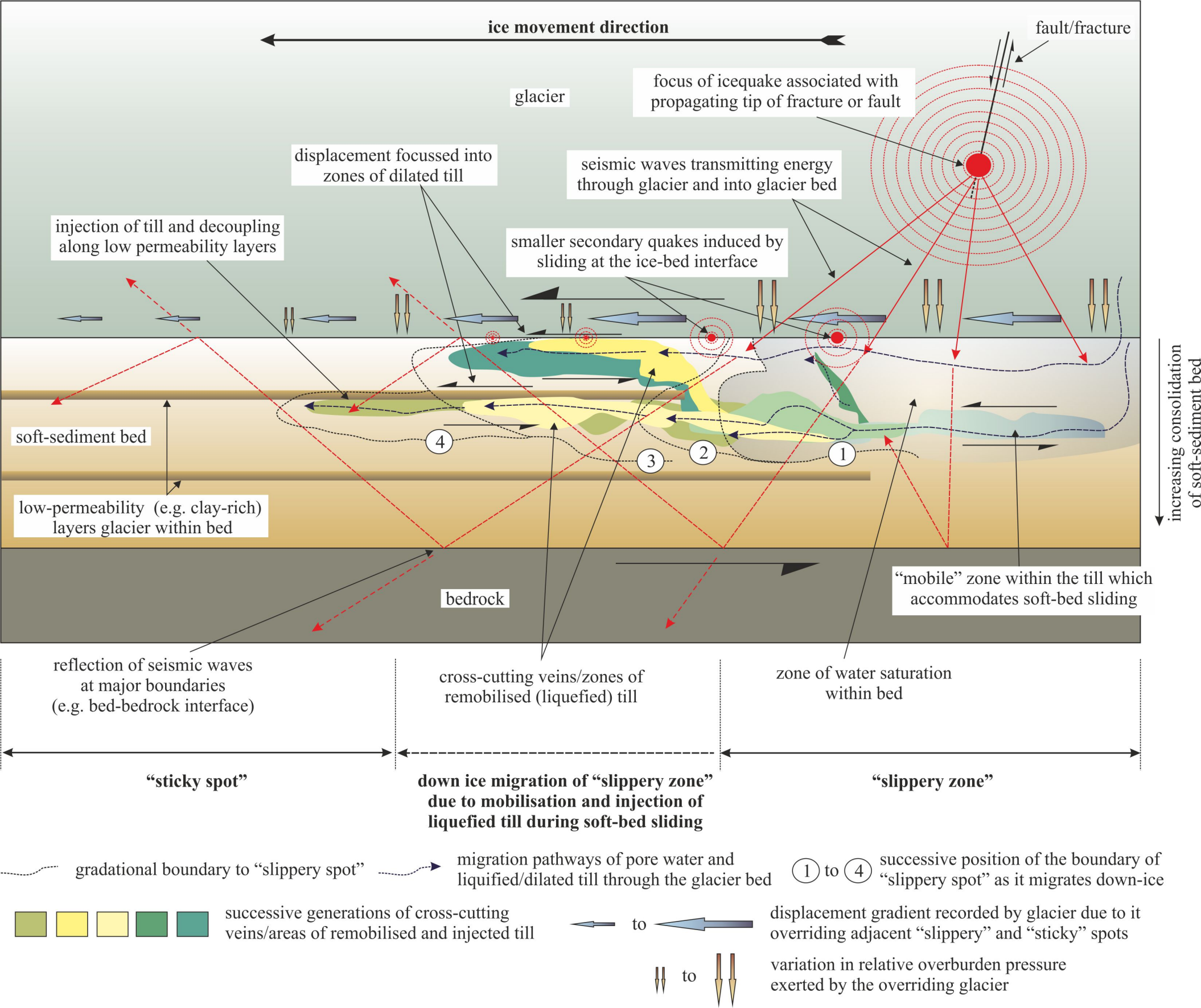


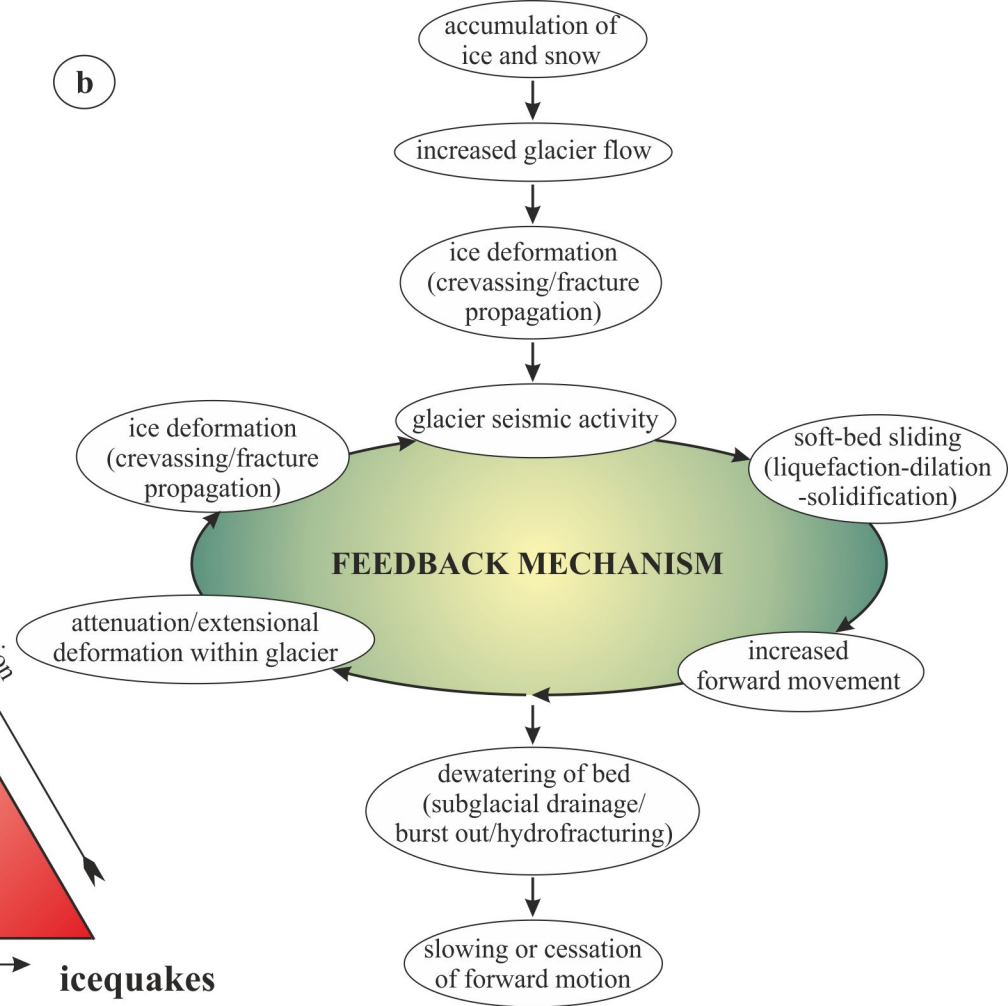
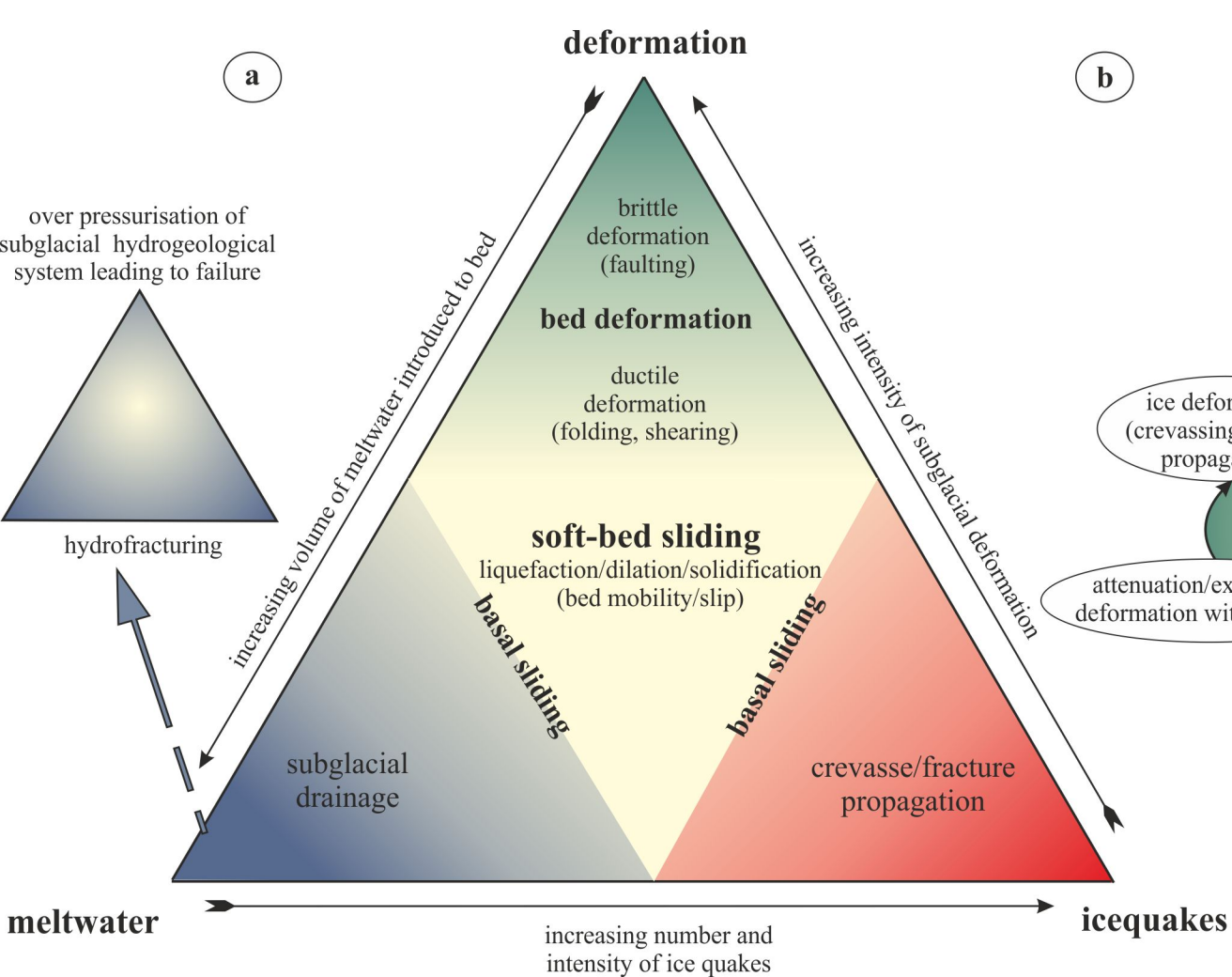
**during icequake**



high proportion of grain to grain contacts, clast vibration caused during icequake induces further compaction and over consolidation

**sediment under saturated or dry  
= consolidation  
= sticky spot**





## Highlights

- Subglacial traction tills undergo repeated phases of liquefaction and deformation
- This process lowers the shear strength of the till, facilitating glacier movement
- This soft-bed sliding occurs in a series of 'stick-slip' events
- Soft-bed sliding may be partially facilitated by glacier seismic activity